STRUCTURE-PROPERTY RELATIONSHIPS IN POLY-(PROPYLENE-ETHYLENE) COPOLYMERS

By

Siyabonga Mange

A thesis submitted to the Faculty of Engineering and the Built Environment of the University of Cape Town in fulfilment of the requirements for the degree of Master of Science in Applied Science.

Department of Materials Engineering
University of Cape Town
December 1999

ACKNOWLEDGEMENTS

I would like to express my sincere gratitude to all those people whose contributions made this work possible, in particular:

My supervisor, Dr Kashif Marcus, for sharing his expertise on the subject and the helpful discussion sessions and support;

Dr Brian Sole for his advice, suggestions, and supply of the research material;

The Polifin Polypropylene Division technical staff for the preparation of the test samples;

Mrs Mira Topic for her technical support and encouragement;

Mr Mohamed Jaffer for his help with the TEM;

Mr James Petersen and Mr Adriaan Loedolff for the photographic work;

Mr Glen Newins, Mr Nicholas Dreze and Mr Dave Dean for their help with the testing apparatus;

Miss Julie Henry for the administrative support;

Mrs Doreen Young for making the working environment less stressful;

Mr Derek McAuley and Mr Jerry Vermeulen at the University of Stellenbosch for the DMTA work;

Dr Terrence Marais at the National Accelerator Centre for the XRD work;

Mr Charles Goldman at Plastamid Ltd for the impact tests;

Mr Gavin Jewell for his computer expertise;

Mr Simphiwe Sishuba and Mrs Lungiswa Moyo for their inspirational support;

The staff and students in the Department of Materials Engineering for putting up with me and

The financial support of Polifin Limited is gratefully acknowledged.

GLOSSARY OF ABBREVIATIONS AND SYMBOLS

% C_2	-	Ethylene Content
α	-	Molecular Relaxations Occurring in the Crystalline Regions of the PP matrix / The Monoclinic Form of Crystalline Polypropylene
β	-	The Hexagonal Form of Crystalline Polypropylene
β_1	-	Molecular Relaxations Occurring in the Amorphous Regions of the PP Matrix
β_2	-	Molecular Relaxations Occurring within the EPR
γ	-	The Triclinic Form of Crystalline Polypropylene / Onset of the Local Mode of Relaxation
λ	-	Wavelength of the Incident X-Ray Beam
σ_t	-	Interfacial Tension between the Dispersed Rubber
ηm	-	Matrix Viscosity
Al_2O_3	-	Alumina
b	-	Width of Specimen in mm
C	-	Circumference of Rubber Particle in µm
C_2	-	Ethylene
C_3	-	Propylene
Ca	-	Capillary Number
CCD	-	Centre to Centre Distance
CD	-	Comonomer Distribution
CH_3	-	Methyl Group
$ClSO_3H$	-	Chlorosulphonic Acid
D	-	Cross-Sectional Particle Diameter
d	-	Diagonal Indent in mm
d_c	-	Cross-Sectional Diameter
DMA	-	Dynamic Mechanical Analyser
DMTA	-	Dynamic Mechanical Thermal Analysis
DSC	-	Differential Scanning Calorimetry
DTA	-	Differential Thermal Analysis
E′	-	Storage Modulus
E′′	-	Loss Modulus
E_f	-	Flexural Modulus
EPR	-	Ethylene-Propylene Rubber

E_Y	-	Tensile or Young's Modulus
HV-25 gf	-	Vickers Microhardness at 25 grams-force
i-PP	-	Isotactic Polypropylene
ISO	-	International Standards Organisation
m	-	Slope of Load-Deflection Curve in N/mm
MFI	-	Melt Flow Index
$\overline{M}n$	-	Number Average Molecular Weight Particles and the Matrix
$\overline{M}w$	-	Molecular Weight
$\overline{M}z$	-	*z*-Average Molecular Weight
MWD	-	Molecular Weight Distribution
NAC	-	National Accelerator Centre
$NaIO_4$	-	Sodium Periodate
NaOCl	-	Sodium Hypochlorite
OsO_4	-	Osmium Tetroxide
PE	-	Polyethylene
PP	-	Polypropylene
R21	-	Polifin Internal Standard Directly Related to the Rubber Content
$RuCl_3$	-	Ruthenium Trichloride
RuO_2	-	Ruthenium Dioxide
RuO_4	-	Ruthenium Tetroxide
SD	-	Sequence Distribution
STA	-	Simultaneous Thermal Analysis
t	-	Thickness of Specimen in mm
Tan δ	-	Ratio between Loss and Storage Modulus
T*g*	-	Glass Transition Temperature
TG	-	Thermogravimetry
T*m*	-	Melting Temperature
V_f	-	Volume Fraction
W	-	Load Applied in kgf
XRD	-	X-Ray Diffraction
B	-	Width of Rectangle with Same Area and Height as an XRD Trace Peak
E	-	Average Crystallite Size

ABSTRACT

This thesis examines the relationship between the microstructural and the mechanical properties of poly-(propylene-ethylene) bi-phasic copolymers. The copolymers investigated covered a comonomer content ranging between 4 and 23 percent ethylene. Nine grades were considered, with variables such as the melt flow index, the degree of crystallinity, the molecular weight distribution and the effect of a nucleating agent being examined.

These copolymers have been characterised in order to gain a better understanding of the interrelationship between the morphological structure and their physical, mechanical, thermal and thermo-mechanical properties. The toughness of the copolymers can be enhanced at low temperatures by increasing the ethylene content, at the expense of a loss in stiffness. A study of the microstructure using the scanning electron microscope indicates that a good balance between these two properties can be achieved through a uniform size and spatial distribution of the ethylene-propylene rubber particles within the polypropylene homopolymer matrix. The transmission electron microscope shows the ethylene-propylene rubber (EPR) to be agglomerates of smaller particles, with some crystallinity within the EPR being evident.

X-ray diffraction studies show that an increase in ethylene content broadens the peak widths and decreases the average crystallite size. Some grades show a presence of the $(300)_\beta$ crystallographic peak at $2\theta^\circ = 16.1$. This peak is due to the presence of the β hexagonal form of polypropylene. The degree of crystallinity determined from XRD data shows a decrease with increasing ethylene content. Dynamic Mechanical Thermal Analysis (DMTA) shows that an increase in ethylene content shifts the glass transition temperature to lower temperatures. Differential Scanning Calorimetry (DSC) and Differential Thermal Analysis (DTA) studies of the copolymer grades spanning the ethylene content range show little difference in their melting behaviour. Thermogravimetric (TG) studies for grades with very dissimilar ethylene contents showed similar decomposition patterns.

TABLE OF CONTENTS

CHAPTER 1

GENERAL INTRODUCTION

1.1 INTRODUCTION

Polypropylene is an extremely versatile semicrystalline polymer because its properties can be modified to meet specific requirements. The most important molecular parameters that can be manipulated are its melt flow index (MFI), molecular weight distribution (MWD) and its % crystallinity. Careful control of these parameters leads to the conversion of useful products *via* processing routes such as injection moulding, extrusion and melt spinning. Polypropylene is also often used as the matrix in composite materials. It has a very low density and this leads to a favourable specific- strength and stiffness as well as an advantageous price-performance ratio. Polypropylene occupies a special place amongst synthetic polymers, standing as it does on the dividing line between engineering and commodity polymers[1]. On the one hand, its price makes it desirable for use in low cost applications, whilst on the other hand, its specific properties and performance allows it to be used in engineering applications.

Its major disadvantage though, is its relatively poor toughness at low temperatures. To overcome this problem, polypropylene can be copolymerised with comonomers such as ethylene. The main reason for the poor toughness of the polypropylene homopolymer at low temperatures is its high degree of crystallinity coupled with its glass transition temperature (T*g*) at about −10 °C. The synthesis and development of polypropylene copolymers was a natural development after the initial discovery and industrial manufacture of the polypropylene homopolymer[2]. Copolymerisation lowers the crystallinity of polypropylene by introducing irregularity into the chain structure, thus lowering the close packing density. The glass transition temperature is dependent on the crystallinity of the polymer and the configuration of the

polymer chain. Reducing the crystallinity through copolymerisation allows a controlled decrease in the glass transition temperature hence increasing toughness at low temperatures with an acceptable loss in stiffness.

The incorporation of the ethylene-propylene rubber (EPR) particles as the dispersed rubber phase into the polypropylene matrix can be done either in the reactor or in the extruder[3]. The reactor-made copolymer can be made either in a single reactor where the resulting product is a random copolymer, or with two reactors in tandem, with the matrix produced in the first reactor and the dispersed phase produced and incorporated in the second reactor. Truly block copolymers can only be produced under conditions of[4]:

- Active sites being able to polymerise both ethylene and propylene;
- Active sites sufficiently stable along the polymerisation period and a
- Long average life of the growing macromolecules.

The above conditions are not all usually fulfilled; hence the copolymer is strictly speaking a bi-phasic polymer but is commonly referred to as a block or impact copolymer. The reactor-made method is considered more advantageous than the post-reactor process since[5]:

- Products are polymerised directly from the monomers, thus the reduced variability in raw materials imparts better material consistency;
- There are fewer manufacturing steps, thus cost savings are possible;
- Elastomers are finely dispersed in the matrix and therefore improved physical properties and melt uniformity are achieved and
- The viscosity ratio does not restrict the selection as severely as in blends and so a wider range of elastomeric compositions is possible.

The commercial application of the random copolymer is mainly in the packaging industry where its low melting and softening points, as well as improved clarity offer significant benefits. The block copolymer is considered to be both a commodity and an engineering polymer, and is used in the manufacture of items such as kitchenware, car bumpers and electrical appliance casings. The copolymer grades produced by Polifin

are custom made, and to this end different operating variables are introduced in the polymerisation process as well as through different additives packages added in the extruder. Since the production process is continuous, the grades produced show a great deal of property variation between batches. The above statement brings us to the objectives of this study.

1.2 RESEARCH OBJECTIVES

This study was undertaken to:

- Fully characterise the copolymer grades;
- Seek to understand the influence that each of the variables has on the mechanical properties of the copolymers;
- Determine the physical and structural parameters that give the optimum stiffness to toughness ratio;
- Determine the optimum conditions that ensure the production of copolymers with such physical and structural parameters and
- Ultimately, the thesis aims to be a valuable contribution to Polifin in the drive to ensure the production of copolymers with highly reproducible and desirable properties.

1.3 OVERVIEW OF THESIS

This thesis is divided into 6 chapters.

- Chapter 2 gives a *review of the literature* pertaining to the aspects of research in polypropylene with a strong emphasis on poly-(propylene-ethylene) copolymers;
- Chapter 3 gives detailed information about the *experimental techniques* used in this study;
- Chapter 4 is a presentation of the *results* in the form of tables, graphs, SEM and TEM micrographs;
- Chapter 5 is a *discussion* and interpretation of these results and
- Chapter 6 *summarises* the work completed.

CHAPTER 2

LITERATURE REVIEW

2.1 POLYMER STRUCTURE

2.1.1 Molecular Structure

Isotactic polypropylene is a semicrystalline, linear chain macromolecule composed of propylene -(CH (CH_3) CH_2)- repeat units added in a tail-to-head fashion. Depending on the spatial arrangement of the methyl (-CH_3) groups, three stereoisomers of polypropylene are found. In atactic polypropylene the methyl groups are randomly distributed, in syndiotactic polypropylene the methyl groups are situated in an alternating fashion around the chain, while in the isotactic form of polypropylene the methyl groups are all positioned on the same side of the chain (see Figure 2.1).

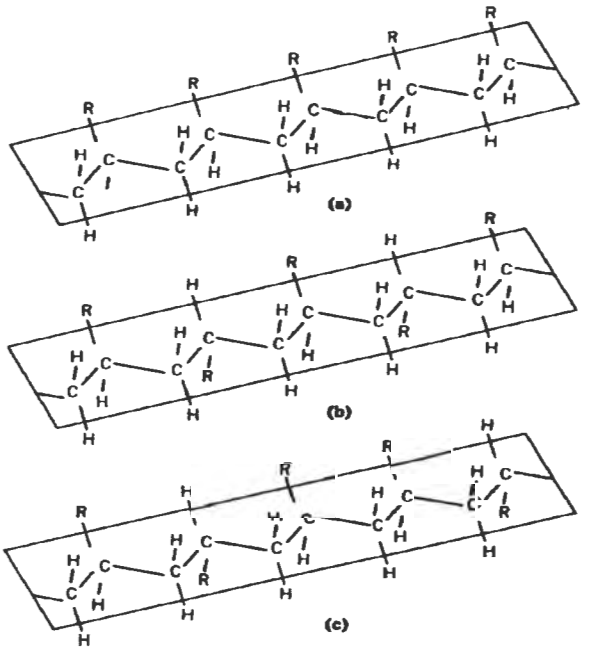

Figure 2.1: Stereoisomers of polypropylene (a) isotactic, (b) syndiotactic and (c) atactic, R = -CH_3 (methyl group), [after ref. 2].

During copolymerisation the propylene molecules combine with ethylene monomer molecules. This introduces irregularity to the polymer chain; hence the copolymers are less crystalline than the homopolymer. The arrangement of the chains can be depicted as shown below[6]:

- **Homopolymer**: This phase is highly crystalline and imparts stiffness to the copolymer. The polymer chains consist of propylene units only.
  P-P-P-P-P-P------P-P-P-P-P-P-P
- **Random copolymer**: This is a tough single-phase polymer with an amorphous structure. The polymer chains consist of propylene units and randomly distributed comonomer units.
  P-P-P-C-P-P-C-P--------P-P-C-P-P-P
- **Block copolymer**: This polymer is bi-phasic and is a composite of the stiff homopolymer phase and the tough ethylene-propylene rubber phase.
  P-P-P-P-E-E-P-P-E-P-P-E-E-P-P-P-E-P-P-P

2.1.2 Crystalline Structure

The building blocks of the polymer structure are the chain macromolecules, lamellae and spherulites. Three monomer units combine to form one full helix rotation. The helices repeatedly fold in a three dimensional fashion to form lamellae, as shown in Figure 2.2[7].

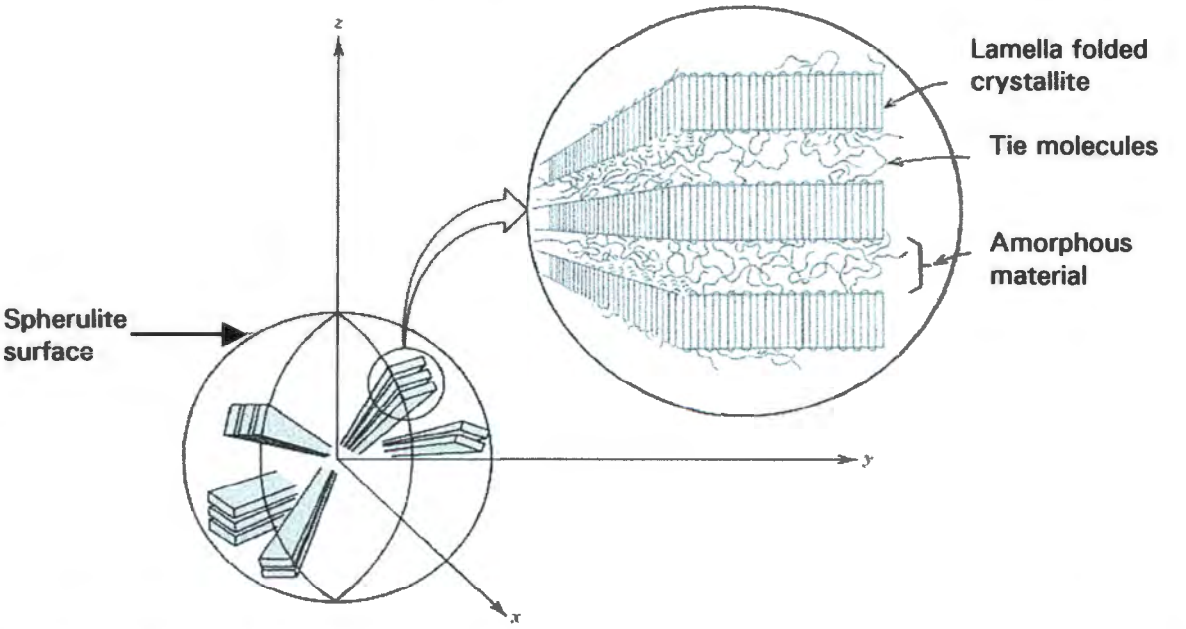

Figure 2.2: A simplified model of isotactic polypropylene lamella crystallites, [after ref. 7].

The size of the lamellae ranges from 10 to 50 nm and is a function of the crystallisation conditions. The direction of growth of the lamellae is perpendicular to the surface of the lamellae crystal. Spherulites are a higher order structure composed of these lamellae, trapping amorphous material as they radiate and grow from a centre of nucleation. When thin films of polypropylene are viewed using polarised optical microscopy, the characteristic Maltese cross patterns are observed, as shown in Figure 2.3[8]. The size of the spherulites can range from a few microns up to about 100 μm.

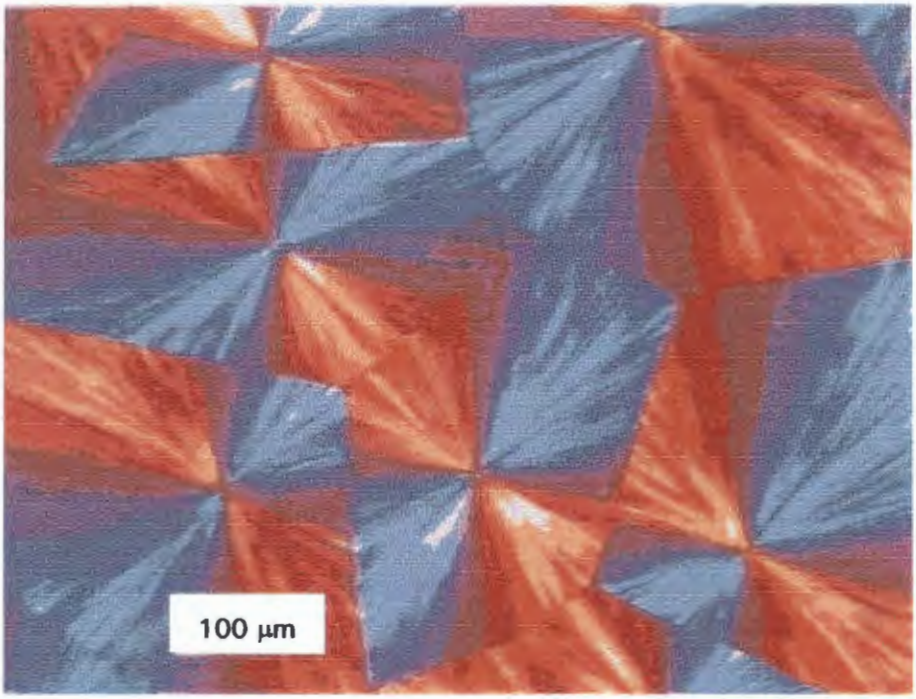

Figure 2.3: The spherulitic structure of isotactic polypropylene, viewed under polarised light, [after ref. 8].

Isotactic polypropylene (i-PP) is known to exist in at least four different crystal structures: the monoclinic (α-) form[9], the hexagonal (β-) form[10], the triclinic (γ-) form[11] and the quenched form[9]. The α form is the most common crystalline form of polypropylene. These different crystal structures arise as a result of the packing geometries of the right handed (*d*) and left handed (*l*) helices that are made to rotate in specific directions by the asymmetry of the substituent groups. The presence of ethylene as the co-monomer disturbs the regular order of the chains and hence diminishes the α peak intensity in an x-ray diffractogram.

Feng *et al*[12] recently studied the effect of ethylene as the co-monomer on the characteristics of the crystal structure. It was found that the proportion of the γ form increased with increasing crystallisation temperature. Increasing the comonomer content results in an increase in γ and a maximum in γ content is reached at an ethylene content of about 15%. For the copolymers studied, a characteristic polyethylene peak at $2\theta = 23.4°$, ascribed to the polyethylene (200) crystallographic plane, was found at elution temperatures between 65 °C and 110 °C. In this elution temperature range, polyethylene chains were long enough to be able to diffract the x-rays.

Conditions that favour the formation of γ crystals in copolymers include isothermal crystallisation close to the melt temperature (T*m*), very slow cooling and crystallisation at elevated pressure. Insertion of the ethylene units into isotactic polypropylene (i-PP) chains makes the crystallisable sequence shorter, resulting in an easy formation of the γ crystals.

According to Karger-Kocsis *et al*[13], in pure i-PP, the β form has a much higher toughness than the α form. This is due to a phase transformation toughening (PTT) that occurs when the β form is mechanically stressed during an impact event. This transformation is from a metastable, less dense β form to a more stable and denser crystalline α form. The β form can be obtained by the use of special nucleating agents. The relative amount of the β form present in the copolymer is usually described in terms of the K value, defined as[14,15]:

$$K = H(300)_\beta / [H(300)_\beta + H(110)_\alpha + H(040)_\alpha + H(130)_\alpha \quad (2.1)$$

where,
$H(110)_\alpha$, $H(040)_\alpha$ and $H(130)_\alpha$ are the heights of three strong α form peaks (110), (040) and (130), and H (300) is the height of the strong single β form peak.

2.2 MECHANICAL PROPERTIES

2.2.1 Introduction

The mechanical properties that need to be optimised in copolymers are impact strength and stiffness. This task is made challenging by the inverse relationship between the two, as shown in Figure 2.4[16]. The two properties are always affected in opposite ways by variables such as the molecular weight, the morphology, the crystallinity and the glass transition temperature. The effect of some of the above factors is difficult to realise as some are inter-linked and are more or less dependent on the ethylene content.

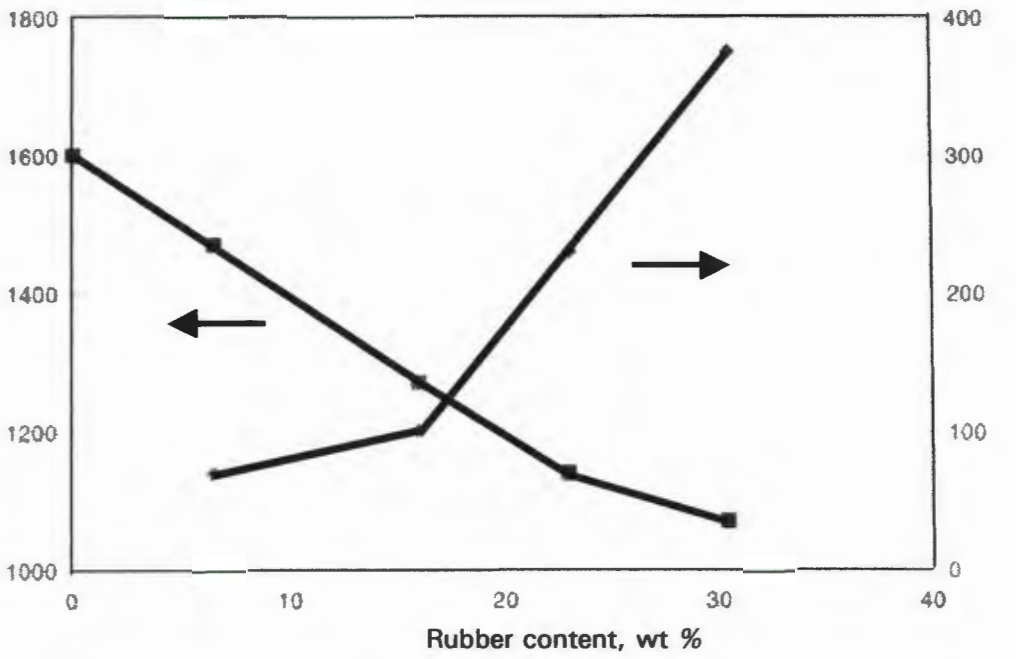

Figure 2.4: Relationship between stiffness and impact strength as a function of the rubber content, [after ref. 16].

When considering the physical or mechanical properties of the copolymers, it should be borne in mind that the processing or rheological variables also play an interconnected role with these outcomes as shown in the schematic below in Figure 2.5[17]. An item such as the microstructure in the figure below is controlled through the molecular parameters such as molecular weight (or MFI), the molecular weight

distribution (MWD), the comonomer distribution (CD), the sequence distribution (SD), the tacticity distribution (TD) and the amount and type of branching. The molecular structure, in turn, affects the viscosity or melt elasticity, which is also affected by the temperature or flow rate in an extruder, for example. Finally, the mechanical properties are affected by the crystallisation conditions after processing.

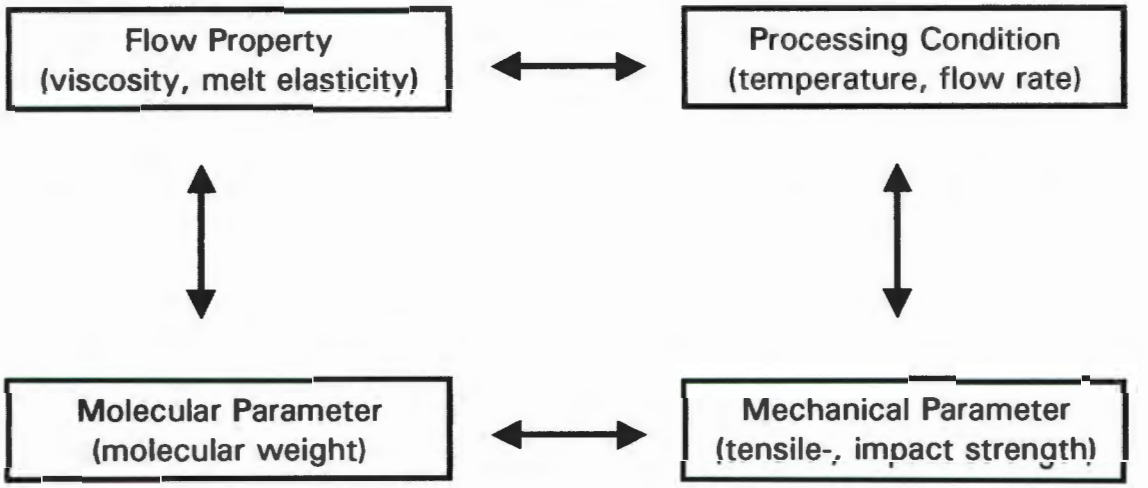

Figure 2.5: **Interrelationship between processing variables, molecular parameters, flow and mechanical properties, [after ref. 17].**

2.2.2 Impact Strength

The Izod impact strength is measured by releasing a pendulum hammer of known mass at a given height to strike a notched or unnotched impact test specimen clamped at the lowest point in its swing. Some of the energy from the pendulum is absorbed by the test specimen and, as a result the upward swing of the pendulum, is retarded. The amplitude to which the pendulum ultimately rises is recorded and converted to energy per unit cross sectional area or per unit thickness of the test piece.

The impact strength of the polymer at the test temperature employed is dependent on its glass transition temperature (T*g*). Certain parameters affect the T*g* of a polymer. According to Eisenberg[18] these can be grouped into two categories, *viz.* molecular parameters such as chain stiffness and intermolecular forces, and controllable parameters such as

glass transition temperature, pressure, plasticizers, molecular weight, monomers, cross-linking, crystallinity, tacticity and % elongation. For polypropylene copolymers, impact strength enhancement depends on:

- The amount of EPR;
- The EPR particle size and distribution;
- The T*g* of the EPR and
- The adhesion between the EPR and the matrix.

The effect of the presence of EPR as the dispersed phase is evident when the impact strength values of the random and block copolymers are compared, as shown in Table 2.1[19]. The random copolymer has a single-phase structure whereas the block copolymer has the EPR as the dispersed phase in a bi-phasic structure.

POLYMER TYPE	*IMPACT STRENGTH (kJ/m²)*
Isotactic polypropylene	82
Random copolymer	190
Block copolymer	385

Table 2.1: **Typical impact strength values of the different polypropylene types, [after ref. 19].**

According to Dwyer *et al*[5] an optimum toughness in PP/EPR systems is achieved at a particle size of about 0.4 μm. The ratio of the ethylene (C_2) and the propylene (C_3) in the EPR is very important. Increasing the amount of C_2 lowers the T*g*. As the % C_2 is increased, polyethylene crystallinity develops and the impact strength reaches a maximum at a certain level of C_2. The optimum concentration of ethylene for a maximum in impact strength is around 50 to 60 mole percent C_2. A much higher % C_2 lowers the adhesion between the rubber phase and the matrix due to a decreased compatibility between these two phases.

For homopolymer polypropylene, the xylene solubles and R21 ratio are used to describe the stereo-regularity of the polymer. The xylene solubles test dissolves atactic polypropylene. The R21 ratio represents the magnetisation of free induction decay at two different relaxation times.

For polypropylene copolymers, the R21 ratio is directly correlated with the rubber content and also includes a contribution from the atactic polypropylene. The impact strength is also dependent on the length of the ethylene sequences in the rubber particle. The relative length of ethylene to propylene sequences is defined as the Long/Short (L/S) ratio, where typically more than five ethylene monomers would be considered to be a long sequence. If the rubber particle is relatively rich in ethylene then the L/S ratio is high and the impact strength is low. On the other hand, if the L/S ratio is low, the impact strength will also be negatively affected. Ideally, the L/S ratio should be between 0.4 and 0.7 for impact copolymers.

There is a tendency for impact strength, expressed as energy per unit thickness (J/m), to lie in one of two areas. The specimens either fail in a high fracture energy area of around 600 J/m exhibiting ductile failure, or in a low fracture energy area of around 30 J/m exhibiting brittle failure. An intermediate transition region between these two zones shows a high scatter in impact energy[16]. In copolymers it is believed that the toughening occurs through a number of mechanisms. According to Kim *et al*[20] toughening occurs in three stages:

- The particles act as stress concentrators;
- Void formation occurs mainly at the interface of the EPR inclusions and
- Further increases in strain ultimately result in the interaction of the voids and shear yielding of the matrix finally occurs.

According to Del Duca *et al*[16] the toughening in impact copolymers is mainly due to the generation of many small crazes and the interruption of a propagating crack in the matrix. The toughening occurs when rubber particles of a proper size (of say 0.4 μm) initiate many subcritical crazes that absorb significant energy during the stressing of the polymer and also act to interrupt the crazes before they become critical. The above mechanism operates above the glass transition temperature of the dispersed phase.

The toughness of the copolymer is dependent on the particle size (D), the interparticle distance, *i.e.* the centre-to-centre distance between rubber particles (CCD) and the ratio of the interparticle distance to particle size (CCD/D). The smaller the CCD/D ratio, the tougher the copolymer. The interparticle distance CCD, is related to the volume fraction of rubber V_f, the % C_2 and the particle size D, by the formula[21]:

$$CCD = D\,[(\pi/6V_f)^{1/3} - 1] \qquad (2.2)$$

A reduction of CCD can be achieved by either reducing D or by increasing V_f. Increasing the % C_2 is not always beneficial. Although there might be an increase in toughness, the stiffness can be drastically reduced. A reduction of D can be achieved by manipulating the variables in the formula used to determine the Capillary Number (C*a*):

$$Ca = \eta_m \dot{\gamma} R/\sigma \qquad (2.3)$$

where,

- η_m - is the matrix viscosity;
- $\dot{\gamma}$ - is the shear rate applied to the matrix;
- R - is the radius of the rubber particle (R = 0.5 D) and
- σ - is the interfacial tension between the rubber particles and the matrix

C*a* should be kept below a critical minimum, Ca_{cr}. Since R = 0.5 D, at a constant value of C*a*, an increase in η_m or $\dot{\gamma}$ will decrease D. By making the homopolymer chains longer, η_m is increased but chain length is a variable in grades of different MFI's. Although chain length is a variable, there are limitations as a result of the viscosity ratio between the dispersed phase and the matrix, as it controls the resultant particle size. During extrusion, $\dot{\gamma}$ can be increased but there is a limit to the shear rate of the extruder. Lessening the ethylene content in the rubber phase can lower the interfacial tension but this is not a viable solution as there is a need to lower the crystallinity in the matrix in order to increase toughness and this requires a minimum in the amount of ethylene in the rubber.

In a study conducted by Marcus *et al*[22] on the effect of molecular parameters on mechanical properties of a 23_ _ and a 25_ _ series

copolymers, the following observations from Figure 2.5 can be made concerning impact strength:

- Molecular weight has a greater influence on impact strength than ethylene content, at low MFI;
- For both series, the impact strength decreases exponentially with increasing MFI;
- An increase in ethylene content increases impact strength between grades;
- At very high MFI, the impact strength is independent of ethylene content;
- The nucleated grades show an increased impact strength at low MFI but the effect diminishes at high MFI and
- An increase in modulus is associated with a decrease in impact strength.

It was also noted that there is more scatter in impact strength for low MFI grades, hence quoting average values may be unrealistic. The low MFI grades are mainly the non-visbroken copolymers (see Section 2.2.4) and as such the broad molecular weight distribution might have a significant effect on the impact properties.

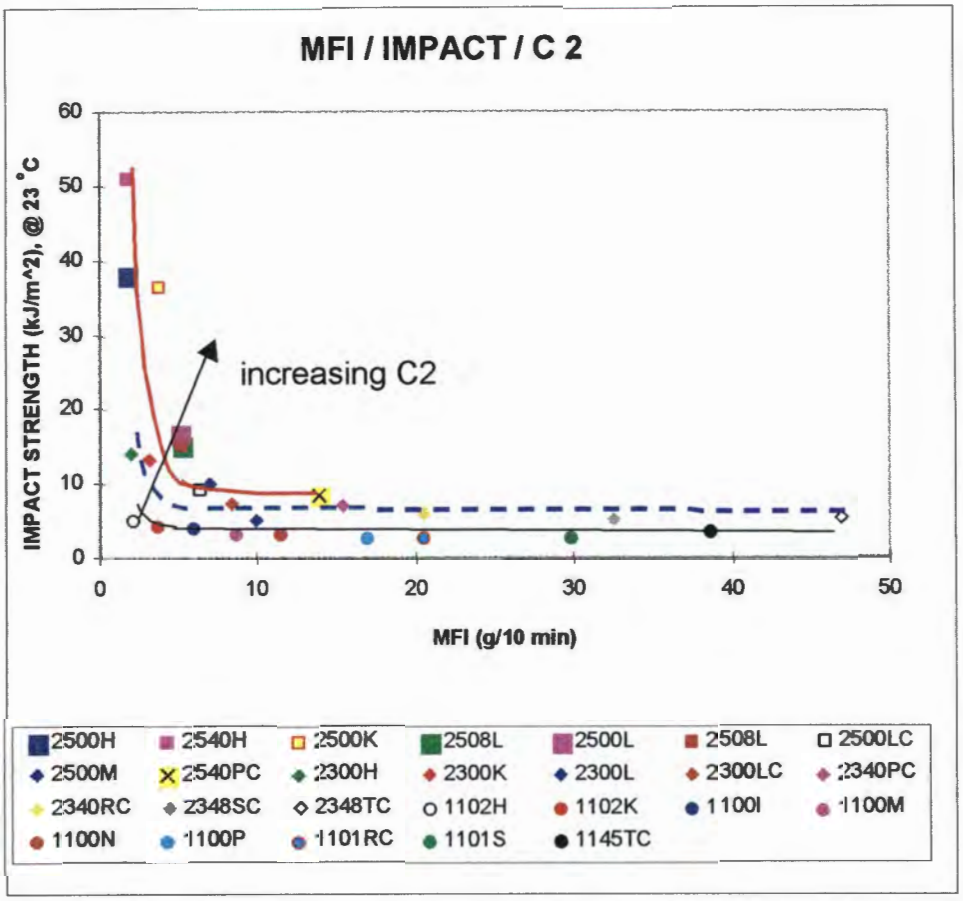

Figure 2.5: Notched Izod impact strength as a function of MFI and ethylene content for various copolymer grades, [after ref. 22].

2.2.3 Flexural Modulus

Modulus or stiffness involves the stretching of covalent atomic bonds and the energy barrier associated to rotations about these bonds. Small strain properties such as the flexural modulus, are dependent on the % crystallinity, hence any factors that will increase the crystallinity of the matrix, will also increase the modulus of the composite. Marcus *et al*[22] showed that:

- An increase in average ethylene content (*i.e.* from one series to the other) resulted in a decrease in modulus;
- The addition of nucleating agents increased the modulus and
- There was a small negative correlation between modulus and MFI.

The study also noted that there was no strong correlation between impact strength and modulus. The above observations are summarised in Figure 2.6.

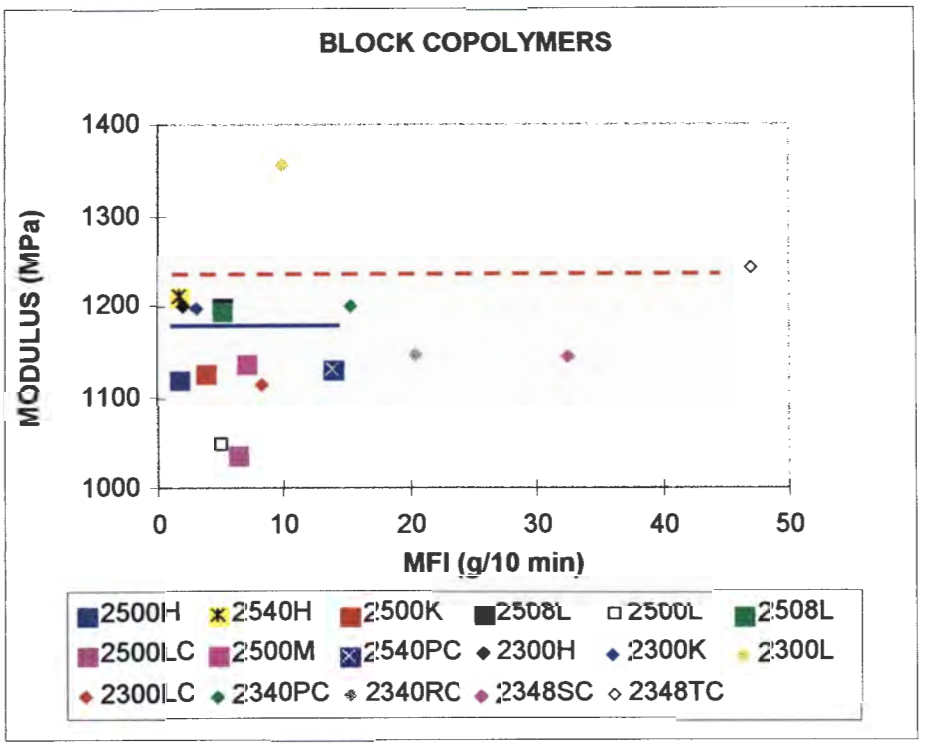

Figure 2.6: Flexural modulus as a function of MFI and ethylene content for various copolymer grades, [after ref. 22].

2.2.4 Effect of Molecular Weight and Molecular Weight Distribution on Mechanical Properties

The statistical nature of the polymerisation process results in a distribution of molecular sizes, which in turn depend on reactants' residence time and the concentration of the chain transfer agent (hydrogen). The molecular weight distribution (MWD) is mainly due to the fact that the Ziegler-Natta catalyst system used in the polymerisation process has multiple reaction sites that differ in their activity. The molar mass can be expressed as any one of the three arithmetic averages[23]. Gel permeation chromatography (GPC) can be used to determine the three molecular parameters[24]. In these expressions n_i is the number of molecules of species i in the sample and M_i is the molar mass of the molecular species, i. The number-, mass-

and z-average molar masses are defined as follows, using a summation from $i = 1$ to n:

- $\overline{M}n$ - $\Sigma n_i M_i / \Sigma n_i$;
- $\overline{M}w$ - $\Sigma n_i M_i^2 / \Sigma n_i M_i$ and
- $\overline{M}z$ - $\Sigma n_i M_i^3 / \Sigma n_i M_i^2$.

In poly-(propylene-ethylene) block copolymers, the molecular weight distribution (MWD) is a very important molecular parameter and is expressed as the ratio of $\overline{M}w/\overline{M}n$. Depending on the catalyst system used, the MWD is either narrow when using the third generation Z-N catalyst system, or wider with the second generation Z-N catalyst system. A narrow MWD at constant MFI would result in a higher impact strength for polypropylene[17].

Besides the catalyst system used, the MWD can also be controlled through a process known as vis-breaking. This is achieved by reacting the polymer powder with peroxide in an extruder[24,25]. The peroxide promotes extrusion degradation of the starting polymer resin. The final resins are known as controlled rheology (CR) grades. The controlled rheology grades consist of shorter chains having a more uniform length and thus narrower molecular weight distribution. Longer chains are broken down more easily as there is a higher probability of the peroxide attacking the longer chain molecules. This lowering in molecular weight results in an increase in the melt flow index (MFI) and a narrowing in MWD, which promotes improved processability in the polymer. The MFI and MWD affect the impact strength in opposite ways. An increase in MFI lowers impact strength whilst a reduction in MWD (at constant MFI) increases the impact strength. According to Becker *et al*[25] the amount of peroxide needed depends on:

- The MFI of the starting resin;
- The desired MFI of the final resin and
- The antioxidant system used in the formulation.

Narrow MWD grades generally show superior processing characteristics in high speed melt spinning of very thin fibres, high-speed extrusion of thin films and injection moulding of thin-walled articles. Controlled rheology gives grades with higher gloss, enhanced transparency, higher flowability, higher toughness at comparable flowability, less warpage, less shrinkage and shorter cycle times. All the above are gained at the expense of lowering the stiffness and the melt strength[26].

For long-chain polymers, many mechanical properties can be improved by an increase in molecular weight. This effect reaches a limiting value at a relatively high molecular weight after which no appreciable change in the property is apparent. Eventually, at very high molecular weight, the melt viscosity becomes so high that the polymers cannot be dissolved, worked mechanically or be made to flow in the molten state. The stress-strain properties of an amorphous polymer depend on chain entanglements, and thus the molecular weight. In semicrystalline polymers, like polypropylene, this influence is not as apparent, due to the presence of crystallites, which also contribute to the strength.

2.2.5 Effect of Morphology on Mechanical Properties

The morphology of the copolymers determines the balance between the stiffness and the impact strength. The scanning electron microscope (SEM) and the transmission electron microscope (TEM) can be used to study the morphology of the copolymers. The TEM is used to study the finer details of the structure of the copolymer, especially the rubber phase and the interfacial properties between the phases.

The similarity in electron density between polypropylene (PP) and polyethylene (PE) makes it impossible to get good contrast between the matrix and the dispersed rubbery phase. In order to enhance the contrast, the copolymers are stained with various staining solutions. Some of the work done on the staining procedures can be found in papers by Sano *et al*[27] and Reimschuessel *et al*[28]. The use of osmium tetroxide (OsO_4) as a staining agent is well documented for ethylene-containing systems, but it

has been shown to work best for systems containing an unsaturated bond[27,29]. According to Khandpur *et al*[30] staining with ruthenium tetroxide (RuO_4) seems to be ideal for staining saturated polymer systems such as poly-(propylene-ethylene) copolymers. The preparation of the RuO_4 can be done in two ways, either by the oxidation of hydrated ruthenium dioxide using sodium periodate,

$$2\ NaIO_4\ (4g) + RuO_2\ (0.6g) \xrightarrow[H_2O]{0°C} RuO_4 + 2\ NaIO_3$$

or by the oxidation of ruthenium trichloride with sodium hypochlorite,

$$2\ RuCl_3.3H_2O + 8\ NaOCl \xrightarrow{H_2O} 2\ RuO_4 + 8\ NaCl + 3\ Cl_2 + 3\ H_2O$$
$$(0.1g) \qquad (5\ ml\ 13\ \%\ aq.)$$

According to Sano *et al*[27] the RuO_4 crosslinks the polymer system and this has been confirmed by various structural investigation techniques. The staining with RuO_4 is sometimes preceded by treatment with chlorosulphonic acid ($ClSO_3H$). According to Bassett[31] the sulphur and the chlorine molecules crosslink the ethylene. The staining effect comes from the conversion of RuO_4 to RuO_2, which gives colour to the sample. The sample becomes harder by crosslinking through the formation of carboxylate linkages. The increased hardness also makes sectioning easier. The staining effect in PP is much less than in PE due to the limited amount of carbonyl groups in the former[27].

Typical results of TEM studies, as shown in Figure 2.7, show a matrix of semi-crystalline polypropylene containing lamellae, an amorphous region within the rubber particles and inclusions of semi-crystalline polyethylene[20].

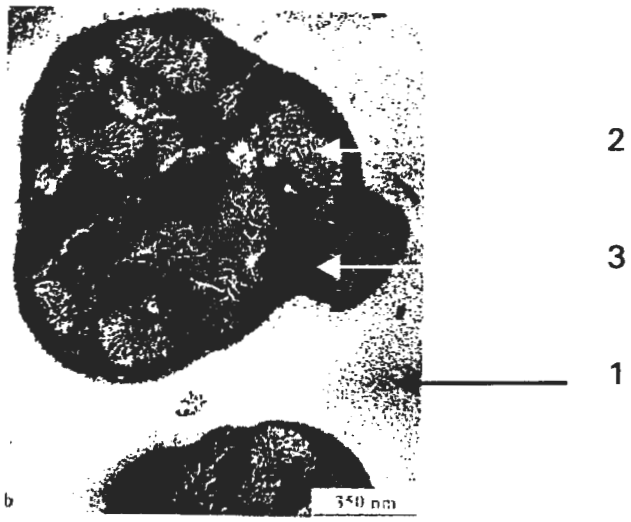

Figure 2.7: Typical structure of a polypropylene-ethylene block copolymer, 1 – semi-crystalline polypropylene matrix, 2 – semi-crystalline ethylene within the rubber particle, 3 – amorphous rubber phase, [after ref. 20].

The ethylene-propylene rubber (EPR) composition is significantly different to that of the PP homopolymer and is usually immiscible in the homopolymer phase even in the melt, thus the final rubber morphology is strongly affected by the shear and deformation during melt processing operations[32].

The effect of injection temperature on the copolymer microstructure is shown in Figure 2.8(a) and Figure 2.8(b). In Figure 2.8(a), the EPR is well dispersed and of an almost uniform size. Raising the injection temperature results in the EPR particles coalescing and causing the average particle diameter to increase, as shown in Figure 2.8(b).

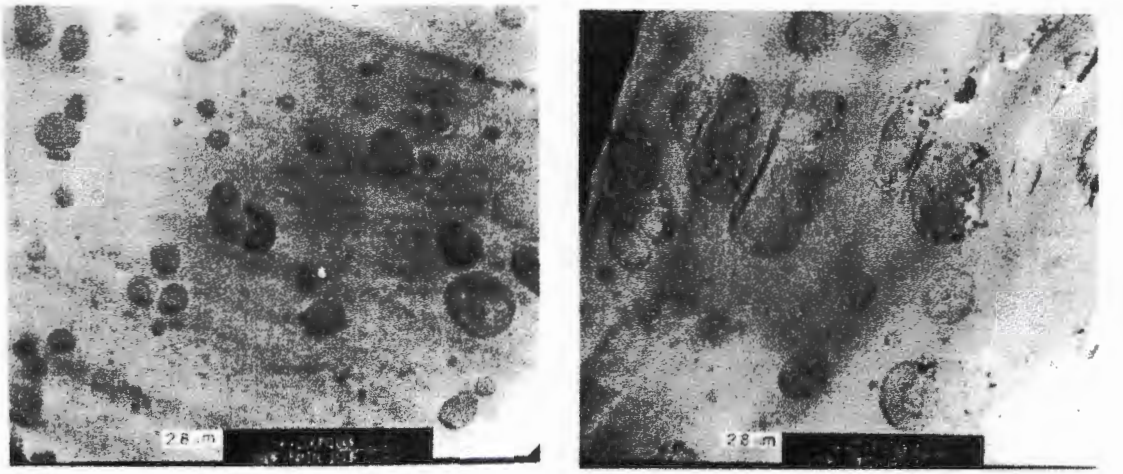

(a) (b)

Figure 2.8: Effect of injection moulding temperature on the copolymer microstructure at, (a) 193 °C and (b) 215 °C, [after ref. 32].

The viscosity ratio ($\eta_{dispersed}/\eta_{matrix}$) is the ratio in viscosity between the dispersed phase and the matrix. Changing the viscosity ratio results in a change in morphology as shown in Figure 2.9(a) and Figure 2.9(b). A low viscosity ratio gives rubber particles of even distribution and small size, (see Figure 2.9(a)). Increasing the viscosity ratio gives large particles of an uneven distribution, (see Figure 2.9(b)). The matrix cannot transfer enough shear to the rubber particles to break them up during processing.

The SEM is mainly used for quantitative analysis and fracture surface studies. It is necessary to first cryogenically fracture injection-moulded specimens to reveal the rubber particles on the exposed surface. A quantitative analysis of the rubber particles in such specimens is made difficult by the poor contrast and the incomplete exposure of some of the rubber particles. Etching of the polymer samples alleviates this situation. A number of etching techniques are in use but the use of *n*-heptane at 70 °C for 30 minutes seems to work well for the poly-(propylene-ethylene) copolymers[19]. The rubber particle size and spatial distribution can then be measured using various image analysis software packages.

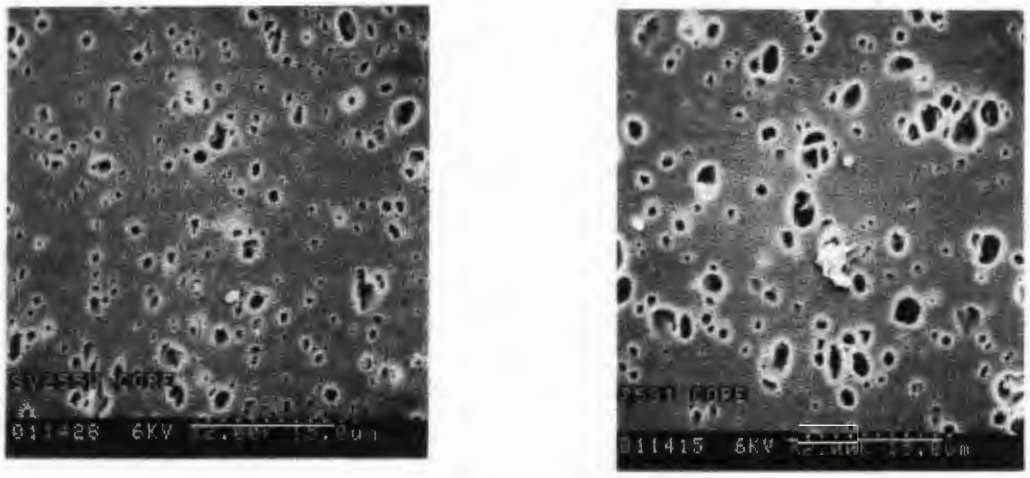

(a) (b)

Figure 2.9: The effect of the viscosity ratio on the morphology of polypropylene copolymers at a, (a) low ratio and (b) high ratio, [after ref. 32].

2.2.6 Effect of % Crystallinity on Mechanical Properties

Crystallinity is a function of the crystallisation temperature. The higher the crystallisation temperature (below T*m*), the higher the crystallinity. The molecular weight ($\overline{M}w$), stereo-regularity of the chain and the size of the substituent groups around the chain limit the degree of crystallinity. The degree of crystallinity is relatively high for the lower molecular weight polymers. An increase in $\overline{M}w$ lowers the degree of crystallinity until a limiting value of about 25 to 30 % is reached[33].

The effect of stereo-regularity can be seen when comparing atactic and isotactic polypropylene. Atactic polypropylene is amorphous whereas isotactic polypropylene is semi-crystalline[34]. If the substituent groups around the chain are big, the chains cannot pack closer and therefore crystallinity is reduced. Crystallinity plays an important role in most polymer properties, especially those influenced by small strain properties. For the copolymers to have high impact strength, the EPR should be amorphous and the matrix should be crystalline to give the rigidity required. Some crystallinity within the EPR is also required as this helps to lower stresses within the matrix and also influences the shrinkage of

the rubber phase. Stress whitening is also lowered by crystallisation of ethylene within the rubber particle[8].

2.2.7 Effect of the Glass Transition Temperature, Tg, on Mechanical Properties

The glass transition temperature (T*g*) is the discontinuity in the rate of change of volume with respect to temperature in volume *vs.* temperature plots[18]. The glass transition temperature can also be defined as the temperature at which the polymer properties change from a glassy to a rubbery nature with increasing temperature, as shown in Figure 2.10[7]. At the T*g* there is enough volume for the side chains or groups to start rotating around the backbone carbon chain. The chain rotation at the T*g* and above gives a mechanism for impact energy absorption by the copolymers. Isotactic polypropylene is brittle at low temperatures because its glass transition temperature of about -10 °C is relatively high.

The Dynamic Mechanical Thermal Analyser (DMTA) can be used to measure the viscoelastic behaviour of polymers, *i.e.* the ability to recover elastically and to flow when stressed[35]. The two properties can be expressed as storage modulus, E′, and loss modulus, E″. The storage modulus quantifies the material's ability to store energy whereas the loss modulus quantifies the material's ability to dissipate energy by viscous flow. E′ is measured by quantifying that part of the material's resistance to deformation that is in phase with the applied stress, while E″ is the quantification of the part that is out of phase. The ratio of the loss modulus and the storage modulus is expressed as tan delta, *i.e.* E″/E′ = tan δ. The EPR in impact copolymers provides a means by which energy can be dissipated.

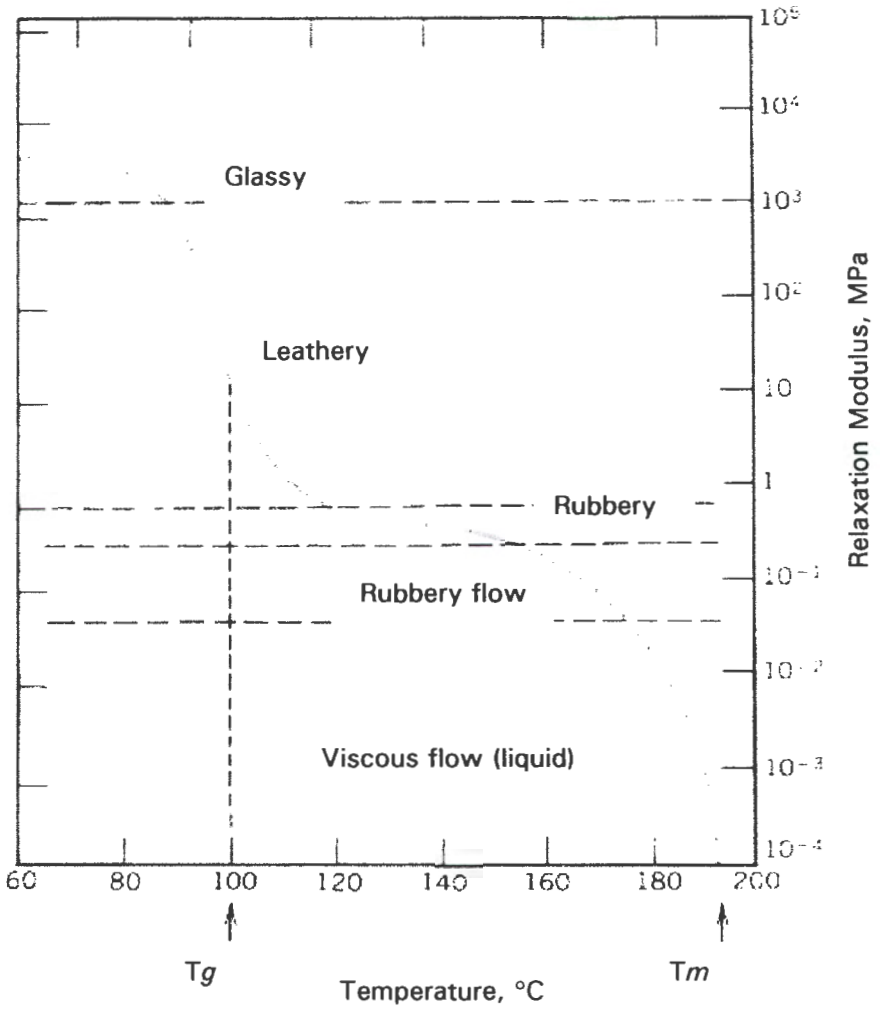

Figure 2.10: A plot showing the thermal events occurring in a semi-crystalline polymer as a function of temperature, [after ref. 7].

Bi-phasic copolymers show two glass transition temperatures, one for the isotactic polypropylene phase and the second one for the EPR phase. The bigger the difference between the two, the more immiscible the components are. When the difference is smaller, there is a stronger interaction between the polymer chains of the individual phases and this results in good cohesion between the two phases and therefore better impact properties, as shown in Table 2.2[36].

ITEM	*COPOLYMER B*	*COPOLYMER J*
T*g* PP (°C)	26	17
T*g* EPR (°C)	-46	-33
Impact Strength (kJ/m^2) at 25°C	52	116
Impact Strength (kJ/m^2) at -20°C	35	52

Table 2.2: The effect of differences in T*g* on impact properties for two copolymers, [after ref. 36].

Melt crystallised i-PP exhibits three relaxation peaks in the -150 to 150 °C temperature range (see Figure 2.11(a)). The α peak is due to molecular relaxations in the crystalline phase, the β peak is due to the transition from the glassy to the rubbery state and the γ peak is assigned to the local mode of relaxation in the amorphous phase.

Copolymerisation with ethylene makes it possible for relaxations to occur below the T*g*. Dynamic Mechanical Thermal Analysis (DMTA) was used by Feng *et al*[19] on polypropylene copolymers to study their relaxation behaviour as a function of temperature. In Figure 2.11(b), the β peak splits into a doublet designated as β_1 and β_2, with β_2 occurring at a lower temperature of about -50 °C, which is attributed to molecular relaxations within the rubber phase (EPR). These relaxations in the EPR phase give high impact strength at low temperatures in the block copolymers.

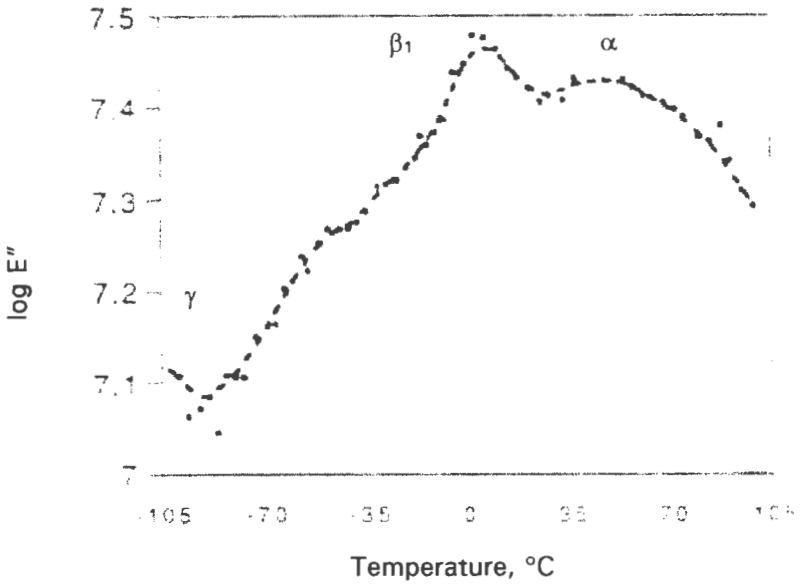

(a)

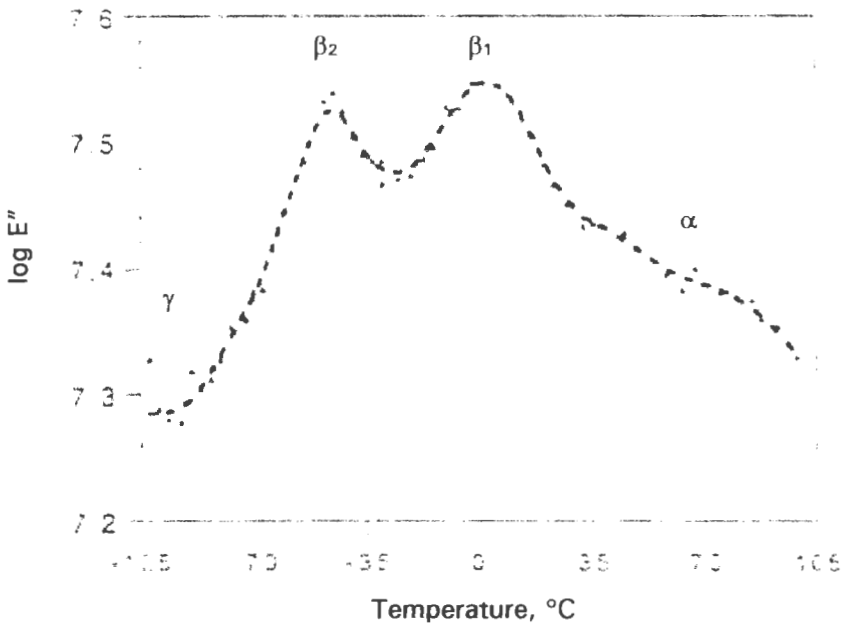

(b)

Figure 2.11: DMTA curves for (a) the PP homopolymer and (b) the PP block copolymer, [after ref. 19].

CHAPTER 3

MATERIALS AND EXPERIMENTAL TECHNIQUES

3.1 INTRODUCTION

This chapter gives a detailed description of the copolymers investigated and the techniques employed to measure the physical, mechanical, thermal and thermo-mechanical properties and also to elucidate the microstructural features of the copolymers.

3.1.1 Materials Tested

The polymeric materials investigated in this study were nine grades of bi-phasic poly-(propylene-ethylene) impact copolymers as classified in Table 3.1. The grades were obtained from the supplier Polifin Ltd. South Africa and, as indicated in Table 3.1, two of the grades included for a comparative study, were obtained from Targor in Germany. The copolymers cover an ethylene content range of between 6 and 23 % and an MFI range of between 0.8 and 46 g/10 minutes. The MFI is a measure of the flow rate in g/10 minutes of polymer flowing through a die at a given temperature and dead weight on a piston. For polypropylene the test conditions are 230 °C and a load of 2.16 kg (ISO 1133).

The other variables amongst the grades are the presence or absence of nucleating agents, the molecular weight distribution (MWD) and the additive package. Some of the physical and mechanical properties of these materials as supplied by the producer appear in Appendix A. The copolymer grades are differentiated from one another by codes as

explained in Table 3.2. As an example, the grade 2340 PC is a controlled rheology, medium impact copolymer containing a nucleating agent.

Grade Code	*Ethylene Content (wt %)*	*Melt Flow Index (g/10 min)*
2340 PC	6.17	15.67
2349 MC	7.71	8.33
2448 TC	9.53	46.11
2540 H	11.75	1.67
2600 PC*	11.76	17.2
2602 E	12.7	0.85
2648 PC	11.76	15.57
2648 RC	11.65	22.67
2900 H*	22.35	1.84

Table 3.1: Experimental matrix showing the range of copolymers used. *The 2600 PC and 2900 H material were supplied by Targor in Germany.

Code Digit or Letter	*Explanation*
First Digit	An indication of the type of polymer
1	Homopolymer
2	Block copolymer
3	Random copolymer
Second Digit	An indication of the ethylene content or impact strength
Third Digit	An indication of the additive package
0	General additive package
4	Nucleating agent additive package
Fourth Digit	Interdepartmental code and additives
First Letter	Target Melt Flow Index, (MFI)
H	1.8
M	8.0
P/PC	15
R/RC	22
TC	45
Second Letter, C	Controlled rheology grade or narrow MWD

Table 3.2: Explanation of the terminology and codes used to identify the copolymers.

3.1.2 Production of Copolymers

The technology used to make the copolymers is the BASF Gas-Phase Process[37] (see Figure 3.1). The stages of the production process are illustrated below:

3.1.2.1 Polymerisation

The copolymers are polymerised in a continuous process in two vertically stirred reactors in series as shown in Figure 3.1. Liquid propylene is fed through the bottom of the first reactor. Hydrogen is added to control the molecular weight of the resulting polymer. The product produced in the first reactor is the homopolymer polypropylene that forms the matrix of the copolymer. Polymerisation is done at temperatures of between 50 and 90 °C and the pressure is between 10 and 40 bar. The catalyst system used is the BASF's PTK 4W, which is capable of producing polymers with a narrow molecular weight distribution.

Copolymerisation takes place in the second reactor. The feedstock consists of the powder homopolymer from the first reactor, ethylene and propylene. The ethylene and the propylene react to form the ethylene-propylene rubber, which forms the dispersed phase and is incorporated in the polypropylene homopolymer matrix. Chain-to-chain linkage is achieved between the dispersed phase and the matrix.

The reaction is exothermic and cooling is achieved by cooling the gas taken from the space above the polymer powder bed. This cooling is very critical as temperature affects the MFI of the polymer produced. The MFI ratio of the polymer powder between the first reactor and the second reactor has to fall within a specified range in order to produce grades of a given final MFI and impact strength to stiffness ratio.

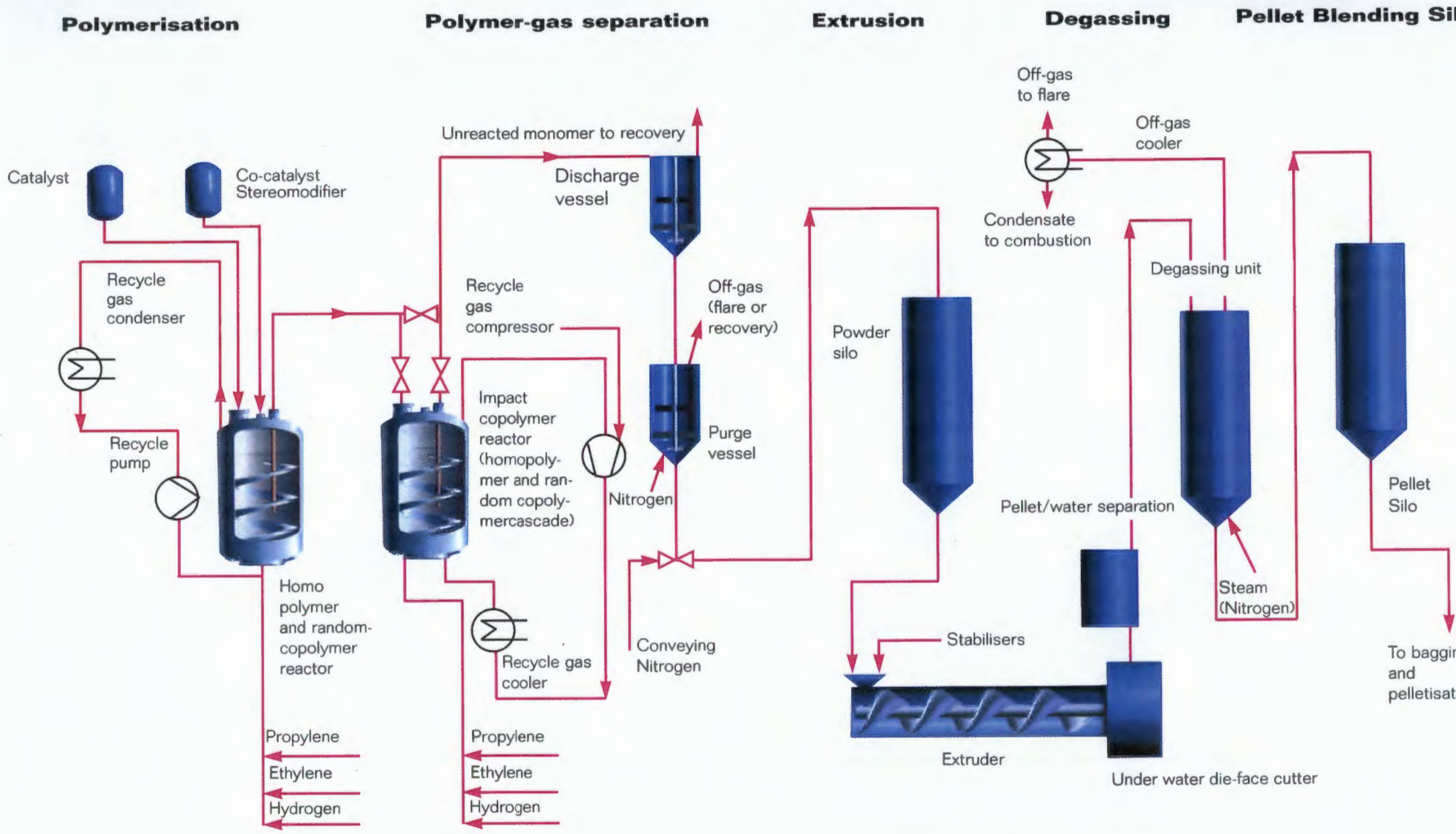

Figure 3.1: A schematic of The BASF Gas-Phase polypropylene production process, [after ref. 37].

3.1.2.2 Polymer-Gas Separation

The polymer mixture of powder and monomers is transferred to discharge vessels *via* dip legs such that the polymer powder bed level is maintained at a constant height. The polymer powder and carrier gas are separated in the discharge vessels. The polymer powder is then stripped of residual propylene by flushing it with nitrogen gas in a stirred purge vessel. The powder then gets sent to the powder silos.

3.1.2.2 Extrusion

The powder from the powder silos is converted into pellets in a twin-screw extruder where stabilisers and other additives are added through the throat of the extruder. The vis-breaking process also takes place in the extruder using peroxides in order to manufacture controlled rheology grades. Underwater die-face cutters then pelletise the material.

3.1.2.3 Degassing

The pellets are transferred to a degassing unit to remove volatiles and odours in order to meet the stringent quality demands for the food and health packaging industries.

3.1.2.4 Blending Silos

The degassed pellets are then conveyed to blending silos that serve both to ensure homogeneity in the product and as temporary storage before bagging.

3.1.3 Sample Preparation

The samples tested were injection-moulded on a 150 ton Engel Injection Moulder-DTE26 at the Polifin Polypropylene Plant. International Standards Organisation (ISO) standard tensile and impact specimens were moulded under standard operating conditions. Specimens were moulded using an injection speed of 50 mm/s and at an injection pressure of 50 bar. An operating temperature of 230 °C was used along the length of the screw barrel. The mould temperature was kept constant at 30 °C, while the cooling time was set for 10 seconds. Prior to testing, the specimens were left for at least 48 hours in the testing room and at least 5 tests were carried out on each batch of polymer.

3.2 PHYSICAL CHARACTERISATION

3.2.1 Differential Scanning Calorimetry (DSC)

Differential Scanning Calorimetry (DSC) was performed on a Perkin-Elmer DSC 2 in the analytical laboratory of Polifin PP Division. In order to determine the percentage crystallinity, an average of the heat of fusion (ΔH_f) of the copolymers was obtained using the known heat of fusion of a 100 % crystalline isotactic polypropylene (ΔH_f *i-PP) which is assumed to be 209 J/g[38]. The percentage crystallinity of the copolymers can be calculated from the equation:

$$\% \text{ crystallinity} = \frac{\Delta H_f \text{ copolymer}}{\Delta H_f \text{ *i-PP}} \times 100 \qquad (3.1)$$

$$= \frac{\Delta H_f \text{ copolymer}}{209 \text{ J/g}} \times 100$$

3.2.2 X-Ray Diffraction (XRD)

X-ray diffraction (XRD) scans for the injection-moulded copolymer specimens were acquired on a Bruker XAS machine at the National Accelerator Centre (NAC) at Faure in Cape Town. The specimens were mounted on a cold setting polymer resin for easy polishing of the surface, prior to taking the XRD scans. A blank (resin only) run was made to determine the contribution of the resin to the peaks. There were no peaks that could be attributed to the resin only. The software supplied with the machine then automatically subtracted the amorphous contribution of the resin from the samples.

The 2θ range covered was from 5 to 50° with the sample holder rotating at 30 rpm. A step size of 0.1° was used and the duration of each step was 2 seconds. The scans were taken at room temperature. The width, β, of a rectangle with the same area and height as the peak, was used to calculate the average crystallite size using the equation from Hay *et al*[39]:

$$E = \lambda/(B\cos\theta) \qquad (3.2)$$

where,

- E is the average crystallite size;
- λ is the wavelength of the incident x-ray beam at 1.54 Angström;
- B is the width of a rectangle with the same area and height as the peak in radians and
- θ is half the angle at which the peak maximum is taken (in radians).

The crystallinity, Xc, of the copolymers was determined from the XRD traces by measuring the area under the crystalline peaks and the amorphous background, using[12,39]:

$$Xc = Ac / [Ac + Aa] \qquad (3.3)$$

where,
Ac is the area under the crystalline peak and Aa is the area of the amorphous background.

The relative amount of the hexagonal β form, K, was determined from the XRD traces in grades in which the $(300)_\beta$ crystallographic plane was present using[14,15]:

$$K = H(300)_\beta / [H(300)_\beta + H(110)_\alpha + H(040)_\alpha + H(130)_\alpha \qquad (3.4)$$

where,
$H(110)_\alpha$, $H(040)_\alpha$ and $H(130)_\alpha$ are the heights of three strong α form peaks (110), (040) and (130), and H (300) is the height of the strong single β form peak.

3.3 MECHANICAL CHARACTERISATION

3.3.1 Hardness Testing

The Vickers micro-hardness (HV), of the specimens was measured on a Matsuzawa MXT-α7 Digital Micro-Hardness Tester using a 25-gf load over a loading period of 10 seconds. The Vickers micro-hardness was calculated from the formula:

$$HV = \text{load / area} = 1.854\ W/\ d^2 \qquad (3.5)$$

where,
W is the load in kgf and d is the diagonal indent in mm.

3.3.2 Impact Testing

Izod impact testing was done at Polifin on a Zwick Materials Testing Machine. The test specimens were of dimensions 8 mm thick and 4 mm wide with a notch radius of 0.25 mm.

3.3.3 Flexural-Bend Testing

The flexural-bend tests were carried out under the conditions as set out in ASTM D 790M – 92[40] using *Test Method 1 - Procedure B*. The 3-point bend tests were performed on a Zwick Universal Tensile Testing Machine using an in-house built cage as shown in Figure 3.2. The test parameters employed on specimens of dimensions of width 10 mm and thickness of 4 mm were; a test speed of 17 mm/min and a support span of 64 mm. The flexural modulus was determined from the force/deflection curves obtained from the tests using the equation:

$$E_f = (0.17L^3m)/(bt^3) \quad (3.6)$$

where,

- E_f is the flexural modulus of elasticity in MPa;
- L is the support span in mm;
- b is the width of the specimen in mm;
- t is the thickness of the specimen in mm and
- m is the slope of the load/deflection curve in N/mm.

The flexural strengths were not determined, as the specimens were not strained to failure.

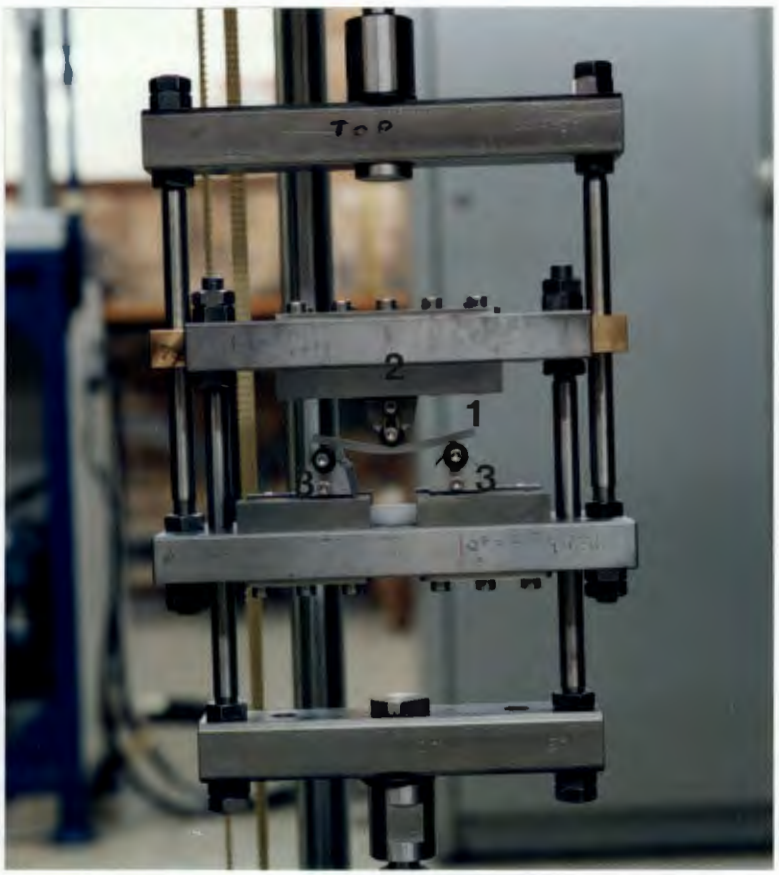

Figure 3.2: The 3-point bending cage for flexural-bend tests, 1 – polymer specimen under load, 2 – central loading roller and 3 – support rollers.

3.3.4 Tensile Testing

The tensile test specimens were pulled in tension on the Zwick 1484 Universal Tensile Testing Machine. The tests were carried out according to ASTM D 638M - 91a[41]. It was necessary to use a test speed of 50 mm/min because the specimens elongated to more than 200 % of the original gauge length. The test parameters employed were a test speed of 50 mm/min, *i.e.* at a strain rate of 9.8 X 10^{-3} s^{-1}. The tensile specimens had a gauge length of 85 mm, a thickness of 4 mm and a width of 10 mm. The slope of the initial linear part of the curves was used to calculate the tensile modulus using the formula:

$$E_y = (W/A_o) / (\Delta L/L_o) = \sigma/\varepsilon \qquad (3.7)$$

where,

- E_y is the tensile (Young's) modulus in MPa;
- W is the load in N;
- A_o is the initial cross sectional area in mm^2;
- ΔL is the change in gauge length in mm;
- L_o is the original gauge length in mm;
- σ is the engineering stress in MPa and
- ε is the strain.

The tensile strength of the copolymers was determined from the maximum load reached after the initial elastic portion of the curve. The tensile yield strength could not be accurately determined as the material displayed a continuous yielding. The maximum elongation was obtained from the reading on the machine.

3.4 MORPHOLOGICAL CHARACTERISATION

3.4.1 Scanning Electron Microscopy (SEM)

A Cambridge Stereo-scan 2000 Scanning Electron Microscope (SEM) operating at 15 kV, was used to quantify the rubber particle size and spatial distribution. From the SEM micrographs, the average particle size and the average interparticle spacing of the rubber particles were determined. Notched impact test specimens were immersed in liquid nitrogen for approximately one minute, quickly clamped in a vice and fractured using a plastic hammer. The fracture surface was then etched in *n*-heptane at 70 °C for 30 minutes. After cleaning in methanol for 5 minutes in an ultrasonic bath, the specimens were mounted on aluminium stubs. They were then sputter-coated at 2 kV and 16 mA for 10 minutes using a *gold / palladium* mixture, to render them electrically conducting. To minimise charging of the polymer specimens, a conducting path of silver dab was applied between the specimen and the stub.

The interparticle spacing was determined by measuring the distance from the centre of one rubber particle to the nearest with a ruler. The particle size was determined by measuring the perimeter of the rubber particles using a Joyce Loebl Image Analysis Software Package. The rubber particles were assumed to be spherical, hence the relation between the perimeter (circumference) and the diameter was used to convert the circumference values, C, to diameter, d_c, *i.e.* $C = \pi d_c$.

3.4.2 Transmission Electron Microscopy (TEM)

The transmission electron microscopy (TEM) was used to study the microstructure of the rubber phase. For this purpose a JEOL JEM-200CX Transmission Electron Microscope operating at 200 kV was used. The polymer specimens were first prepared into blocks that could fit into a microtome sample holding pin. The blocks were then submerged in

concentrated chlorosulphonic acid for 4 hours at room temperature and then rinsed thoroughly in distilled water. The chlorosulphonic acid hardens the blocks and makes sectioning easier.

The blocks were dried and then submerged in a 0.1% staining solution of ruthenium tetroxide (RuO_4) for 4 to 8 hours. The staining solution was buffered at a pH of 7.2 with sodium dimethylarsonate in order to maximise the diffusion of the stain into the block. The purpose of the RuO_4 solution is to give contrast between the polypropylene matrix and the dispersed ethylene-propylene rubber phase. The stock solution was prepared by reacting 4 grams of sodium periodate with 0.6 grams of hydrated ruthenium dioxide in 100 ml of water. The reaction mixture was left to react at a temperature of 0 °C in a fume-hood for 3 hours. The reaction is as follows:

$$2NaIO_4\,(s) + RuO_2\,(s) \rightarrow RuO_4 + 2NaIO_3$$

The polymer block was immersed in a 0.1% solution that was prepared from the stock solution. The blocks were then thoroughly rinsed in distilled water and left to dry. Thin sections of about 80 nm thick were microtomed either at room temperature or at −120 °C on a Reichert Ultracut S microtome. The sections were then put on a copper grid for viewing in the TEM. Photographs were taken for a more detailed investigation of the microstructural constituents.

3.5 THERMAL CHARACTERISATION

3.5.1 Dynamic Mechanical Thermal Analysis (DMTA)

The dynamic mechanical thermal analysis (DMTA) of the polymer samples was performed on a Perkin-Elmer DMA 7e Analyser at the Polymer Institute at the University of Stellenbosch. The tests were conducted at an operating frequency of 3.6 Hz over a temperature range of −70 to 100 °C, using a heating rate of 5 °C/min. The test specimens were machined from the injection-moulded tensile test specimens to fit into the specimen holder of the machine. A parallel plate measuring configuration was used. A probe measures the material's response to the applied frequency over the temperature range. The results were recorded as either loss modulus, storage modulus or tan δ, as a function of temperature but in this thesis only the loss modulus results are reported as they were the more meaningful of the three.

3.5.2 Simultaneous Thermal Analysis (STA)

The response to temperature increase of the copolymer material was investigated by looking at the Differential Thermal Analysis (DTA) and the Thermogravimetric (TG) curves for the 2349 MC and 2900 H grades. Specifically, the influence of % C_2 on transition temperatures and decomposition behaviour was studied. The tests were run on a Netzsch Thermal Analysis STA 409 machine shown in Figure 3.3. The machine is equipped with two Al_2O_3 crucibles for the sample and the reference material. The reference crucible was kept empty during testing. The tests were run from 20 °C to 500 °C at a heating rate of 5 °C/min in a dynamic atmosphere of argon flowing through the furnace chamber at 100 ml/min. The data is collected and processed via a computer with the necessary software.

Figure 3.3: The Netzsch Thermal Analysis STA 409 machine used to obtain the data for DTA and TG analysis, 1 – specimen chamber, 2 – weighing balance system, 3 – pressure gauge, 4 – vacuum pump and 5 – argon gas cylinder.

CHAPTER 4

RESULTS

4.1 INTRODUCTION

This chapter presents a systematic characterisation and analysis of the various poly-(propylene-ethylene) copolymers. In the case where more than one batch per grade was analysed the results are reported with a standard deviation. For the mechanical tests results at least five measurements were taken. Various correlations were established and in cases where there was a common denominator between two different correlations, care was taken not to repeat a correlation between the two dependent variables and a reference to this is made accordingly in the text. The experimental results are presented in the following order:

1. PHYSICAL CHARACTERISATION,
2. MECHANICAL CHARACTERISATION,
3. MORPHOLOGICAL CHARACTERISATION AND
4. THERMAL CHARACTERISATION.

4.2 PHYSICAL CHARACTERISATION

4.2.1 Effect of Ethylene Content (% C_2) on the Crystalline Structure

The melt flow index (MFI), the R21 and the degree of crystallinity as determined by DSC are presented in Table 4.1 as a function of ethylene content. The R21 value is a Polifin internal standard that is directly related to the rubber content and also includes a contribution from the atactic polypropylene. Figure 4.1 shows that the R21 is directly proportional and increases with an increase in ethylene content. The ethylene content is an indication of the amount of rubber contained in the copolymer. Since R21 is directly proportional to the ethylene content, it should be expected that plots of physical and mechanical properties against R21 would show trends similar to those against ethylene content, hence such plots are not shown. Figure 4.2 shows a decrease in the degree of crystallinity as the ethylene content increases. It should be noted that the nucleated grades generally have a slightly higher percentage crystallinity at comparable ethylene contents.

Grade	Ethylene Content (%)	MFI (g/10 min)	R21	Degree of Xc (%)	Min. Value	Max. Value
2340 PC	6.2	15.7	15.1	31.7±2.9	29.2	34.8
2349 MC	7.7	8.3	16.2	31.0±3.3	27.2	33.3
2448 TC	9.5	46.1	19.7	29.8±4.3	23.5	32.8
2540 H	11.8	1.7	24.5	27.4	--	--
2600 PC	11.8	17.2	24.7	28.7	--	--
2602 E	12.7	0.9	26.3	24.4±3.2	24.1	24.8
2648 PC	11.8	15.6	25.4	28.9±1.5	27.4	31.5
2648 RC	11.7	22.7	23.7	29.3±4.1	24.8	32.9
2900 H	22.4	1.8	39.5	20.3	--	--

Table 4.1: Data for the copolymer properties: % C2, MFI, R21 and % crystallinity.

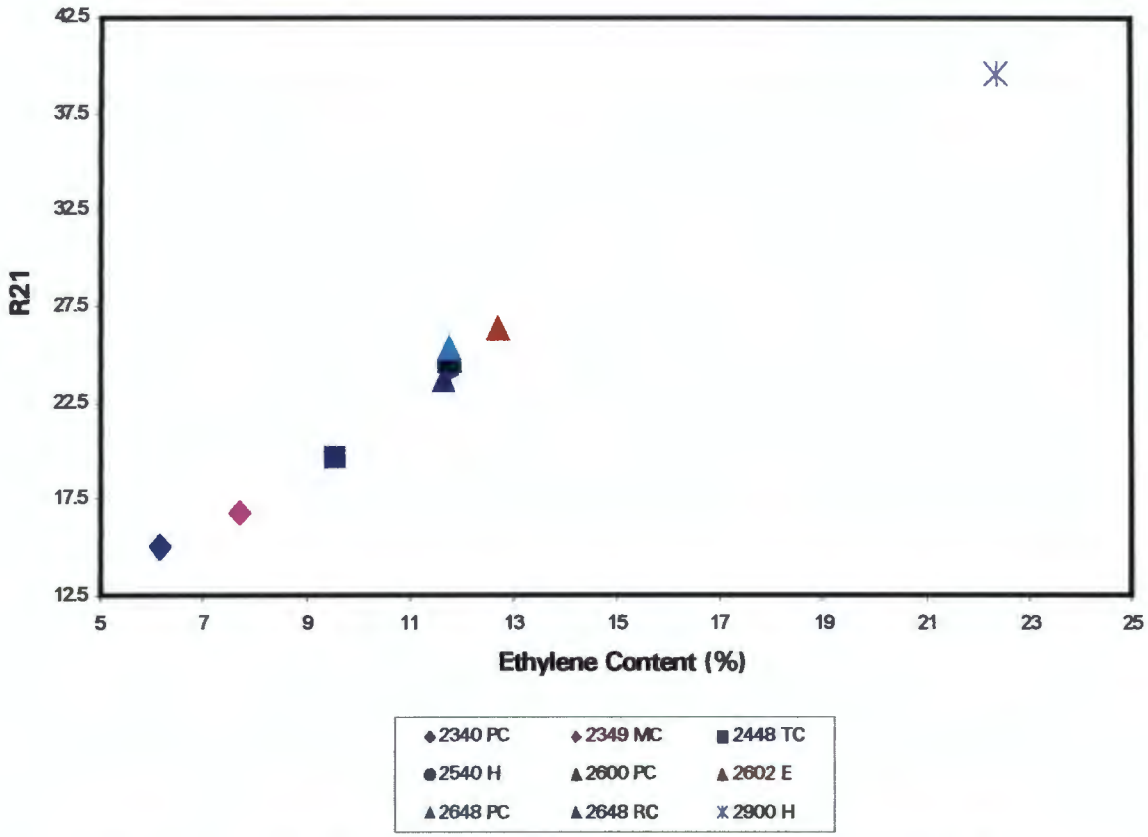

Figure 4.1: The R21 is linearly correlated with the ethylene content, % C_2.

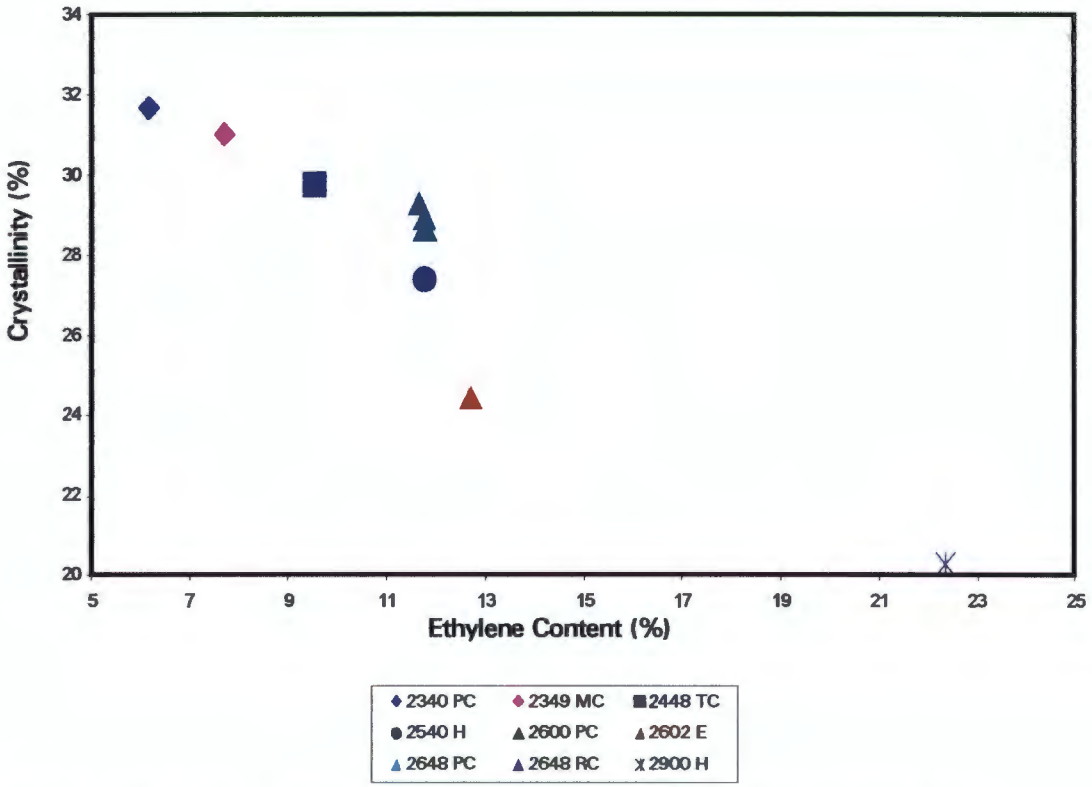

Figure 4.2: The % Xc, determined from DSC data, decreases with increasing %C_2.

4.2.2 X-Ray Diffraction Studies

Wide-angle x-ray diffraction (WAXD) studies were carried out in order to obtain information on the crystal level of the copolymers. Selected diffractograms are shown in Figures 4.3 (a) to (d). These traces all show a broad amorphous background superimposed on diffraction peaks ascribed to the crystallographic planes $(110)_\alpha$, $(040)_\alpha$, $(130)_\alpha$, $(111)_\alpha$, $(131)_\alpha$, $(041)_\alpha$ and in some grades $(300)_\beta$. Sometimes the β peak, occurring at $2\theta = 16.1°$, also appeared in traces within some of the batches in grades where they were generally not present. From this it can tentatively be concluded that the proportion of the β hexagonal form and the α monoclinic form depends on the ethylene content, the presence of a nucleating agent, the plant processing- and / the moulding conditions.

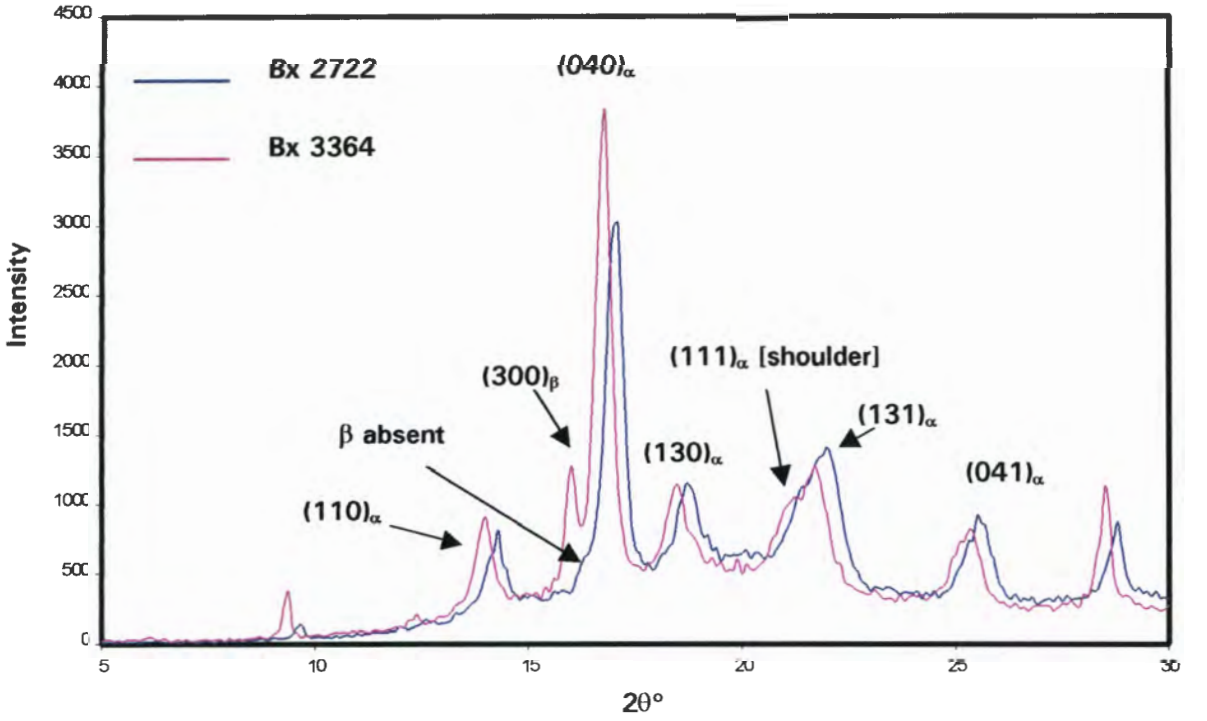

(a)

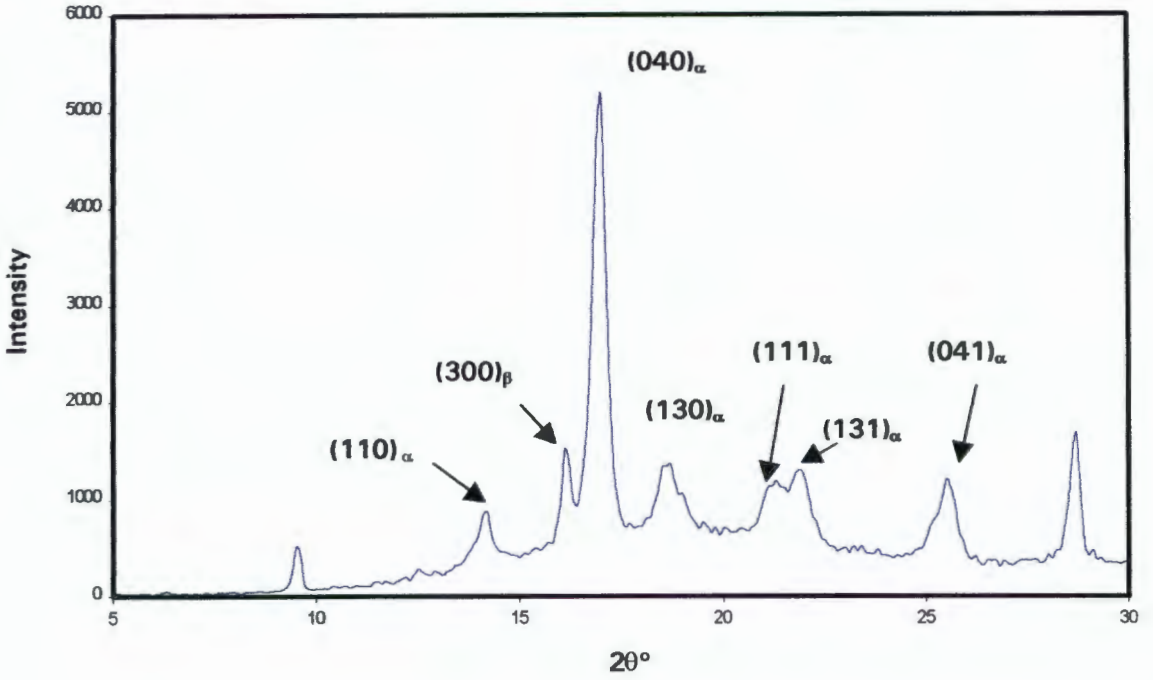
Intensity
2θ°
(040)α
(300)β
(110)α
(130)α
(111)α
(131)α
(041)α

(b)

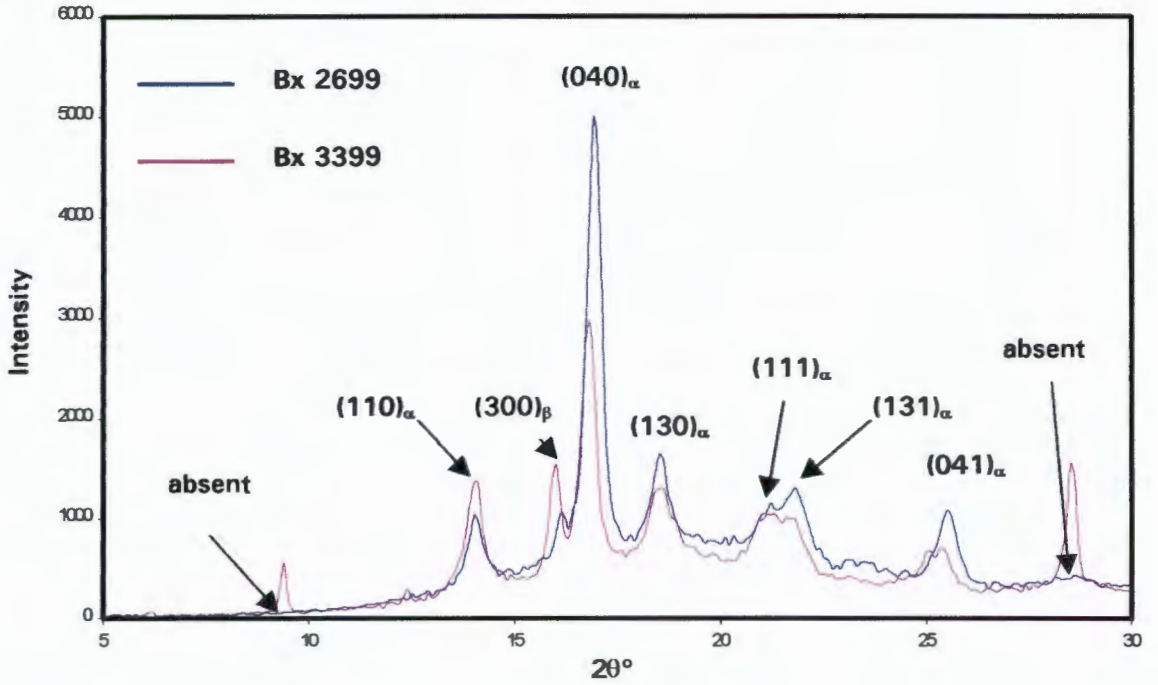
Bx 2699
Bx 3399
Intensity
2θ°
(040)α
(110)α
(300)β
(130)α
(111)α
(131)α
(041)α
absent
absent

(c)

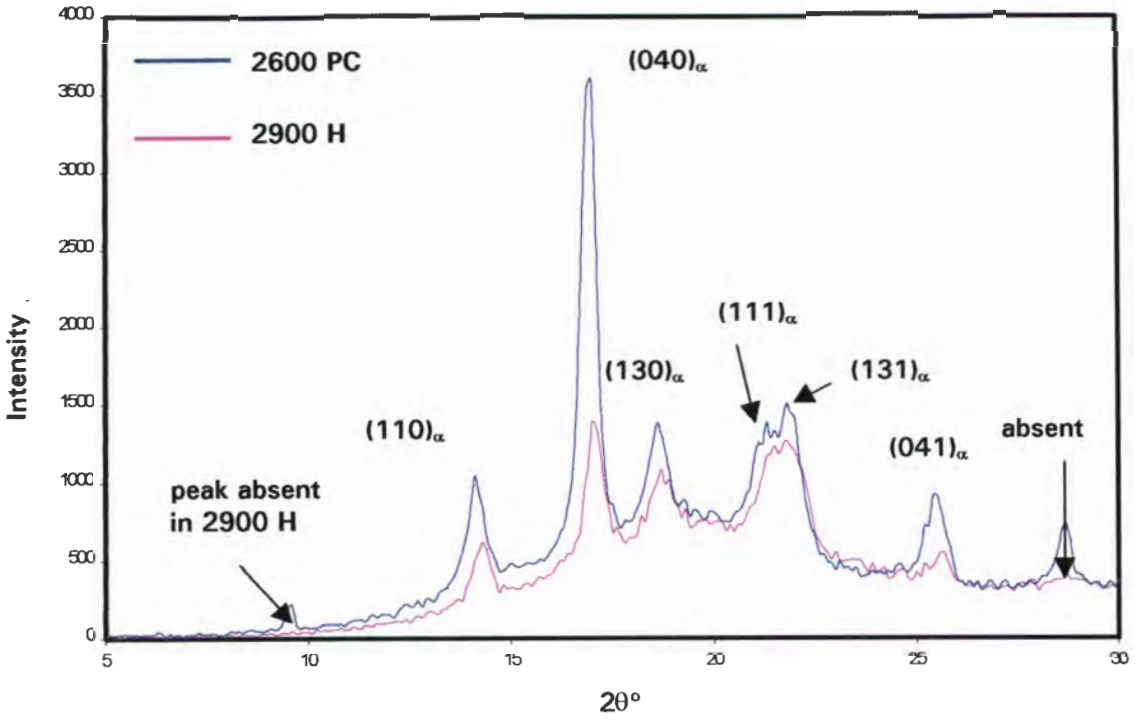

(d)

Figure 4.3: Selected XRD traces for the copolymers showing (a) two different batches of grade 2349 MC, one with the $(300)_\beta$ peak present; (b) grade 2540 H with all the peaks present and a clear split in the peaks for $(111)_\alpha$ and $(131)_\alpha$; (c) two batches of grade 2602 E with one batch showing an absence of peaks at $2\theta° = 9.5$ and 28.6 and (d) Targor grades 2600 PC and 2900 H with the $(300)_\beta$ peak absent in both grades; the 2900 H grade also shows an absence of the peaks at $2\theta° = 9.5$ and 28.6.

Figure 4.3 (a) shows two different batches (Bx's 2722 and 3364) of grade 2349 MC, with batch 3364 showing the $(300)_\beta$ peak. The peaks for the trace with no $(300)_\beta$ peak (Bx 2722) also show a shift to slightly higher diffraction angles. For both batches a shoulder can be attributed to the $(111)_\alpha$ plane at $2\theta° = 21.2$. Figure 4.3 (b) shows a trace of grade 2540 H with all the peaks present and a clear split between the $(111)_\alpha$ and $(131)_\alpha$ peaks is now evident. Figure 4.3 (c) shows two different batches (Bx's 2699 and 3399) of grade 2602 E with batch 2699 showing an absence of peaks at $2\theta° = 9.5$ and 28.6. Furthermore, the percentage crystallinities calculated from the XRD traces are 54.8 for batch 2699 and 62.4 for batch 3399. Figure 4.3 (d) shows the two Targor grades 2600 PC and 2900 H with the $(300)_\beta$ peak absent in both

grades whilst the 2900 H grade also shows an absence of the peaks at $2\theta° = 9.5$ and 28.6.

Table 4.2 summarises an analysis of the data obtained from the x-ray diffraction traces for the various copolymers. The average values of the peak position, peak width and apparent crystallite size obtained from the $(040)_\alpha$ crystallographic plane are reported here. There appears to be a slight shift to a higher diffraction angle and also a peak broadening with an increase in ethylene content.

Grade	*Ethylene Content (%)*	*Peak Position (2θ) Degrees*	*Peak Width (2θ) Degrees*	*Crystallite size (Å)*
2340 PC	6.2	16.82±0.05	0.41±0.04	216.4±19.2
2349 MC	7.7	16.88±0.16	0.43±0.03	204.4±14.6
2448 TC	9.5	16.85±0.07	0.45±0.03	199.2±14.7
2540 H	11.8	16.98	0.42	210.2
2600 PC	11.8	16.96	0.46	191.9
2602 E	12.7	16.86±0.11	0.43±0.01	205.4±6.7
2648 PC	11.8	16.84±0.04	0.44±0.02	199.7±9.9
2648 RC	11.7	16.85±0.18	0.43±0.03	204.2±11.7
2900 H	22.4	17.03	0.62	142.4

Table 4.2: X-ray diffraction data as a function of % C_2 in polypropylene copolymers.

Figure 4.4 shows a decrease in average crystallite size as the ethylene content increases. The decrease in crystallite size can be attributed to an increase in the amorphous content within the copolymers with increasing ethylene content. Molecular weight does not seem to have a significant effect on crystallite size.

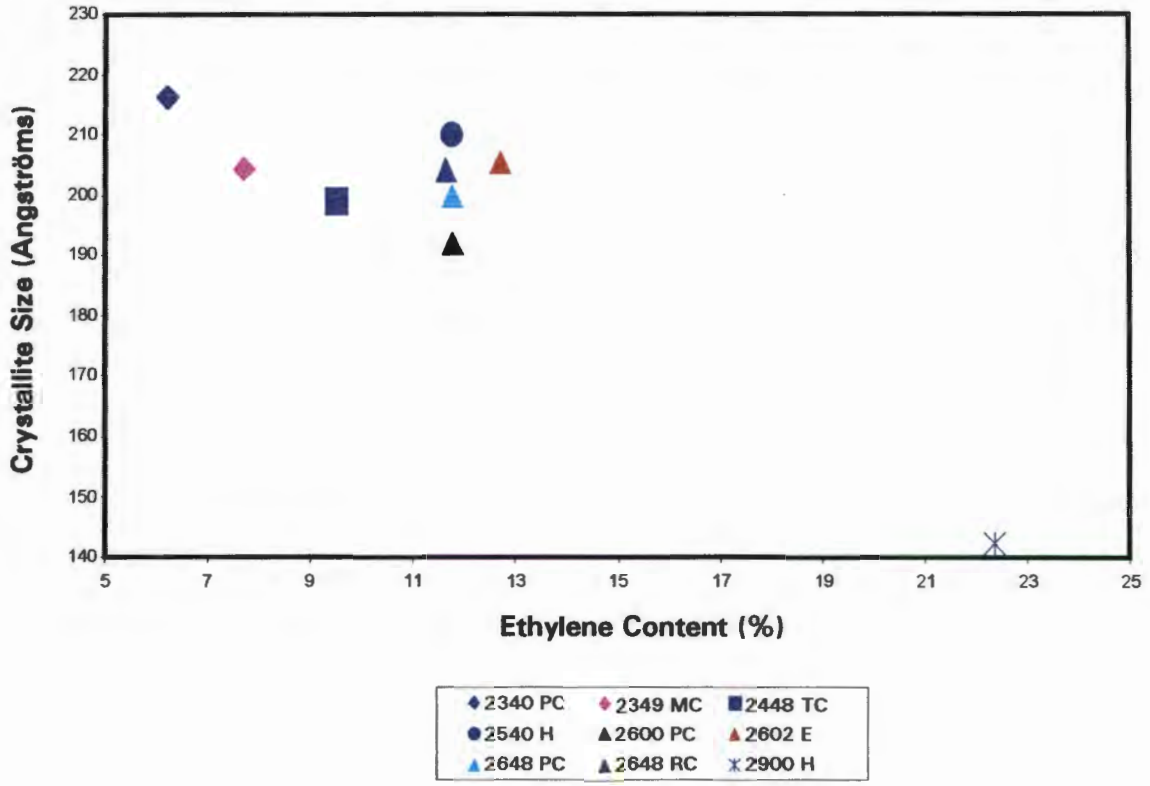

Figure 4.4: Apparent crystallite size showing a general decrease as % C_2 increases.

The relative amount of the β form is described in terms of the K value, which gives the relative content of the β hexagonal form in terms of the diffracting crystallographic planes[14,15]:

$$K = H(300)_\beta / [H(300)_\beta + H(110)_\alpha + H(040)_\alpha + H(130)_\alpha] \quad (4.1)$$

where,
$H(110)_\alpha$, $H(040)_\alpha$, and $H(130)_\alpha$ are the heights of the α form peak and $H(300)_\beta$ is the height of the β form peak.

The diffractograms were also used to determine the % crystallinity (Xc) of the copolymers[12,39]:

$$Xc = Ac/[Ac + Aa] \quad (4.2)$$

where,
Ac and Aa are the areas under the crystalline and amorphous peaks, respectively.

The K and Xc values determined by DSC and XRD are shown in Table 4.3. The degree of crystallinity determined from XRD studies also shows a general decrease with increasing ethylene content as was determined from DSC data. Figure 4.5 shows that a linear relationship exists between crystallinity determined by XRD and that by DSC. It is surmised that the presence of the $(300)_\beta$ peak is a contributing factor to the higher crystallinity obtained for the two grades 2540 H and 2602 E. Where the β hexagonal form is present, the $(040)_\alpha$ peak is broader thus further contributing to the observed higher degree of crystallinity in these grades. The degree of crystallinity, % Xc, from XRD is almost twice as much as that obtained from DSC. For the high MFI grades, only batch 3388 of grade 2648 RC showed the β peak.

Grade	*Ethylene Content (%)*	*Xc (%) from DSC*	*Xc (%) from XRD*	*β Content, K (%)*
2340 PC	6.2	31.7±2.9	66.73±0.98	--
2349 MC	7.7	31.0±3.3	61.38±4.33	16.9
2448 TC	9.5	29.8±4.3	57.38±2.73	--
2540 H	11.8	27.4	58.28	16.9
2600 PC	11.8	28.7	52.67	--
2602 E	12.7	24.4±3.2	58.59±5.41	16.7
2648 PC	11.8	28.9±1.5	51.17±2.72	--
2648 RC	11.7	29.3±4.1	54.84±3.45	12.9
2900 H	22.4	20.3	37.07	--

Table 4.3: Comparison of the crystallinity measurement results from DSC and XRD and results for the β content determination.

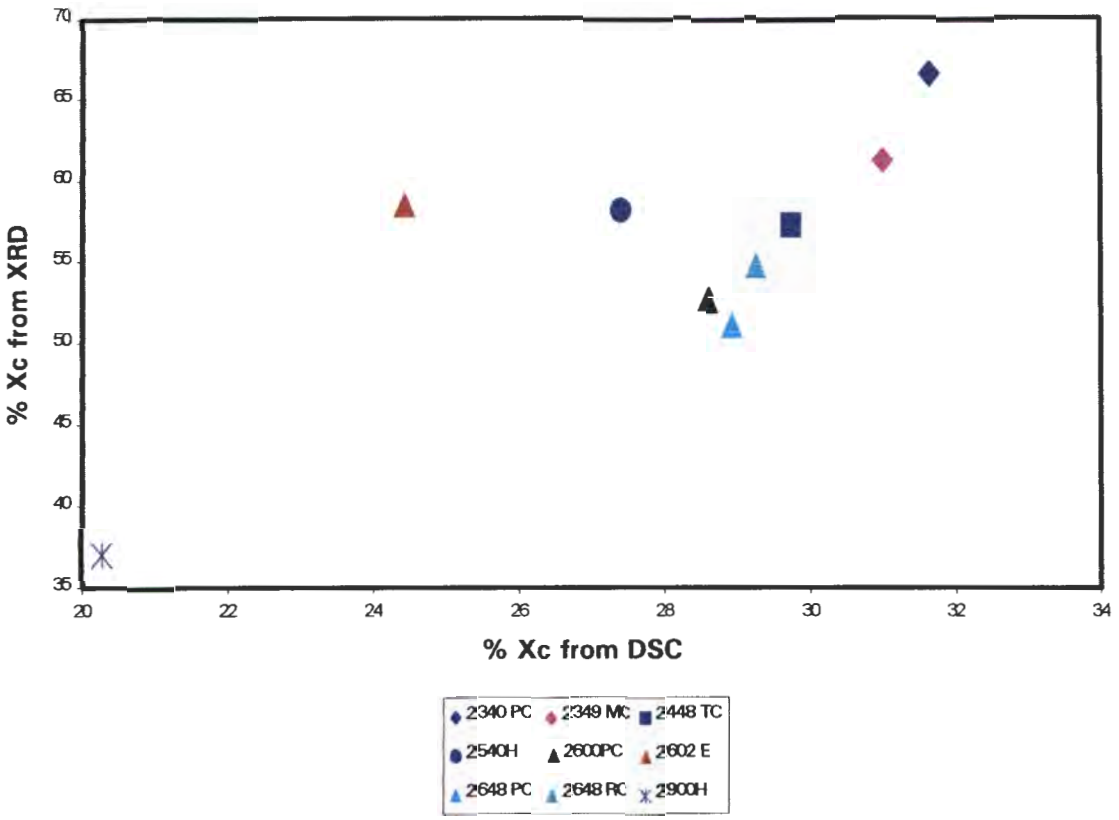

Figure 4.5: A comparison of the % Xc determined from XRD and DSC data.

4.3 MECHANICAL CHARACTERISATION

4.3.1 Hardness Test Results

Table 4.4 shows the average, minimum and maximum values with the standard deviation of the average for the micro-hardness test results. The results show a general decrease in hardness with increasing ethylene content. The size and distribution of the rubber particles would not affect the hardness value, as the size of the indent made is of several orders bigger than any specific rubber particle. It would also appear from the data that the ethylene content overrides any increase in hardness that might be attributed to the addition of a nucleating agent.

Grade	*Ethylene Content (%)*	*MFI (g/10 min)*	*Hardness (HV-25gf)*	*Min. Value*	*Max. Value*
2340 PC	6.2	15.7	7.4±0.6	6.7	7.9
2349 MC	7.7	8.3	6.3±1.5	5.4	7.9
2448 TC	9.5	46.1	6.5±0.7	5.8	7.3
2540 H	11.8	1.7	5.0	--	--
2600 PC	11.8	17.2	5.2	--	--
2602 E	12.7	0.9	3.8±1.1	3.1	4.6
2648 PC	11.8	15.6	4.8±0.4	4.1	5.5
2648 RC	11.7	22.7	4.6±0.6	3.9	5.0
2900 H	22.4	1.8	2.4	--	--

Table 4.4: Data for the results of the hardness tests for the various copolymers.

Figure 4.6 plots the general decrease in hardness with increasing ethylene content. The decrease in hardness with ethylene content can be attributed to the increase in the amount of the soft rubber phase with increasing ethylene content. There is some scatter in the hardness results of the grades with an ethylene content of about 12 %. Figure 4.2 showed that an inverse correlation exists between ethylene content and % crystallinity, thus there is a linear and positive correlation between

hardness and crystallinity of the copolymers as shown in Figure D.1 in Appendix D. This trend is normal as hardness is crystallinity dependent and as such factors that affect crystallinity similarly affect hardness. Because of this correlation, plots of properties such as impact strength against hardness would follow the same trend as it would against % crystallinity.

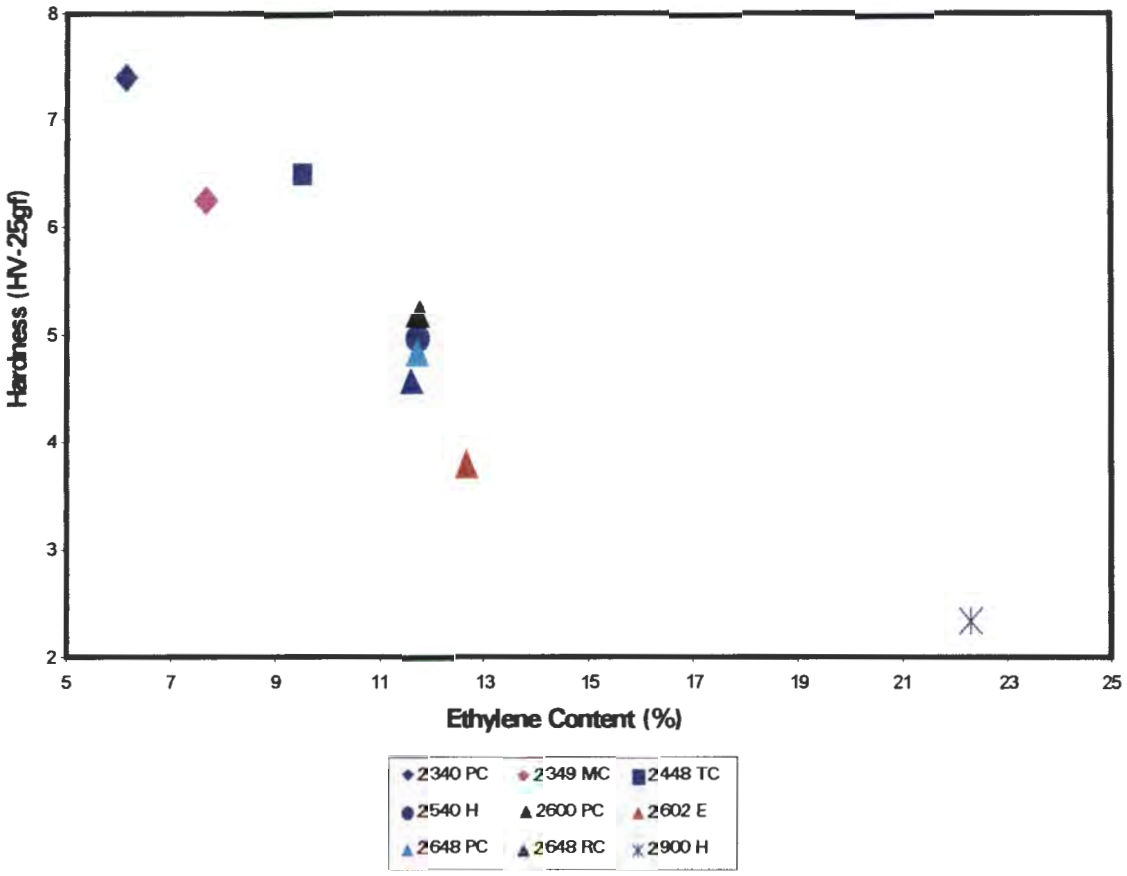

Figure 4.6: The effect of ethylene content on hardness for the various copolymers.

4.3.2 Impact Tests Results

Table 4.5 contains results of the impact tests conducted on notched specimens. In general there is an increase in impact strength with increasing ethylene content and molecular weight (decreasing MFI). The impact strength values show an exponential decrease from high to low toughness with increasing MFI.

Grade	*Ethylene Content (%)*	*MFI (g/10 min)*	*Impact Strength (kJ/m^2)*	*Min. Value*	*Max. Value*
2340 PC	6.2	15.7	8.2±0.7	7.4	8.7
2349 MC	7.7	8.3	9.3±2.6	7.5	12.3
2448 TC	9.5	46.1	6.1±2.1	4.8	9.3
2540 H	11.8	1.7	56.2	--	--
2600 PC	11.8	17.2	12.9	--	--
2602 E	12.7	0.9	54.3±14.7	43.9	64.7
2648 PC	11.8	15.6	21±14.5	9.7	42.2
2648 RC	11.7	22.7	15.7±12.7	7.6	30.3
2900 H	22.4	1.8	54.2	--	--

Table 4.5: Data for the results of the impact tests for the various copolymers.

Figure 4.7 shows two toughness regions separated by a transition at an ethylene content of about 12 %, *viz.*, a low toughness region dominated by low ethylene content (and relatively high MFI) and a high toughness region consisting of low MFI and high ethylene content grades.

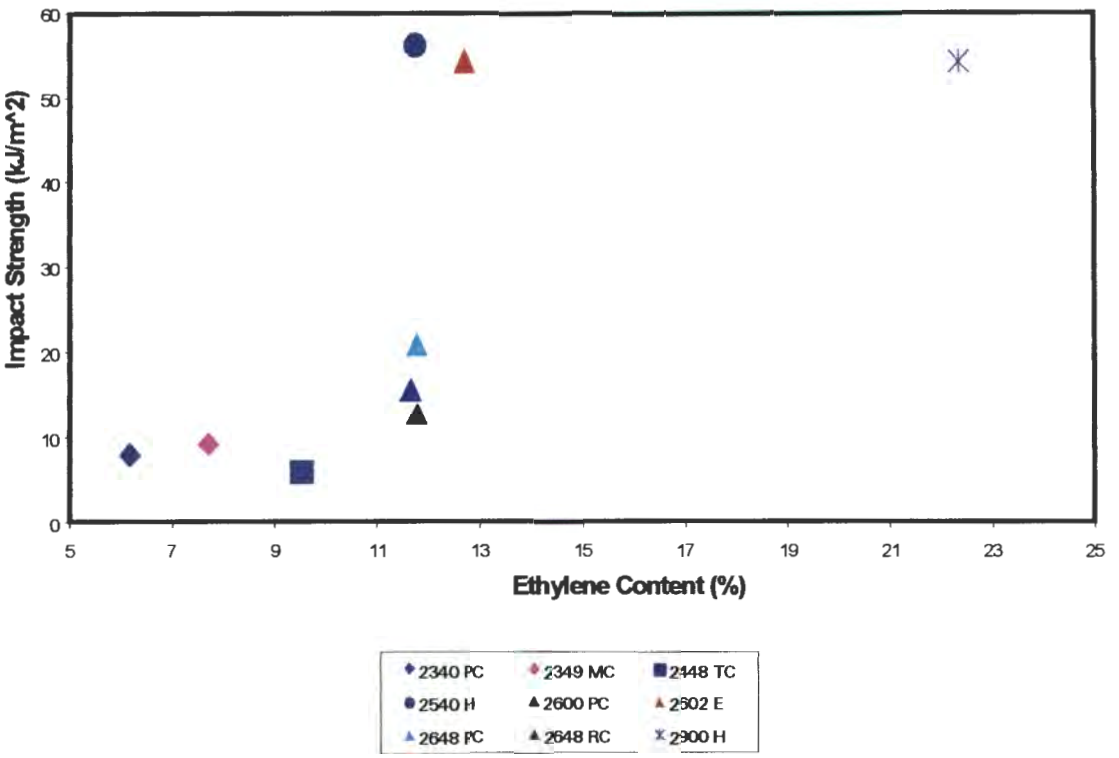

Figure 4.7: The effect of % C_2 on impact strength of the various copolymers.

Figure 4.8 shows a plot of the impact strength against the melt flow index. There is an exponential decrease in impact strength with increasing melt flow index. The MFI is sensitive to the admixture of high molecular weight material *i.e.* to $\overline{M}w$, and as such a small decrease in MFI (at low MFI's) is due to relatively large increases in molecular weight. One would thus expect a rapid increase in impact strength as the MFI is lowered, as confirmed in Figure 4.8. From Figures 4.7 and 4.8 it is clear that both ethylene content and MFI affect the impact strength. The high ethylene content and high molecular weight grades show high impact strength because of mainly two reasons:

1) The high ethylene content lowers the glass transition temperature through lowering the degree of crystallinity and
2) The high molecular weight offers an additional path for fracture energy absorption through changes occurring in chain conformation as well as through the additional tie molecule density.

Since the degree of crystallinity shows an inverse relation to ethylene content, it should be expected that impact strength would also be inversely related to crystallinity as shown in Figure D.2 in Appendix D.

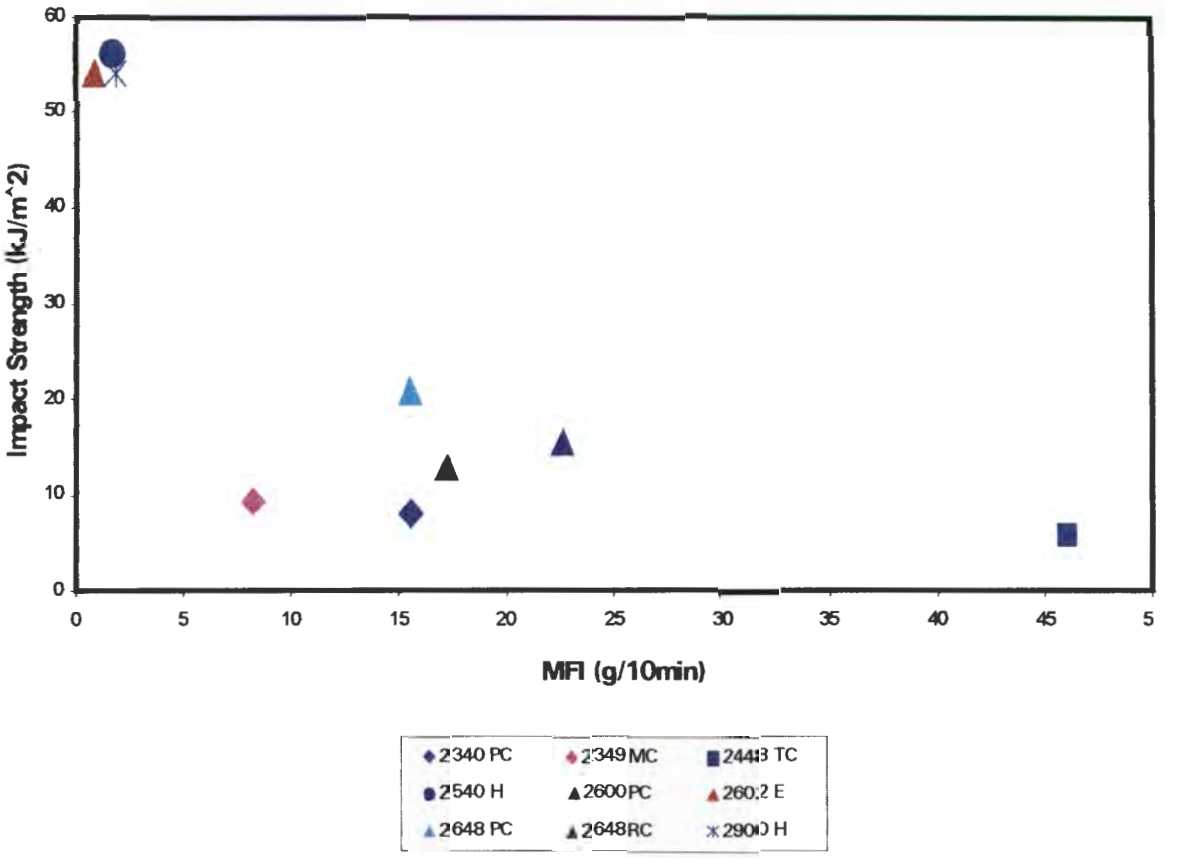

Figure 4.8: The effect of the MFI on impact strength for the various copolymers.

4.3.3 Flexural Tests Results

The load / deflection behaviour of selected copolymer grades during three-point bend tests is shown in Figure 4.9. The grades shown are 2349 MC, 2648 PC and 2900 H. The flexural modulus is determined from the slope of the initial linear part of the load / deflection curves, and as such the magnitude of the slope is directly proportional to the flexural modulus (eqn. 3.6). The slope of a tangent to the curve of the 2349 MC grade is the steepest followed by the 2648 PC and the 2900 H grade. Grade 2349 MC shows the least deflection at a given load because it has a higher degree of crystallinity than the other two grades.

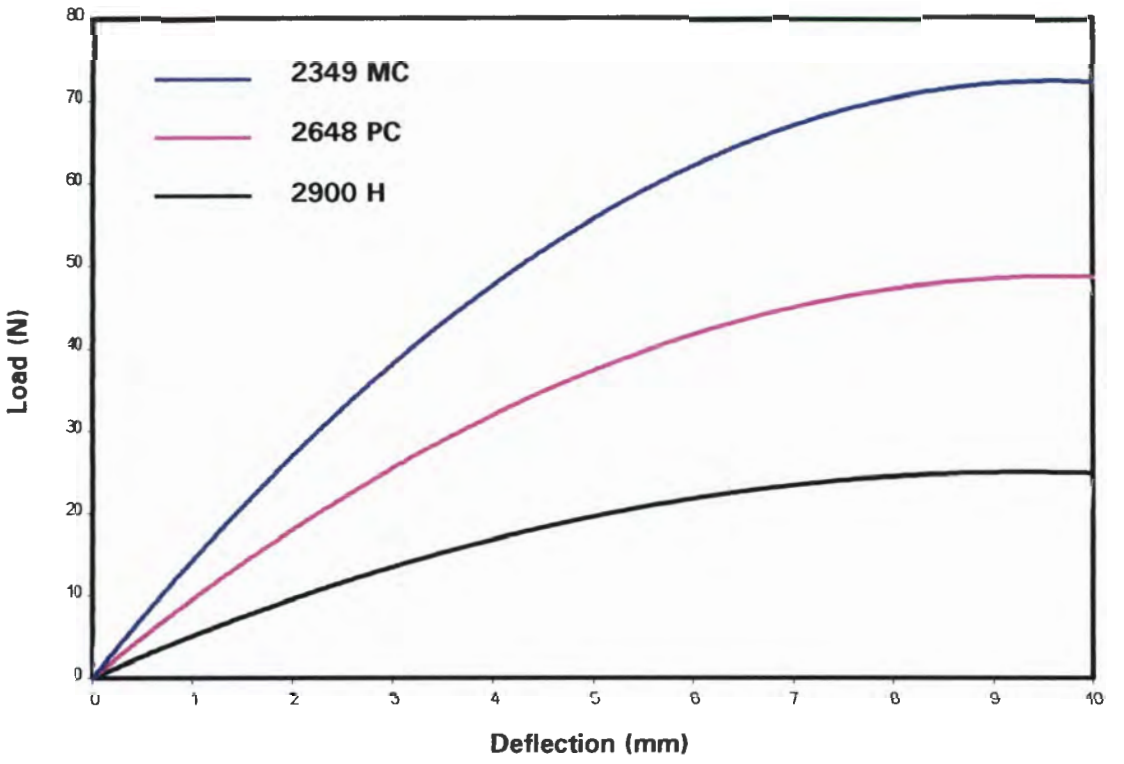

Figure 4.9: Effect of ethylene content on the flexural behaviour of selected copolymers.

The results for the flexural tests are summarised in Table 4.6. There is a general decrease in the flexural modulus as the ethylene content increases as shown in Figure 4.10. This decrease in flexural modulus can be attributed to the modulus being a small strain property dependent on the degree of crystallinity. Some scatter is observed at an ethylene

content of about 12 % with the 2540 H grade showing a significantly high flexural modulus compared to the other grades. The relationship between flexural modulus and crystallinity is shown in Figure D.3 in Appendix D.

Grade	*Ethylene Content (%)*	*MFI (g/10 min)*	*Flexural Modulus (MPa)*	*Min. Value*	*Max. Value*
2340 PC	6.2	15.7	1326±261	1088	1605
2349 MC	7.7	8.3	1137±133	986	1237
2448 TC	9.5	46.1	1083±146	942	1280
2540 H	11.8	1.7	1267	--	--
2600 PC	11.8	17.2	908	--	--
2602 E	12.7	0.9	791±150	685	897
2648 PC	11.8	15.6	811±89	686	904
2648 RC	11.7	22.7	984±187	851	1197
2900 H	22.4	1.8	553	--	--

Table 4.6: Data for results of the flexure-bend tests for the various copolymers.

4.3.3.1 Effect of the Inter-Particle Spacing on Flexural Modulus

Figure 4.11 shows a general increase in flexural modulus with the increase in the ratio between the inter-particle spacing and size of the rubber particles. The data suggests that the grades fall in a broad envelope where a high flexural modulus, at a particular ethylene content, can be obtained by either increasing the inter-particle spacing or by having small rubber particles. In copolymers the stiffness is obtained from the crystallinity of the matrix.

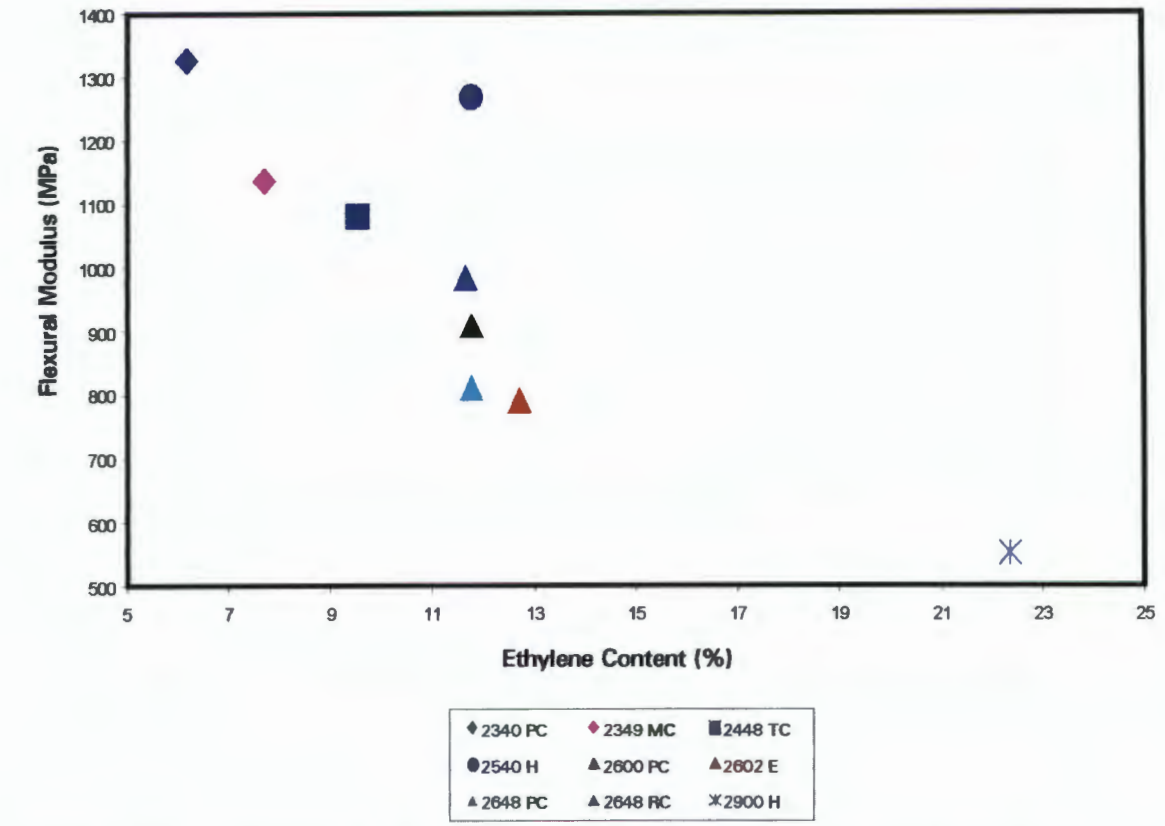

Figure 4.10: The effect of % C_2 on the flexural modulus of the various copolymers.

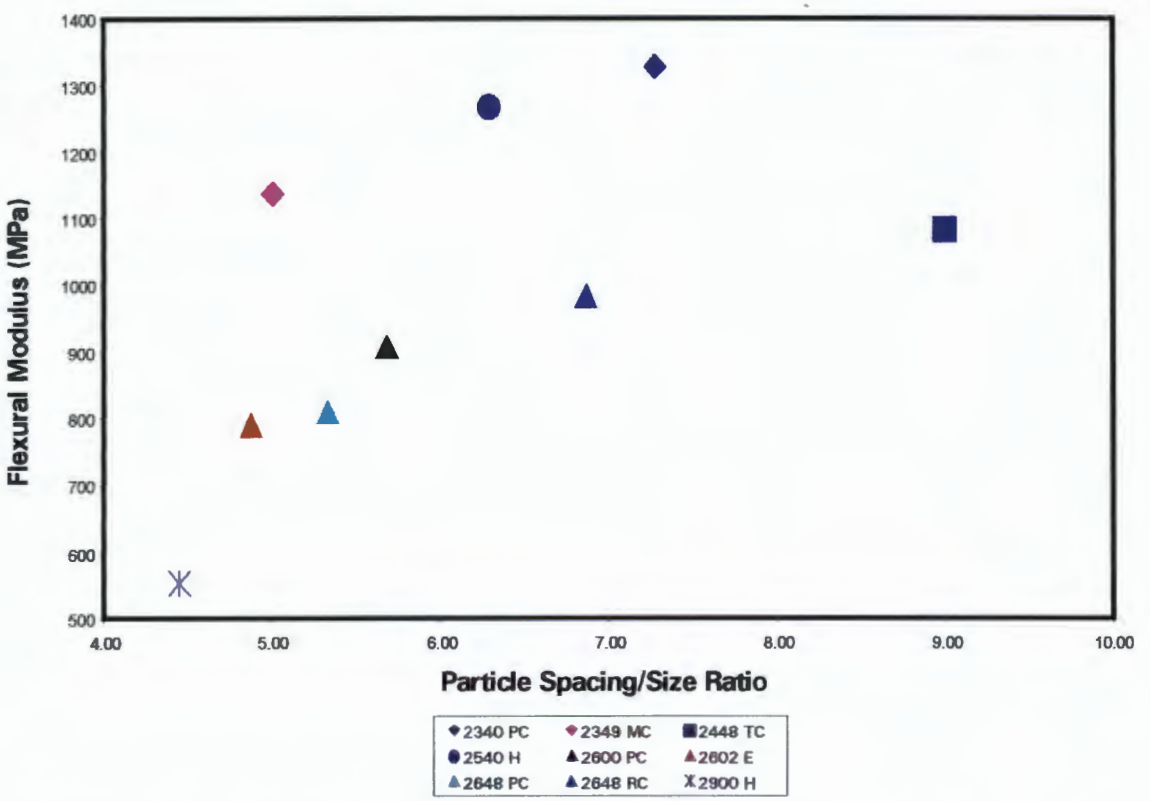

Figure 4.11: A plot of flexural modulus against the particle spacing to size ratio.

4.3.4 Tensile Tests Results

4.3.4.1 Tensile Behaviour

The tensile behaviour as a function of ethylene content of selected copolymer grades during tensile tests is shown in Figures 4.12(a) and (b). The curves shown are for grades 2349 MC, 2648 PC and 2900 H. Figure 4.12 (a) shows the overall tensile behaviour of the copolymers and Figure 4.12 (b) shows the tensile behaviour after 100 % elongation. In Figure 4.12 (a) grade 2349 MC shows the highest ultimate tensile strength and the lowest elongation whilst grade 2900 H shows the lowest ultimate tensile strength and the highest percentage elongation. The test had to be terminated for grade 2900 H as the material continued to strain harden. Grade 2648 PC had tensile properties intermediate between those of the other two grades. The trend observed is that the tensile strength decreases and the elongation increases with increasing ethylene content. This behaviour can be attributed to a decrease in the degree of crystallinity with an increase in ethylene content making chain movement easier. The degree of strain hardening seems to be a function of the ethylene content.

Figure 4.12 (b) shows the tensile behaviour of the copolymers after 100 % elongation. The tensile modulus is determined from the slope of the stress / strain curves (see eqn. 3.7). Grade 2349 MC had the highest tensile modulus followed by 2648 PC and 2900 H. This trend can also be attributed to a decrease in crystallinity with increasing ethylene content. The 2900 H grade has the lowest yield point and seems to neck with more ease than the other two grades.

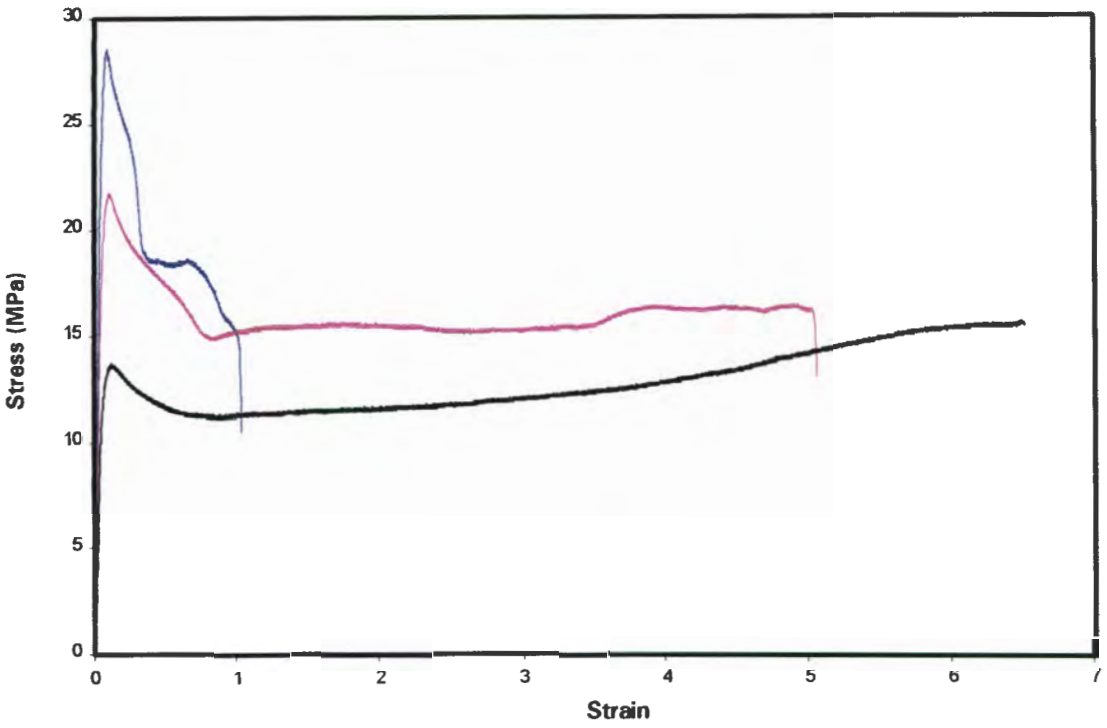

(a)

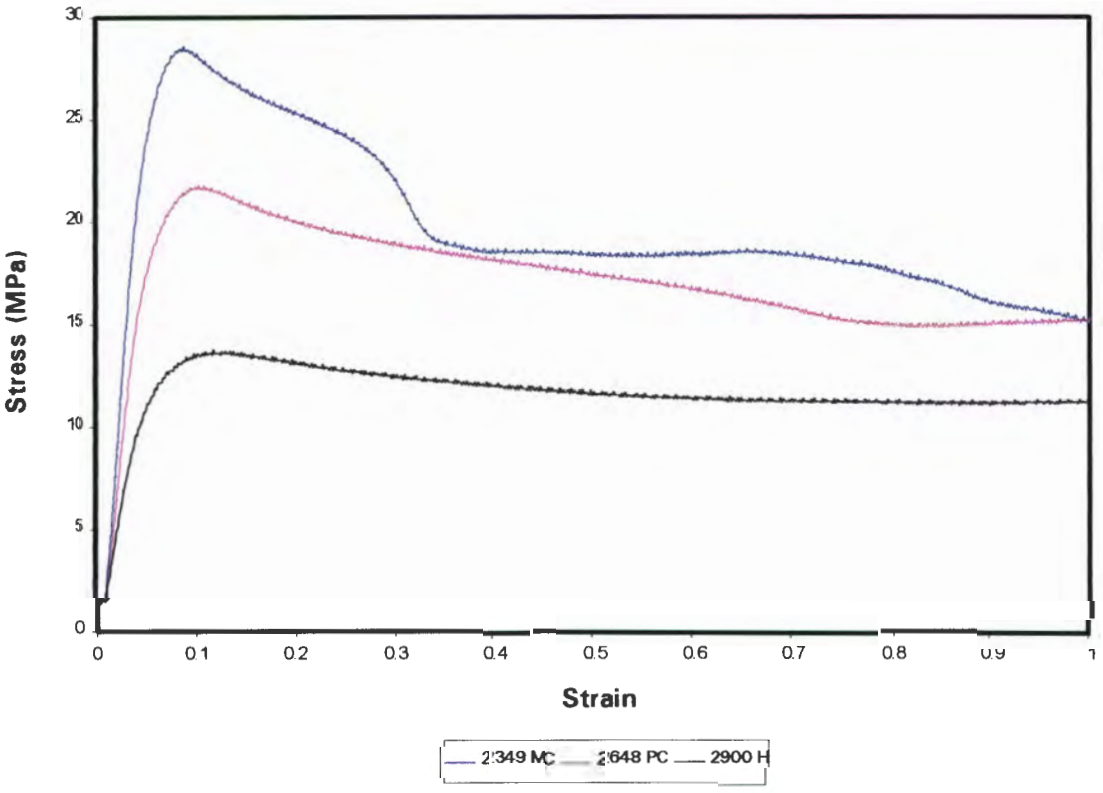

(b)

Figure 4.12: Plots of (a) the overall tensile behaviour and (b) the tensile behaviour at 100 % elongation for selected copolymers.

The tensile test results are summarised in Tables 4.7 below. Both the tensile modulus and tensile strength decrease with increasing ethylene content. This is due to a decrease in the degree of crystallinity as the ethylene content increases, since these tensile properties are small strain properties dependent primarily on crystallinity.

Grade	*Ethylene Content (%)*	*MFI (g/10 min)*	*Tensile Modulus (MPa)*	*Tensile Strength (MPa)*
2340 PC	6.17	15.7	515±52	28.0±1.0
2349 MC	7.71	8.3	493±76	27.0±3.0
2448 TC	9.53	46.1	454±20	23.2±0.7
2540 H	11.75	1.7	436	24
2600 PC	11.76	17.2	504	22.1
2602 E	12.7	0.85	394±15	21±0.2
2648 PC	11.76	15.6	401±32	21.1±1.3
2648 RC	11.65	22.7	391±32	20.5±0.8
2900 H	22.35	1.84	358	17.3

Table 4.7: Data for the tensile modulus and tensile strength determination results of the various grades.

4.3.4.2 Effect of Ethylene Content on Tensile Properties

Figure 4.13 shows that the tensile modulus decreases with increasing ethylene content. At 12 % C_2 there is some scatter in modulus with the Targor grade, 2600 PC, displaying a much higher modulus than the other grades. The decrease in tensile modulus with increasing ethylene content can be attributed to a decrease in the degree of crystallinity with increasing ethylene content, since tensile modulus is a small strain property. Figure D.4 in the Appendix D confirms that tensile modulus does increase with an increase in the degree of crystallinity.

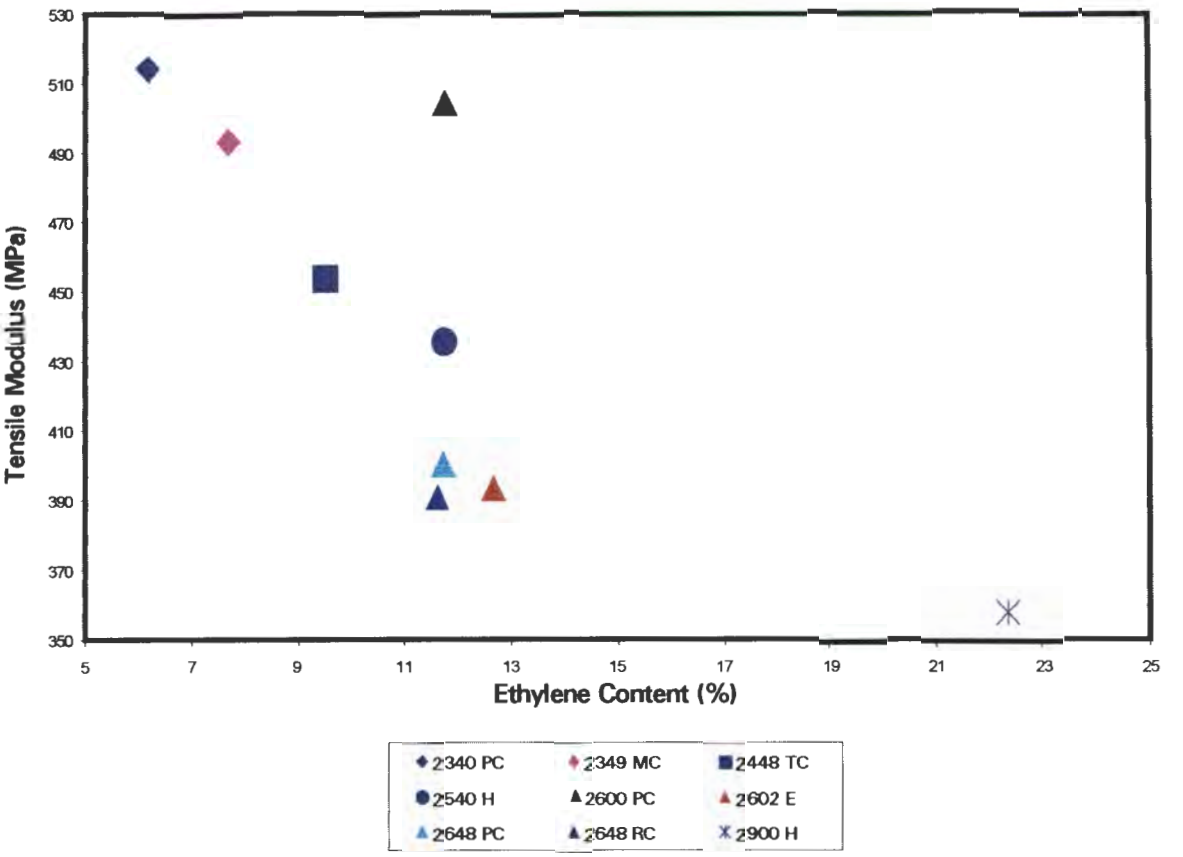

Figure 4.13: Effect of % C_2 on the tensile modulus of the various copolymers.

The tensile strength also decreases with increasing ethylene content as shown in Figure 4.14. The general trend can be attributed to a decrease in the degree of crystallinity with increasing ethylene content. Tensile strength is also a small strain property and therefore depends on the degree of crystallinity. Figure D.5 in Appendix D again confirms that the tensile strength increases with an increase in the degree of crystallinity.

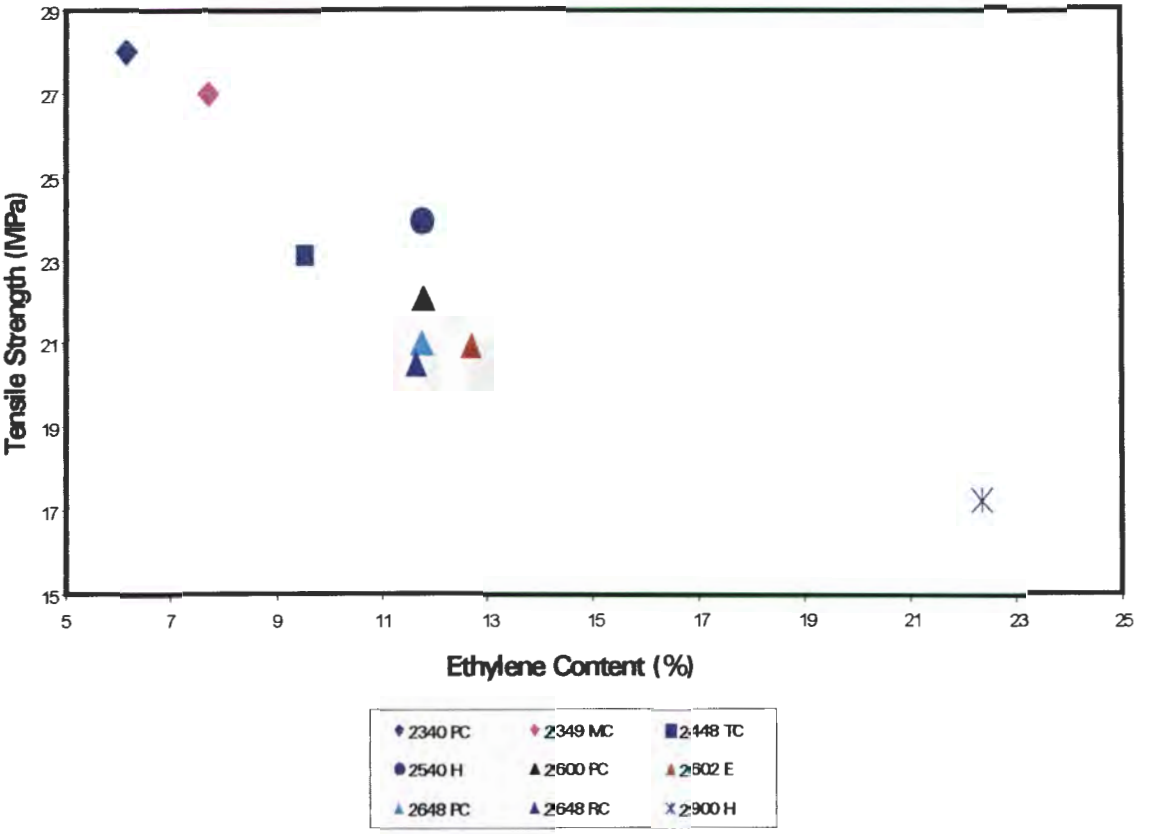

Figure 4.14: Effect of ethylene content on tensile strength of the various copolymers.

4.4 MORPHOLOGICAL CHARACTERISATION

4.4.1 Scanning Electron Microscopy

Micrographs obtained from the scanning electron microscope (SEM) are shown in Figures 4.15 (a) to (j) for the copolymer series. Figures 4.15 (a) to (d) show the microstructure of grades 2349 MC, 2448 TC, 2648 RC and 2900 H at approximately the same magnification. There is a general increase in the density of the ethylene-propylene rubber particles as the ethylene content increases. This can be attributed to an increase in the rubber content with increasing ethylene content. Although the ethylene content for grade 2448 TC is about 3 % higher than that for grade 2349 MC, Figures 4.15 (a) and (b), show that there is no noticeable difference in their respective microstructures. Figures 4.15 (c) and (d) are the microstructures of the 2648 RC and 2900 H grades, respectively. The 2648 RC grade shows a microstructure of small rubber particles with a narrow size distribution and an even spatial distribution.

The 2900 H grade shows a wide range of particle sizes with slightly lower average inter-particle spacing compared to the 2648 RC grade (Table 4.8). The scatter in rubber particle size in grade 2900 H can also be attributed to the agglomeration of smaller rubber particles to form the large particles. This agglomeration is possible because of the higher viscosity ratio between the dispersed phase and the matrix and also due to the fact that at higher C_2 content the rubber phase appears as a separate peak in a DSC scan (see Figures 4.22 (a) and 4.22 (b)).

Figures 4.15 (e) to (h) show the microstructures of the 2340 PC, 2540 H, 2602 E and 2900 H grades at approximately the same but higher magnification. Similar trends to those observed in Figures 4.15 (a) to (d) are observed within these grades. The 2540 H grade has a higher particle density than the 2340 PC grade. The average rubber particle size of the 2602 E grade is slightly smaller than that for the 2900 H grade.

Figures 4.15 (i) and (j) are the microstructures of two different batches of the 2648 PC grade. Figure 4.15 (i) is the microstructure of the batch that showed a very high impact strength, whilst Figure 4.15 (j) shows the microstructure of the batch that showed a much lower impact strength. A visual inspection of the microstructure suggests that the particle size is more uniform for the higher impact. However, there are other factors other than the microstructure that need to be considered for high impact strength.

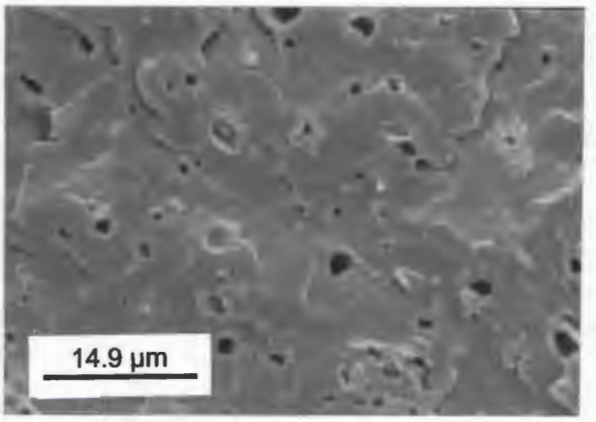

(a)

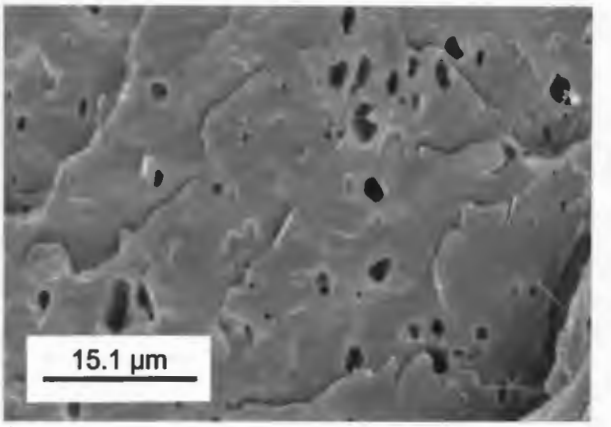

(b)

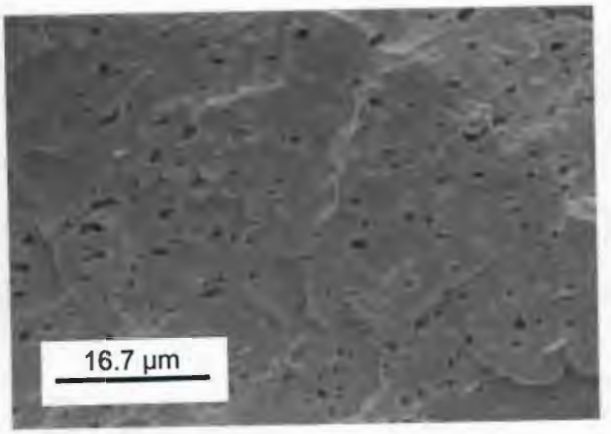

(c)

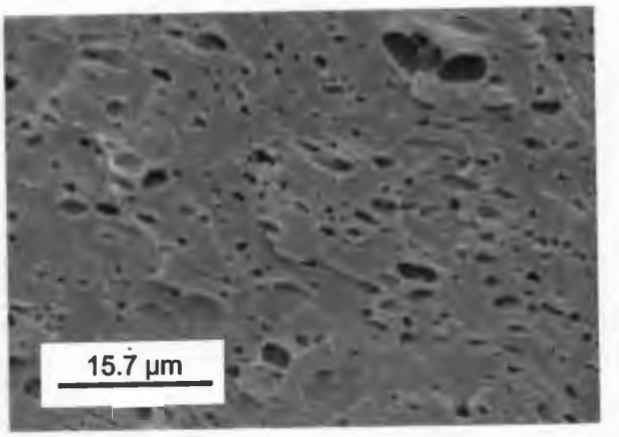

(d)

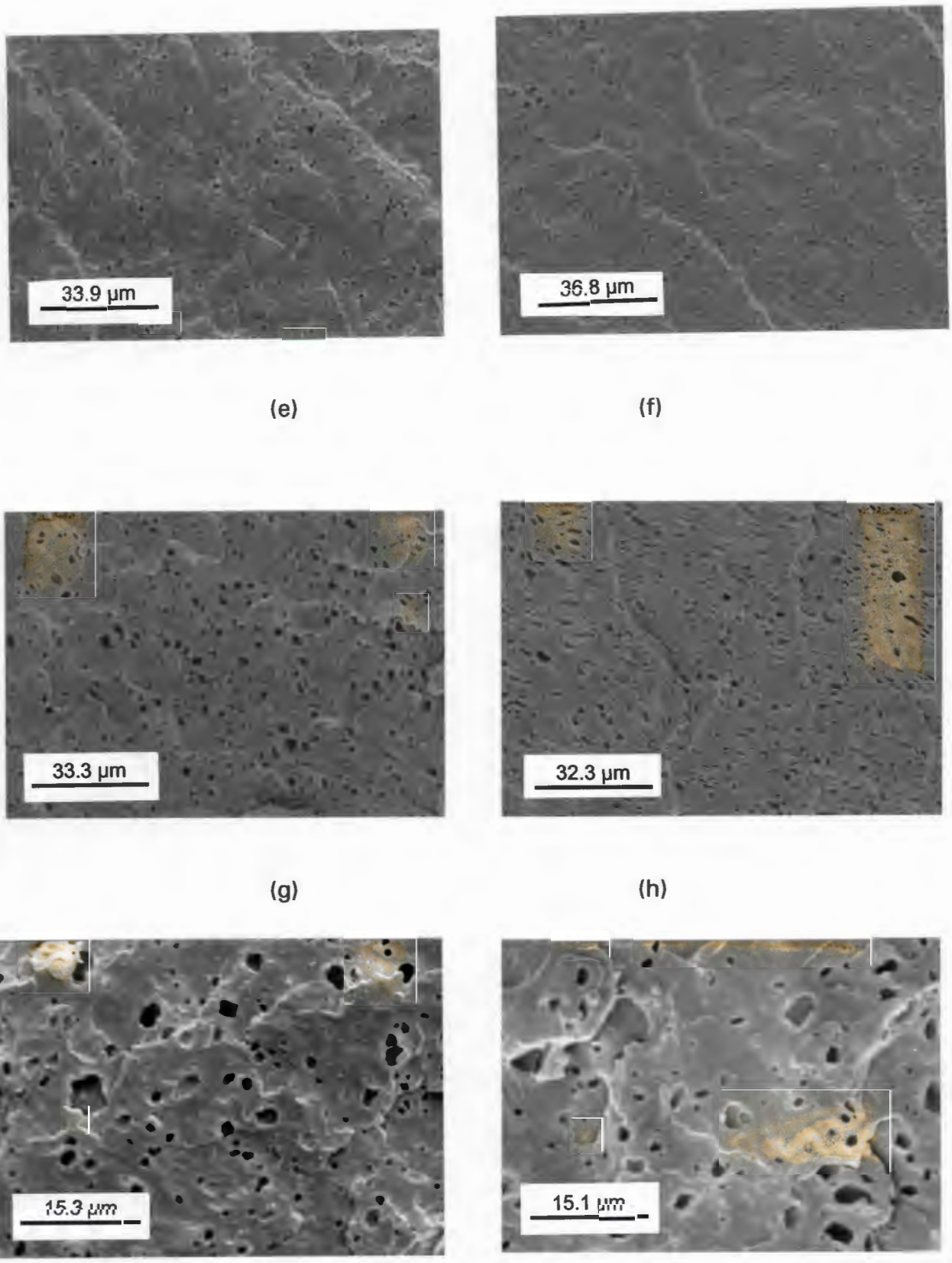

Figure 4.15 SEM micrographs showing the microstructure of the copolymer grades, *viz.*: (a) 2349 MC, (b) 2448 TC, (c) 2648 RC, (d) 2900 H, (e) 2340 PC, (f) 2540 H, (g) 2602 E, (h) 2900 H, (i) 2648 PC-2337 and (j) 2648 PC-2656.

Scanning electron microscopy results are summarised in Table 4.8 as the average values of the cross-sectional diameter, the inter-particle spacing and the ratio between inter-particle spacing and particle size of the ethylene-propylene rubber particles. The data for particle size in Table 4.8 does not show any conclusive trends with respect to ethylene content. This can be attributed to the fact that particle size is also a function of the extrusion and injection moulding processing conditions. The broad molecular weight distribution grades generally show a smaller particle size except for grade 2900 H that shows a slightly higher particle size.

The data in Table 4.8 also shows that there is a general trend of large inter-particle spacing at low ethylene content and a small inter-particle spacing at high ethylene content. Grade 2600 PC shows a high inter-particle spacing when compared to grades of similar ethylene content. The data in Table 4.8 show a relatively higher inter-particle spacing to size ratio is obtained for the low ethylene content grades. This trend can be attributed to the large inter-particle spacing generally displayed by the low ethylene content grades.

Grade	*Ethylene Content (%)*	*Particle Size (μm)*	*Inter-particle Spacing (μm)*	*Inter-particle Spacing/Size*
2340 PC	6.2	0.98±0.3	7.13±3.5	7.05±1.4
2349 MC	7.7	1.81±1.4	9.06±3.9	5.87±2.0
2448 TC	9.5	0.98±0.4	8.81±4.0	8.92±1.2
2540 H	11.8	0.84	5.28	6.29
2600 PC	11.8	1.70	9.65	5.68
2602 E	12.7	0.96±0.3	4.68±0.4	5.04±1.1
2648 PC	11.8	1.22±0.3	6.50±1.5	5.42±0.8
2648 RC	11.7	0.80±0.1	5.49±2.5	6.86±2.8
2900 H	22.4	1.36	6.05	4.45

Table 4.8: Data obtained from the measurements made on the SEM micrographs for the various copolymers.

4.4.1.1 Effect of Ethylene Content on Microstructure

The data for the ratio between inter-particle spacing and particle size is plotted in Figure 4.16 and shows an exponential decrease with increasing ethylene content. The grades in the 23_ _ series do not seem to follow the general trend. The exponential decrease can be understood by considering that increasing the ethylene content ends up balancing the ratio through either increasing the particle size or decreasing the inter-particle spacing.

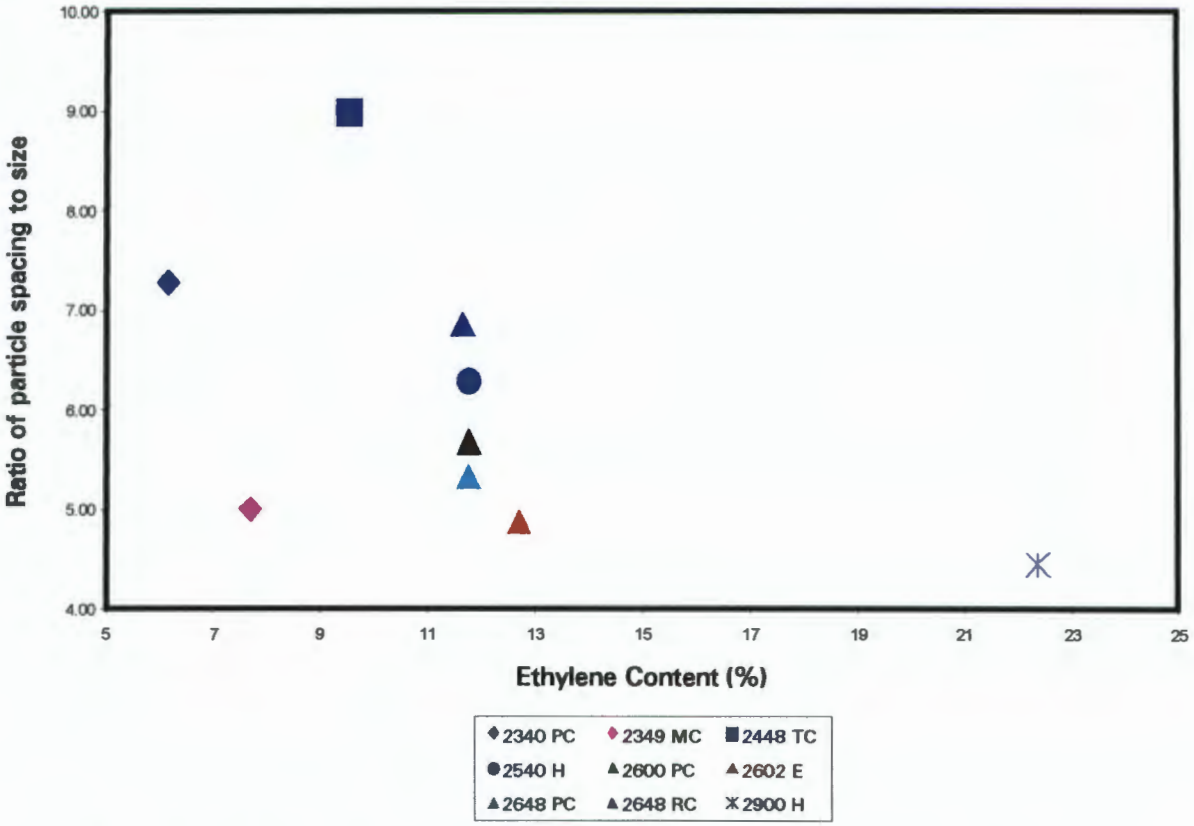

Figure 4.16: The effect of % C_2 on the microstructure of the various copolymers.

4.4.1.2 Effect of the Melt Flow Index on the Microstructure

Figure 4.17 shows a general increase in the ratio between the rubber inter-particle spacing and size as the melt flow index increases. The controlled rheology grades seem to have their own trend, which is more or less a linear increase with increasing MFI. The grades with a broad

molecular weight distribution show a very sharp increase in the ratio between the inter-particle spacing and size with increasing MFI.

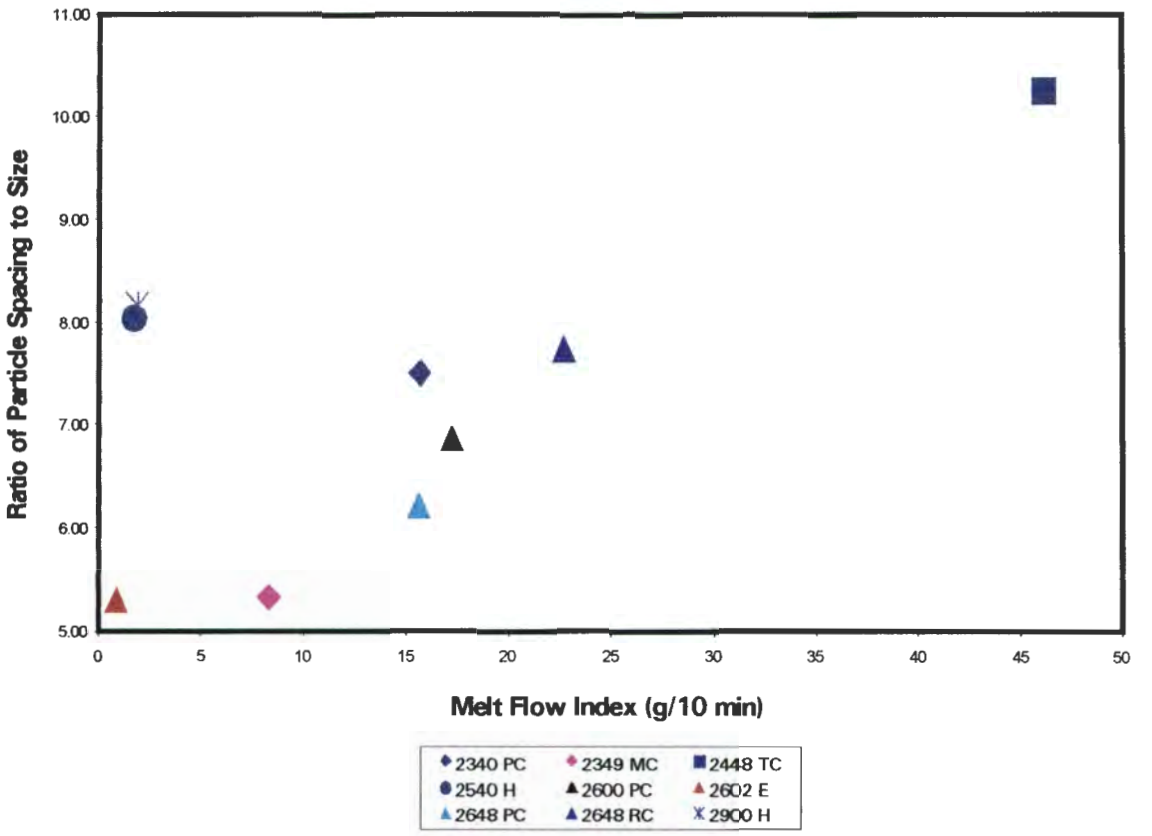

Figure 4.17: The effect of the MFI on the microstructure of the various copolymers.

4.4.2 Transmission Electron Microscopy

Typical micrographs obtained from the transmission electron microscope (TEM) are shown in Figures 4.18 (a) and (b). The pictures show the microstructure of the rubber particles, which was not possible to see with the SEM. Rubber particles were found as single entities although most of the particles were agglomerated as shown in Figure 4.18 (a). This micrograph shows a rubber particle composed of light crystalline regions and dark amorphous regions. In Figure 4.18 (b) thin lamellae (arrowed) of approximately 15 to 20 nm thick are discernible.

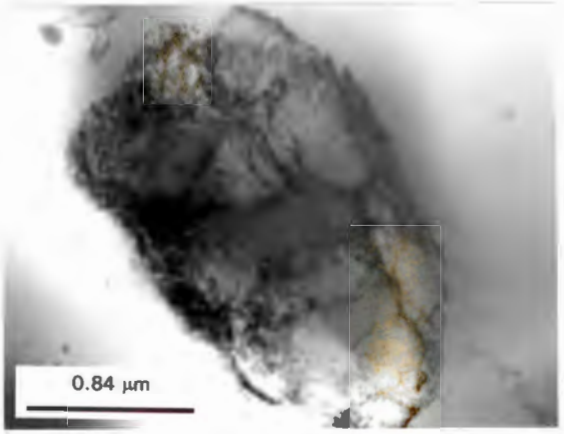

(a)

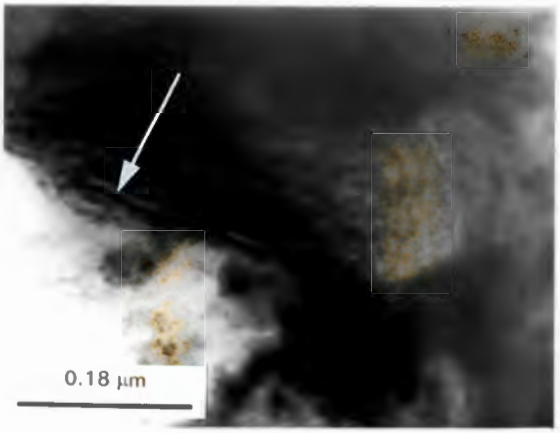

(b)

Figure 4.18: TEM micrographs of grade 2600 PC showing (a) the rubber particle microstructure and (b) the lamellae (arrowed) that can be observed within the EPR.

4.5 THERMAL CHARACTERISATION

4.5.1 Dynamic Mechanical Thermal Analysis (DMTA)

The glass transition temperature of the copolymers was determined from DMTA traces. The limitation of the tests was that the lowest attainable temperature was -65 °C and as such any thermal events occurring below that temperature could not be observed. Figures 4.19 (a) to (c) show the loss modulus (E'') plotted against the temperature scan for three grades of polymers in order of increasing ethylene content.

For grade 2340 PC in Figure 4.19 (a) the β_1 peak for the T*g* of the homopolymer matrix is well defined but the (β_2) peak due to molecular relaxations within the rubber phase is less defined. For grade 2648 PC in Figure 4.19 (b) there is a clear separation of the two β peaks. The β_2 peak has been shifted to much lower temperatures by the increase in ethylene content. In addition, for grade 2900 H in Figure 4.19 (c), the β peaks are well resolved. The β_2 peak appears at a slightly lower temperature than for grade 2648 PC.

In low temperature applications the molecular relaxations within the EPR (β_2 peak) are the most important for high impact strength. The β_2 peak appears to increase in intensity whilst the β_1 peak decreases in intensity with increasing ethylene content. This difference in peak height is in agreement with the observed impact strength of the grades tabulated in Table 4.9. The α peak can be ascribed to the molecular transitions within the crystalline regions of the isotactic polypropylene matrix.

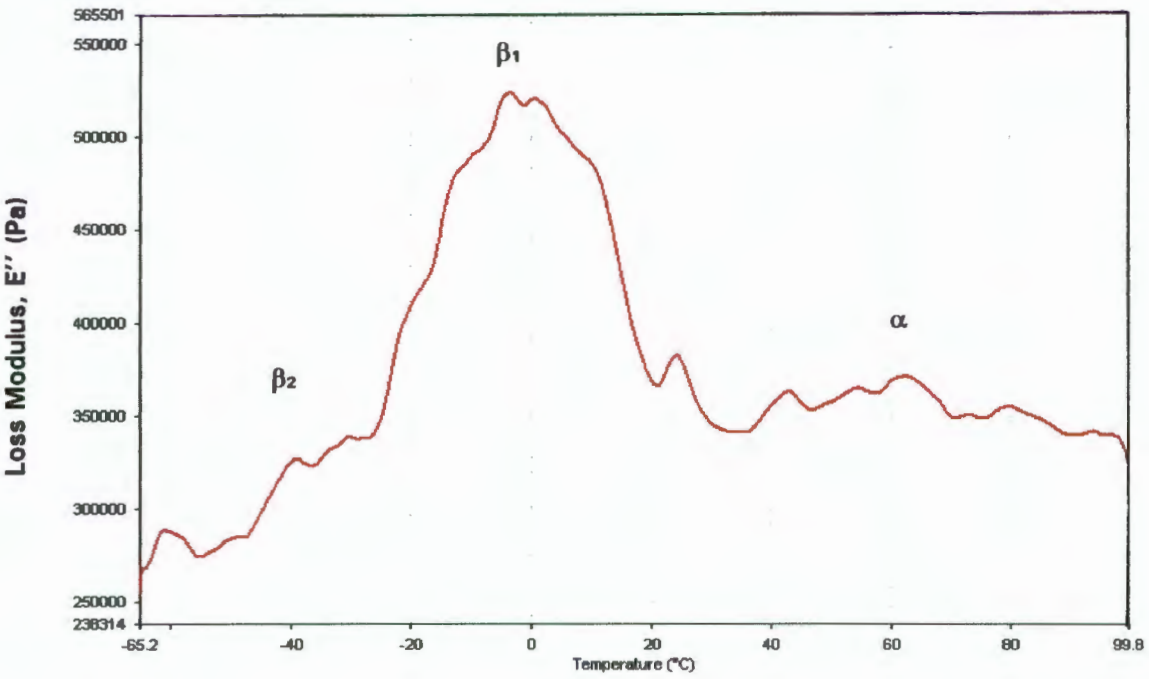
Loss Modulus, E'' (Pa)
565501
550000
500000
450000
400000
350000
300000
250000
238314
β1
β2
α
-65.2
-40
-20
0
20
40
60
80
99.8
Temperature (°C)

(a)

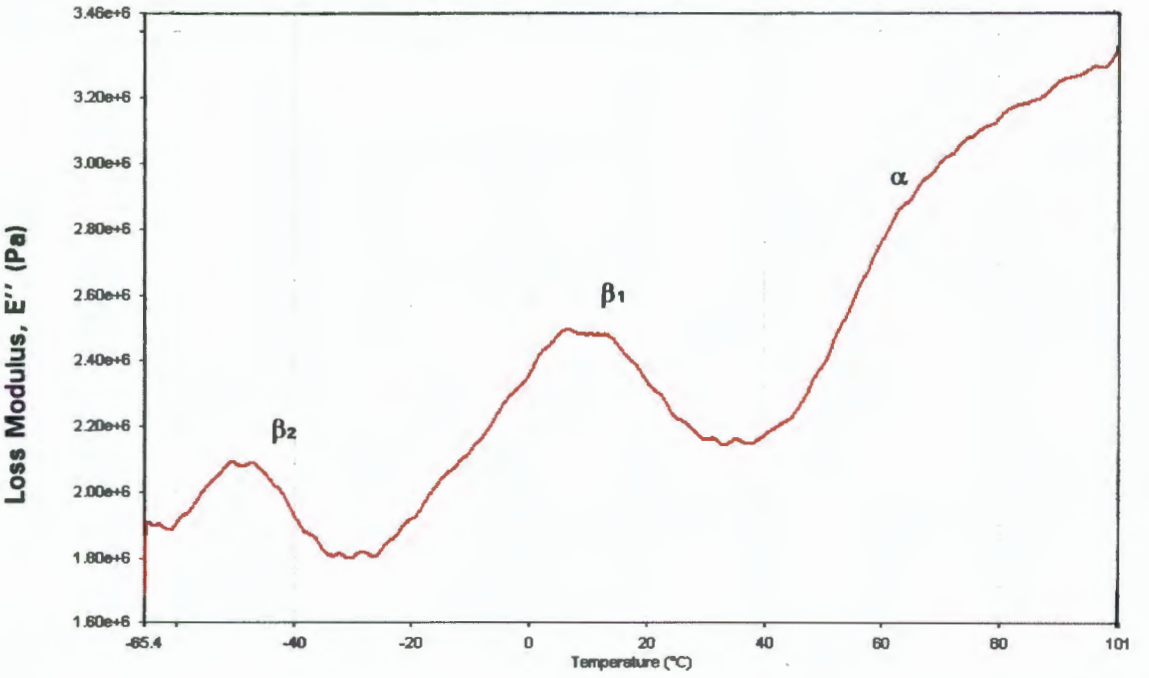
Loss Modulus, E'' (Pa)
3.46e+6
3.20e+6
3.00e+6
2.80e+6
2.60e+6
2.40e+6
2.20e+6
2.00e+6
1.80e+6
1.60e+6
α
β1
β2
-65.4
-40
-20
0
20
40
60
80
101
Temperature (°C)

(b)

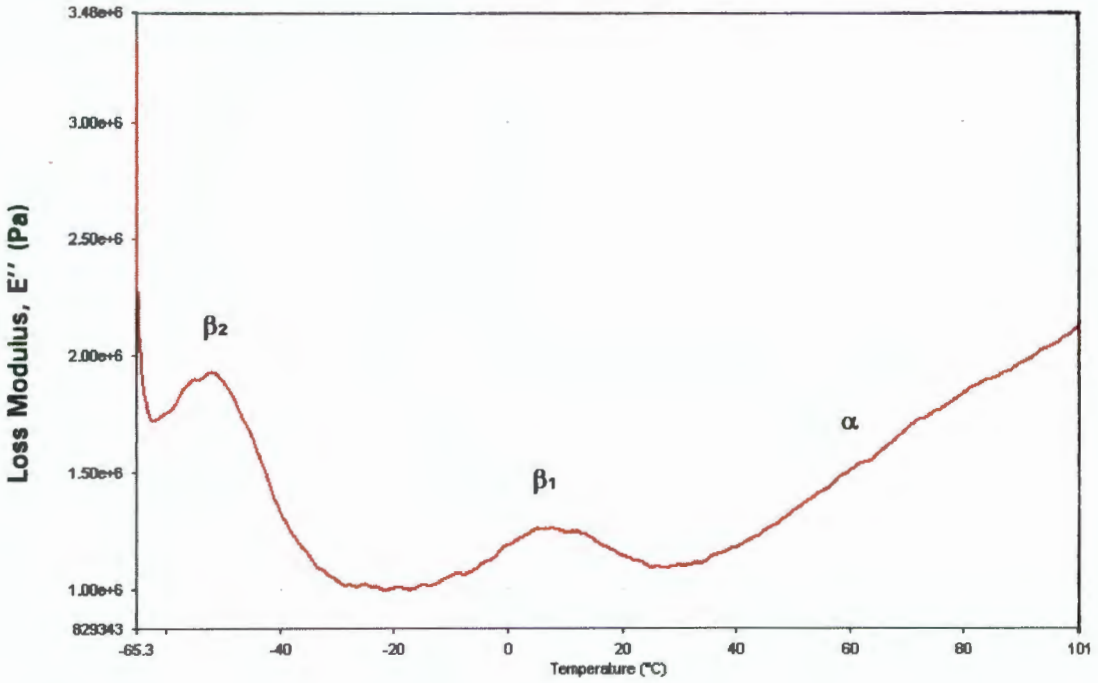

(c)

Figure 4.19: Loss modulus traces for the (a) 2340 PC, (b) 2648 PC and (c) 2900 H grades.

Grade	*Ethylene Content (%)*	*Impact Strength (kJ/m^2)*	*α-Peak (°C)*	*β_1 - Peak (°C)*	*β_2 - Peak (°C)*
2340 PC	7.08	8.72	64.3	1.5	-40
2648 PC	11.36	9.72	64.6	9.8	-48.7
2900 H	22.35	54.22	63.3	8	-52

Table 4.9: The temperatures at which molecular transitions occur as peaks for selected copolymer grades.

4.5.2 Differential Thermal Analysis (DTA)

The curves in Figure 4.20 show the thermal events occurring in the materials as the temperature increases. The DTA curves show the thermal transitions as the copolymers are heated from room temperature to 500 °C. There is more energy absorbed by the 2349 MC grade during the melting process as shown by the sharper and bigger area under the peak at 165 °C.

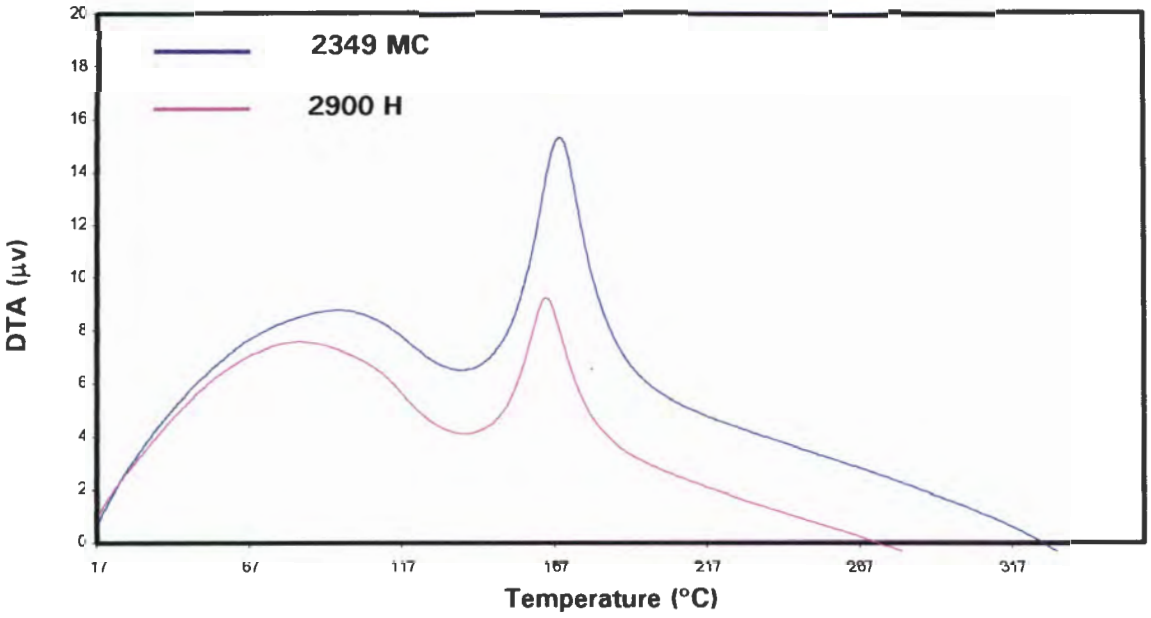

Figure 4.20: Effect of % C_2 on the thermal behaviour of selected copolymers.

4.5.3 Thermogravimetry (TG)

Figure 4.21 shows the thermogravimetric analysis curves for the 2349 MC and 2900 H grades. The copolymer grades investigated show similar degradation behaviour despite the composition differences.

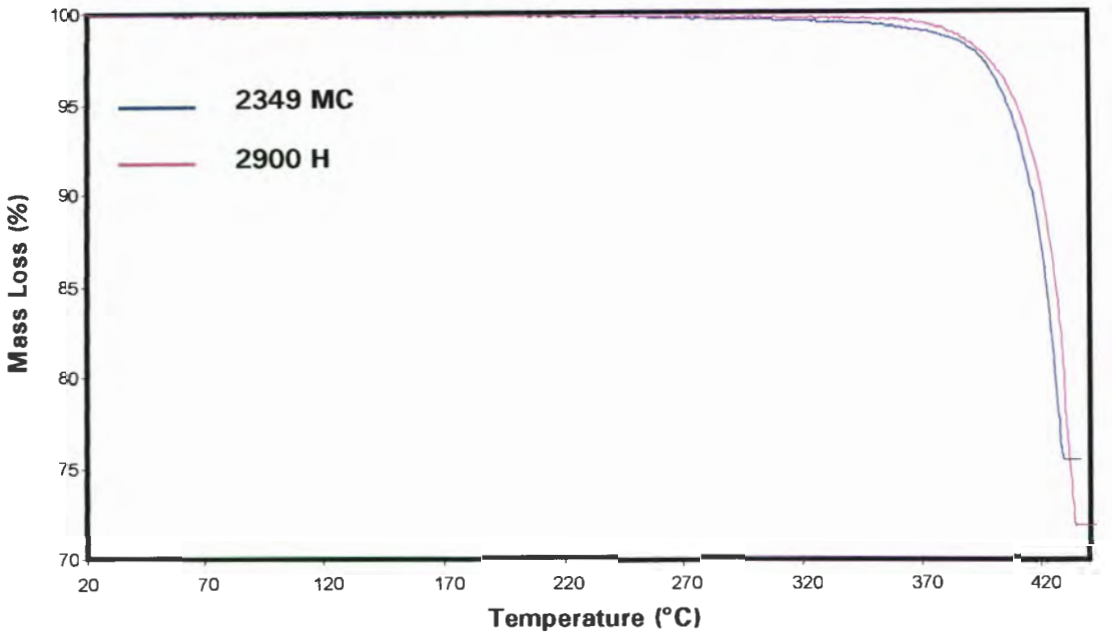

Figure 4.21: The mass loss with temperature for grades 2349 MC and 2900 H.

4.5.4 Differential Scanning Calorimetry (DSC)

DSC scans were used in section 4.2.1 to determine the degree of crystallinity, but from the scans also the melting temperatures as the peak maximum, can be obtained. All the scans showed one endothermic peak at about 165 °C that is attributed to the melting peak of the crystalline polypropylene matrix. Grade 2900 H showed two endothermic peaks, with the extra peak occurring at about 120 °C and is attributed to the melting peak of polyethylene within the copolymer. This phenomenon suggests that the polyethylene is present in the copolymer in such a high percentage that it is able to crystallise on its own. Figure 4.22 (a) shows a DSC scan for grade 2648 RC which is typical of DSC scans of all the other grades, the exception being grade 2900 H which is shown in Figure 4.22 (b).

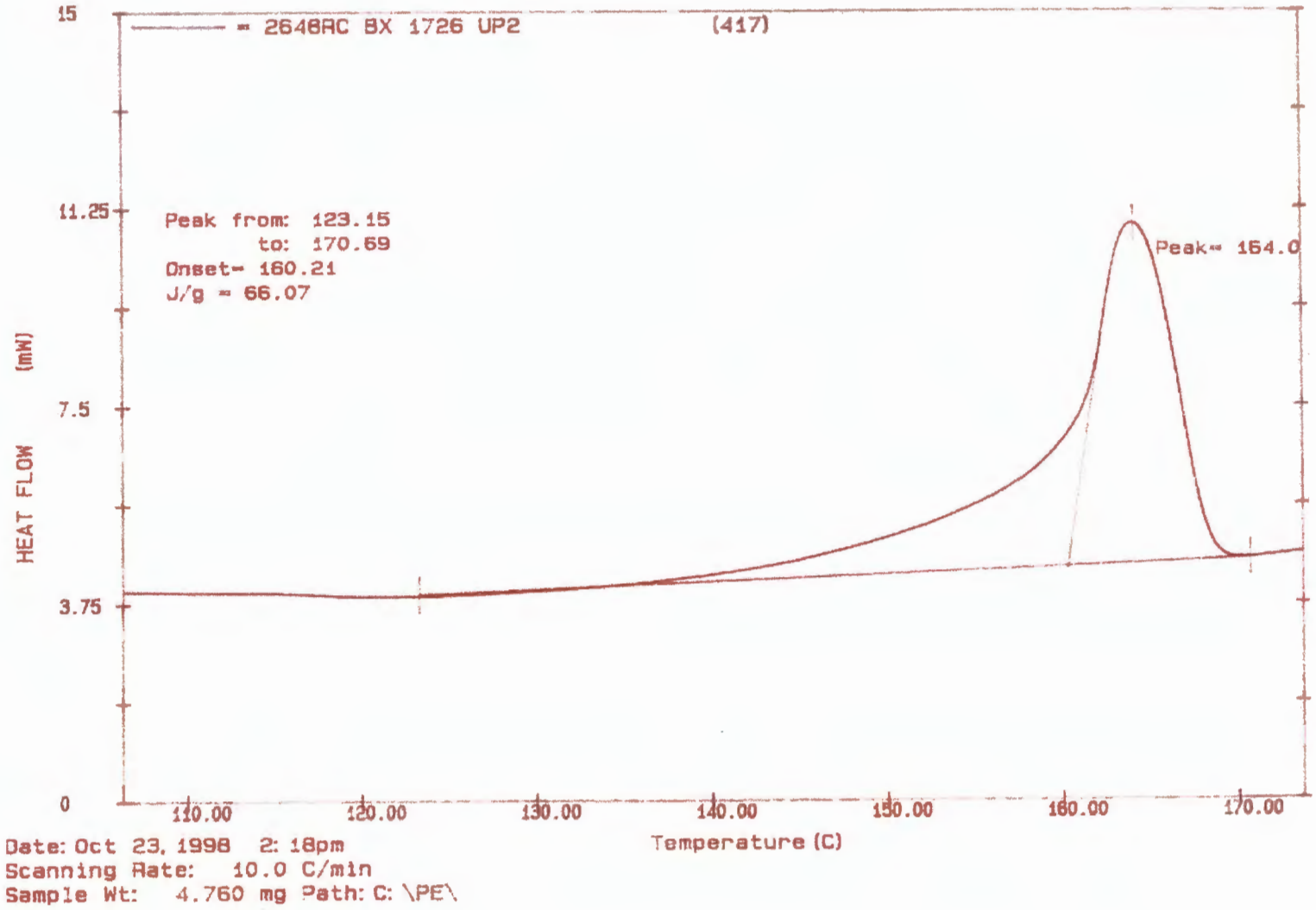

Figure 4.22 (a): A DSC scan of grade 2648 RC showing the typical polypropylene melting peak.

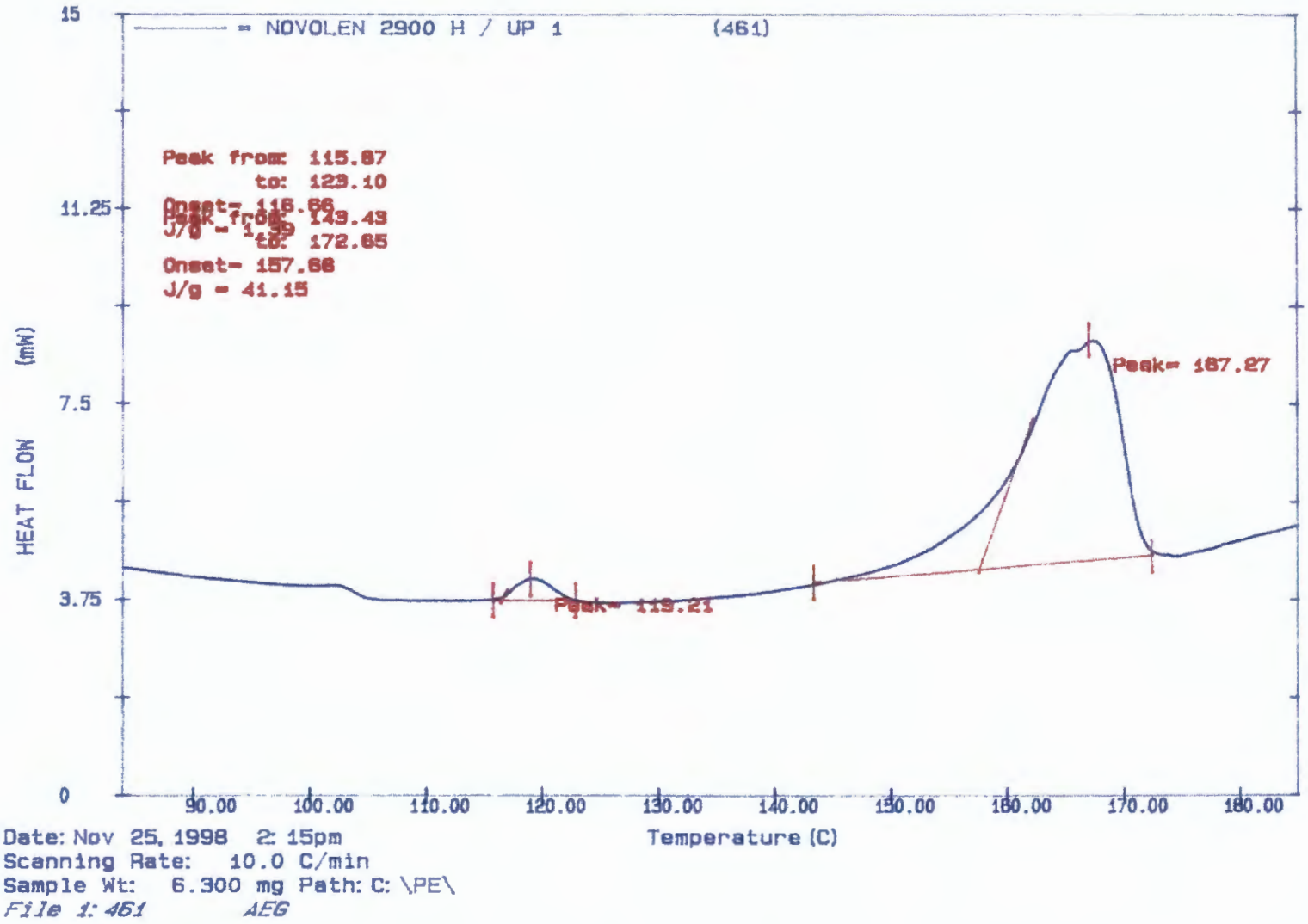

Figure 4.22 (b): A DSC scan of grade 2900 H showing two melting peaks for polyethylene (120 °C) and polypropylene (165 °C).

The results obtained from the DSC scans are presented in Table 4.10 as the average melting temperatures. The effect of ethylene content and molecular weight on the average melting temperature is not apparent from these results since the melting point for all the grades at about 165 °C is due to the polypropylene only.

Grade	*Ethylene Content (%)*	*MFI (g/10 min)*	*Melting Temperature (°C)*
2340 PC	6.2	15.7	166.4±0.2
2349 MC	7.7	8.3	166.5±2.1
2448 TC	9.5	46.1	165.1±0.8
2540 H	11.8	1.7	166.4
2600 PC	11.8	17.2	165.8
2602 E	12.7	0.9	165.5±0.8
2648 PC	11.8	15.6	165.2±0.8
2648 RC	11.7	22.7	164.1±2.1
2900 H	22.4	1.8	165.8

Table 4.10: The average melting temperatures of the various copolymer samples.

CHAPTER 5

DISCUSSION

5.1 INTRODUCTION

It is well known that many molecular parameters operate simultaneously and affect the mechanical and physical properties in complex and often unexpected ways. In addition, small differences in the processing parameters introduce more variability into the product. Hence, any new information of how these parameters govern the properties can lead to valuable contributions to our overall understanding of copolymers. The following discussion describes systematically how parameters and factors such as crystallinity, crystal structure, molecular weight, rubber (or ethylene) content, size and uniformity of the rubber phase and phase morphology can influence the properties. It was deemed necessary to repeat certain concepts in the various sections because of the interplay between the factors governing the properties.

5.2 THE EFFECT OF ETHYLENE CONTENT ON THE MICROSTRUCTURE

5.2.1 XRD and DSC Analysis

Several researchers [19,20,30,42,43-51] have studied the effect of ethylene and other co-monomers on the microstructure of block copolymers. The methods used to improve the low temperature toughness is either blending or copolymerizing polypropylene with the copolymer or

comonomer, respectively. Polyethylene and polypropylene are physically not compatible; hence the microstructure is that of two immiscible blends. The addition of a suitable compatibilizer such as ethylene/propylene/diene copolymer (EPDM) or ethylene vinyl acetate copolymer (EVA) can overcome the incompatibility of polyethylene and polypropylene. The microstructures of copolymers have also been studied with comonomers such as ethylene, butene and hexene[48].

The 'R21' value was used to determine the ethylene content and it was found that a linear relationship exists between these two parameters. The effect of increasing the % ethylene on the crystallinity of the copolymers was determined by both DSC and XRD. The XRD traces were useful in that information on the crystal structure could be obtained in addition to the percentage crystallinity. Although the two techniques gave disparate values of crystallinity, there was nevertheless a positive and linear correlation between the two techniques of crystallinity. As the ethylene content is increased, the amount of rubber (EPR) increases proportionately. An introduction of ethylene into the backbone increases the amount of irregularity and hence decreases the amount of crystallisable material.

The DSC scans showed smaller and less defined melting peaks for polypropylene at approximately 165 °C, with increasing ethylene. This can be attributed to the increased amount of EPR in the copolymers. However, when the ethylene content was relatively high (at ~20 % in 2900 H) separate endothermic peaks at 120 °C and 167 °C were observed. This peak at 120 °C is attributed to crystallisable ethylene sequences in 2900 H. Generally the amount of crystallisable (or crystalline) polyethylene is low and can be determined using techniques such as nuclear magnetic resonance (NMR)[12]. Using the heat of fusion of 100 % crystalline polyethylene (293 J/g[52]) it is estimated that grade 2900 H (see Figure 4.22) contains about 0.5 % crystallisable ethylene segments. The XRD scans, however, did not show the presence of an ethylene peak normally found at $2\theta = 23.4°$ due to the (200) crystallographic plane[12].

The presence of crystallisable ethylene sequences in EPDM was confirmed by Karger-Kocsis[46] using a dynamic mechanical technique and in PP copolymers by Chundury *et al*[49] using DSC. It is thought that the broadening endothermic peaks are due to randomized ethylene and propylene units in the EPR[49].

XRD data showed that the apparent crystal size (E) of isotactic polypropylene in the presence of EPR decreased with increasing ethylene content. These crystals which are of the order of 20 nm are of similar size to those obtained by D'Orazio *et al*[51]. These differences are due to variations in the crystallisation temperatures as well as the moulding conditions. Higher crystallisation and mould temperatures favour thicker crystallite or lamellae sizes. In melt crystallised polypropylene the predominant crystal structure is the α monoclinic form and occasionally the β hexagonal form is observed. The β form was predominantly observed in several of the nucleated batches. For these batches the relative contribution of the β was determined mathematically and was found to be about 17 %. Some researchers have found that the impact resistance of isotactic polypropylene improved when a β-nucleating agent was added [45,53].

In this study, it cannot conclusively be determined if the batches with the β peak had higher impact strength due to variations in ethylene content, although all the batches with the β peaks had good impact strengths. The high ethylene content grades (2900 H and 2600 PC) were non-nucleated grades and did not have the β peak. The XRD traces showed that grade 2349 MC in Figure 4.3 (a) batch 2722 did not have a $(300)_\beta$ peak whereas in batch 3364 it was present. It was also noted that all the latter batches of 2349 MC had the β peak present. If the grade is produced under the same standard conditions, no significant differences between the batches are to be expected. Since differences are observed, the processing conditions at the plant and during injection moulding come under the spotlight. The differences can be attributed to fluctuations in the plant processing variables such as the MFI, reactor temperature, % C_2 and also the formulation and activity of the catalyst system used. In general, the addition of a nucleating agent increases the degree of crystallinity.

5.2.2 SEM and TEM Analysis

In order to understand the relationship between microstructure and mechanical properties, a detailed study was conducted on the effect of EPR particle size, distribution and particle morphology. Heptane was used to etch the copolymers by dissolving the rubber phase and hence it is possible to get an indication of their average size and distribution within the polypropylene matrix. The SEM micrographs were used for this analysis and at least 100 particles are considered for each batch. The rubber particle density increases with increasing ethylene content because the ethylene is used in the formation of the ethylene-propylene rubber (EPR) phase. Particle size varied between 0.8 μm and 1.5 μm. At very high ethylene content the viscosity of the rubber phase becomes significant so that the viscosity ratio becomes very high and the particles coalesce to form large rubber particles[32].

The results indicated no definite relation between either particle size or inter-particle spacing with ethylene content. However, when the *ratio* between the inter-particle spacing and the particle size was plotted, trends against % C_2 and MFI were observed (Figures 4.16 and 4.17). The decrease in the ratio with increasing % C_2 can be attributed to the decrease in inter-particle spacing and at the same time an increase in particle size as the percentage ethylene increases. When considering the rubber morphology factors such as the shear rate in the extruder and injection moulding conditions need to be considered. This can be achieved by increasing the shear rate in the extruder, whilst noting that the viscosity of the matrix and rubber is shear rate dependent. A small and narrow particle size distribution can also be achieved by decreasing the surface tension between the two phases. The better compatibility between the two phases translates into better impact properties. The barrel temperatures should be as low as possible during injection moulding.

A general increase in the ratio between the rubber inter-particle spacing and the particle size as the melt flow index increases is observed (Figure 4.17). The high MFI grades seem to follow a linear trend with increase in inter-particle spacing to size ratio with increasing MFI. This can be

attributed to the further shearing processes, during vis-breaking, which can either break up agglomerated particles, thus resulting in a smaller particle size, or bring together smaller particles to form bigger ones and thus increase inter-particle spacing. A recent study conducted by Kim *et al* showed that the ratio of centre-to-centre-distance to particle diameter (CCD/D) plays an important role in the toughening and micro-mechanical deformation process[20]. In their investigations the copolymers that had several inclusions within the rubber particles had higher toughness values and failed by crazing. These copolymers had a relatively small CCD/D ratio. In this study, the grades with high ethylene content had smaller CCD/D ratios and these copolymers had the higher impact strengths. The limited data that we had suggested that this ratio is important in determining impact strength as inferred from Figure 5.1 below. In order to improve the toughness, the internal phase morphology of the rubber should be considered together with the CCD/D ratio.

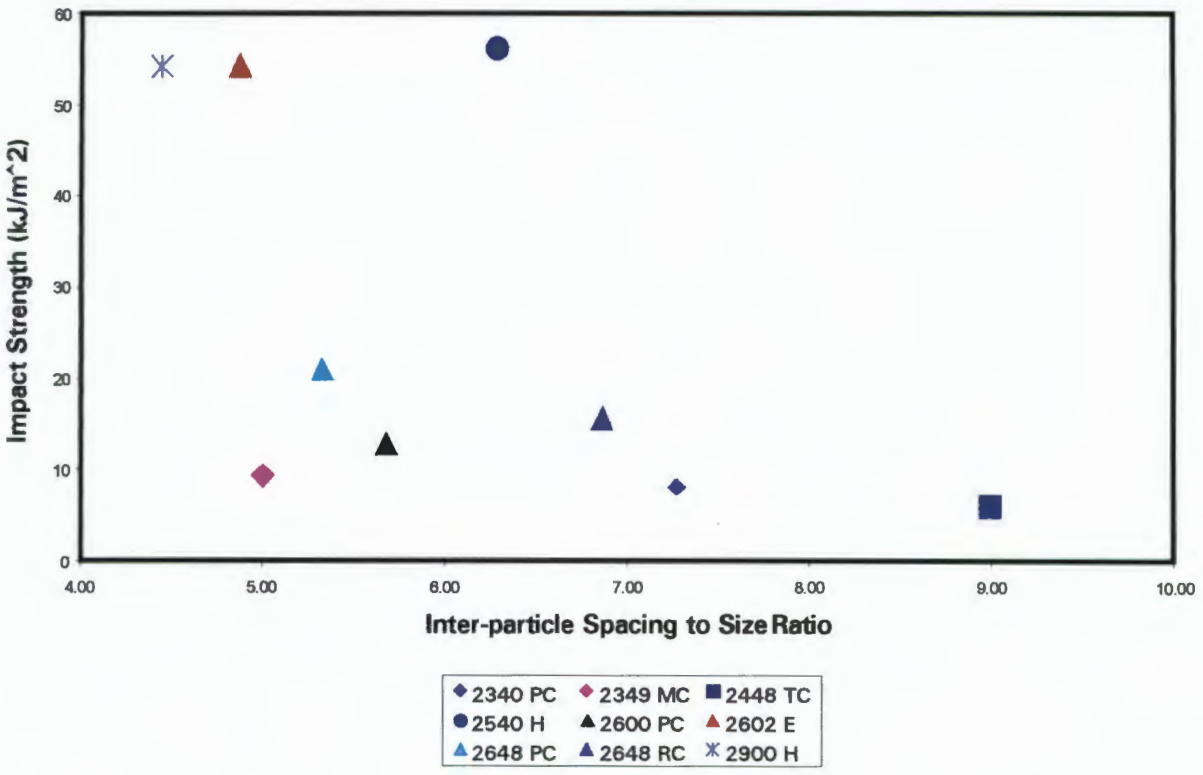

Figure 5.1: Effect of the inter-particle spacing to size ratio on impact strength.

TEM makes it possible to study the individual phases of the copolymer in much more detail. This compensates for the detail lost during the etching process in preparing specimens for the SEM. For a complete structural elucidation, the two techniques should be used to complement each other. TEM studies (Figure 4.18) showed that several of the larger rubber particles are conglomerates of smaller ones. This was confirmed in studies by Kim *et al*[20] and Rűmpler *et al*[54]. These studies showed that in block copolymer systems with a high ethylene content, the EPR particles with several inclusions are more effective for toughening polypropylene. Systems modified with several inclusions dissipate more impact energy through multiple cavitation and crazing processes than single inclusions does through shear yielding[20]. From Figure 4.18, one can see that the rubber particle consists of several 'crystalline' micro-domains. The matrix consists of fine randomly arranged polypropylene lamellae that are distinguished from the coarser lamellae within the rubber phase. The coarser lamellae are believed to be crystallisable PE_xP sequences with a high C_2 content[42].

5.2.3 DMTA and DTA Analysis

Ethylene content seems to be the most important property determining molecular variable in poly–(propylene-ethylene) copolymers as it affects variables such as crystallinity. It occurs in the copolymer as part of the dispersed ethylene-propylene rubber phase. Through factors such as its amount, size, distribution, crystallinity, insertion sequence and adhesion, all the copolymer properties are affected. Multiple transitions by DMA confirm that the phases present in poly–(propylene-ethylene) copolymers are immiscible. It should be noted that the actual values of T*g* and other relaxation temperatures of the copolymer are a function of the frequency and type of thermal analyser used.

The peaks in Figures 4.19 (a) to (c) are summarised in Table 4.8. The grades show a decrease in the temperature at which the β_2 transition occurs as the ethylene content increases. The intensity of the β_2 peak increases whilst the intensity of the β_1 peak decreases. The β_2 peak is the T*g* of the EPR whilst the β_1 is the T*g* of the polypropylene. The

impact strength increases with increase in the intensity of the β_2 peak. The β_2-transition temperature shifts to lower temperatures as the comonomer content increases from grade to grade. The higher intensity indicates an increased capacity of the polymer to absorb mechanical energy through dissipation by rearrangements of chain segments in the amorphous EPR. The α-transition at about 64 °C is displayed by all the copolymer grades and is due to the transitions in the crystalline regions of the copolymer. Techniques such as DMTA is a valuable tool for understanding the impact behaviour of copolymers and should preferably be used in conjunction with other techniques, such as electron microscopy, temperature rising elution fractionation (TREF) and nuclear magnetic resonance (NMR).

The similarity in the degradation behaviour of the copolymers is due to the fact that the copolymers are mainly composed of carbon and hydrogen, the only difference being the respective concentrations of ethylene and propylene in the backbone. It is possible that copolymers with large *%'s* of ethylene concentrations would give different decomposition behaviour than copolymers with relatively small concentrations. DSC thermograms showed that it was possible to obtain the endotherms due to ethylene in those copolymer grades containing a high % ethylene. In addition, the % crystallinity is useful to correlate with mechanical properties that mainly depend on an ordered crystal structure. An increase in ethylene content produced a concomitant decrease in the % crystallinity of the copolymers.

5.3 THE EFFECT OF ETHYLENE CONTENT ON THE MECHANICAL PROPERTIES

5.3.1 Properties that Depend on Crystallinity

The mechanical characterisation of the copolymers shows a clear dependence of the microstructure and composition on various mechanical properties. Small strain properties (elastic properties) such as hardness, tensile yield strength and modulus (or stiffness) depends on the degree of

crystallinity and to a smaller extent on the molecular weight. The micro-hardness was found to decrease with increasing ethylene content. The trend shown (Figure 4.6) is similar to that displayed by crystallinity when plotted against the ethylene content. This is because hardness is a small strain property and therefore depends mainly on the degree of crystallinity. The Vickers micro-hardness test is a simple test that yields information about the microstructure and mechanical behaviour of materials. For polymeric materials, a monotonic increase in hardness with increasing crystallinity can also be related to yield stress and elastic modulus[55].

The tensile properties such as yield strength and elastic modulus also decrease with increasing ethylene content since they are also small strain properties and therefore dependent on the degree of crystallinity. Similar trends of decreasing yield strength and modulus with increasing ethylene content during tensile tests, was observed by Fernando and Williams[56]. Similarly, the three point bending flexural modulus was also found to decrease with increasing ethylene content. This trend is also due to a decrease in the degree of crystallinity since flexural modulus is also a small strain property[16]. The addition of a nucleating agent or fillers such as carbon black or talc have a stiffening and strengthening effect on the copolymers[57,58]. Figure 5.2 shows that the flexural modulus is inversely proportional to ethylene content whilst the impact strength increases with increasing ethylene content. These trends are similar to those shown in Figure 2.4[16].

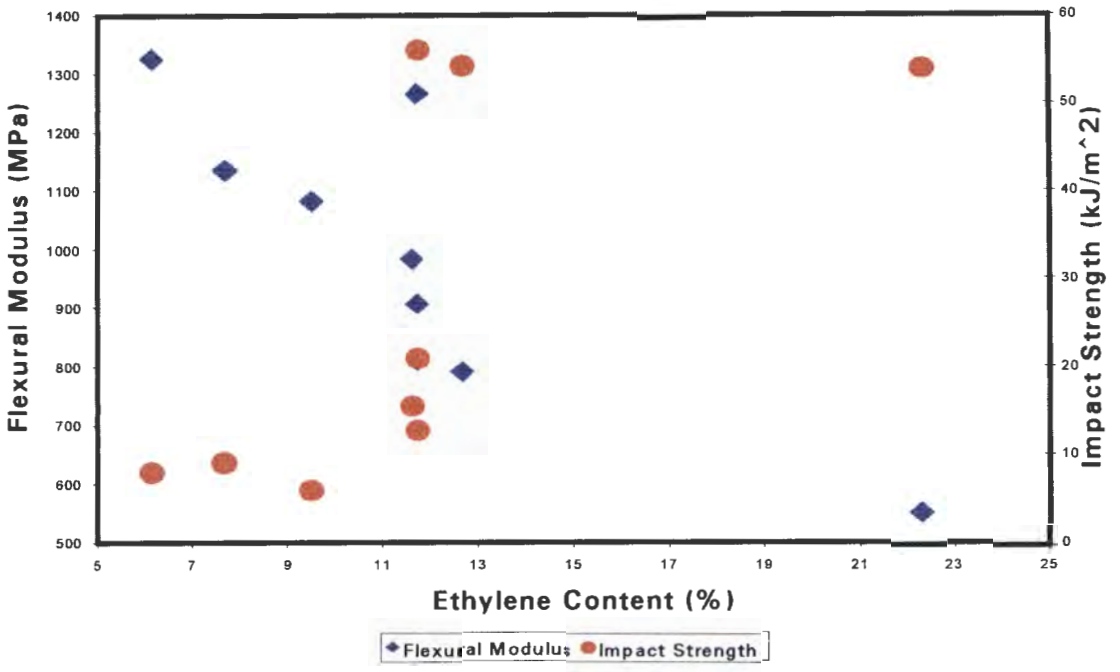

Figure 5.2: Effect of ethylene content on the flexural modulus and impact strength.

5.3.2 *Properties that Depend on Molecular Weight and Molecular Weight Distribution*

In studies conducted with polypropylene homopolymers by Marcus *et al*[24], larger flexural moduli were obtained with broader molecular weight distribution polypropylenes at similar molecular weight and % crystallinities. The authors inferred that the larger flexural moduli obtained for the broad MWD reactor grades is more dependent on the presence of tie molecules rather than small changes in crystallinity in the homopolymers. The tie molecules connecting lamellae are believed to act as a stiffening agent in high molecular weight and broad MWD materials. The flexural moduli decreased substantially on vis-breaking due to the relative absence of long chain tie molecules. It is believed that the vis-breaking process for the copolymers have a similar effect on stiffness but is outweighed by the increase in crystallinity due to the presence of a nucleating agent.

The impact strength is dependent on large strain properties such as % elongation. The long chains in high molecular weight grades are able to

absorb more energy through changes of conformation and through the increased tie molecule density. This renders the high molecular weight copolymers tougher during an impact event[22]. The percentage elongation increases with increasing ethylene content and this can be attributed to the lowered degree of crystallinity. The impact strength also increases with increasing ethylene content alone[16] so that these two molecular parameters together result in a substantial increase in impact strength. Figure 4.7 shows two distinct regions of toughness separated by a transition region at an ethylene content of about 12 %. The high toughness is due to a high ethylene content that reduces the glass transition temperature by reducing the degree of crystallinity[18]. It should be borne in mind that although the ethylene content and molecular weight influence impact strength, modification of the crystal structure through nucleation also contributes to improved overall properties. This can be seen by considering that grade 2540 H has a slightly higher impact strength and much higher stiffness than grade 2900 H, see Tables 4.5 and 4.6.

CHAPTER 6

SUMMARY AND CONCLUSIONS

6.1 SUMMARY

The overall effect of some of the molecular variables studied is summarised in Table 6.1 below. These parameters are by no means exhaustive, whilst it should be borne in mind that if these individual parameters operate together they influence each other in complex and elaborate ways.

Property	↑ *Ethylene Content (%)*	↑ *MFI (g/10 min)*	*+Nucleation*
Impact Strength	↑	↓	↑
Flexural Modulus	↓	↔	↑
Tensile Modulus	↓	↔	↑
Tensile Strength	↓	↓	↑
% Elongation	↑	↔	↔
Melting Point	↔	↔	↑
Tg (EPR)	↓	↔	↔

Table 6.1: Effect of the ethylene content, the melt flow index (MFI) and presence of a nucleating agent on the properties of the copolymers.

6.2 CONCLUSIONS

The work carried out during the course of this thesis has contributed to our understanding of the factors governing the properties of poly-(propylene-ethylene) copolymers. In particular the following conclusions are noteworthy:

1. High ethylene content, high molecular weight and nucleated grades with a narrow molecular weight distribution show the best balance between the impact strength and stiffness.

2. An increase in ethylene content leads to a significant increase in impact strength but has detrimental effects on small strain elastic properties such as flexural- and tensile modulus as well as hardness.

3. The impact toughness can further be improved through controlled manipulation of the EPR microstructure. The inter-particle spacing of the EPR to size ratio (CCD/D) should be as small as possible, at specific ethylene contents. In addition, the inter-particle spacing should be such that their stress fields overlap.

4. Large EPR particles tend to give high impact strength, whilst small particles lead to higher stiffness. A balance of uniformly distributed particle size should be sought for good mechanical properties.

5. The results tentatively show that the formation of the β hexagonal form is advantageous for impact properties.

FUTURE WORK

- The TEM studies should be continued looking specifically on the rubber morphology of grades whose batches display significant differences in properties. The investigator should spend some time on the plant during production of the copolymers to be investigated and gather information such as the fluctuations in process variables. The extrusion process should be optimised with more emphasis on the morphology rather than the final MFI. Ideally, impact tests should be carried out at sub-zero temperatures. The Department of Materials Engineering has an instrumented drop weight impact tester that can be modified to test polymer plates at sub-zero temperatures.

- A more detailed study of the β phase and the influence of the β phase on the spherulitic structure. Some studies have shown that high levels of the β form lead to lower yield stresses and higher % elongations. The drop weight tester could be utilised to study the impact toughness of copolymers enhanced by the addition of say a β-nucleating agent. One could also use of techniques other than SEM and TEM to study the rubber phase. This could be based on interference polarized microscopy such as phase contrast microscopy.

- The impact strengths vary from test to test, for example Izod test values do not necessarily correlate with drop weight test results. The fracture toughness (K_{Ic}) and the fracture energy (G_c) can be found using techniques described in linear elastic fracture mechanics (LEFM).

REFERENCES

1 K. Marcus, N. Marshall and M. Domingo, *"Growth Opportunities for Versatile Polypropylene"*, in **Plastics** '94, The Plastics Institute of Southern Africa, 1994, p. 20.1.

2 R. Lieberman and P. C. Barbe, "*Propylene Polymers*", in **Encyclopaedia of Polymer Science and Engineering,** 2nd Edition, 13, 1998, p. 464.

3 M. R. Rifi, H. K. Ficker and D. A. Wolker, **SPE. ANTEC,** 1986, p. 316.

4 E. Albizzati, U. Giannini, G. Collina, L. Noristi and L. Resconi, *"Catalysts and Polymerizations"*, in **Polypropylene Handbook**, Ed., E. P. Moore, Jr., Hanser Publishers, Munich, 1996, p. 11.

5 S. M. Dwyer, O. M. Boutni and C. Shu, *"Compounded Polypropylene products"*, in **Polypropylene Handbook,** Ed., E. P. Moore, Jr., Hanser Publishers, Munich, 1996, p. 211.

6 H. Schwager, *"PP Reactor Blends"*, in **Polypropylene '92 World Congress,** 1992, p. II-4.1.

7 W. D. Callister, Jr., **Materials Science in Engineering – An Introduction,** 4th Edition, John Wiley & Sons, Inc., New York, 1996.

8 R. A. Phillips and M. D. Wolkowicz, *"Structure and Morphology"*, in **Polypropylene Handbook,** Ed., E. P. Moore, Jr., Hanser Publishers, Munich, 1996, p. 113.

9 G. Natta and P. Corradini, *"Structure and Properties of Isotactic Polypropylene"*, **Nuovo Cimento, Suppl.,** 15, 1960, p. 40.

10 A. Turner-Jones and A. J. Cobbold, *"The β Crystalline Form of Isotactic Polypropylene"*, **J. Polym. Sci. Part B,** 6, 1968, p. 539.

11 D. R. Morrow and B. A. Newman, *"Crystallisation of Low Molecular Weight Polypropylene Fractions"*, **J. Appl. Phys.,** 39, 1968, p.4944.

12 Y. Feng, X. Jin and J. N. Hay, *"Crystalline Structure of Propylene Ethylene Copolymer Fractions"*, **J. Appl. Polym. Sci.,** 68, 1998, p. 381.

13 J. Karger-Kocsis and J. Varga, *"Effects of β-α Transformation on the Static and Dynamic Tensile Behaviour of Isotactic Polypropylene"*, **J. Appl. Polym. Sci.,** 62, 1996, p. 291.

14 X. Zhang, J. Li, Z. Yin and J. Yin, *"Rheological Properties and Cystallisation Behaviour of Yittrium Oxide Filled Low Ethylene Content Polypropylene Copolymer",* **J. Appl. Polym. Sci.,** 63, 1996, p. 313.

15 J. Varga, *"Crystallisation, Melting and Supermolecular Structure of Isotactic Polypropylene",* in **Polypropylene: Structure, Blends and Composites,** Ed., J. Karger-Kocsis, Chapman and Hall, London, 1995, p. 57.

16 D. Del Duca and E. P. Moore, Jr., *"End-Use Properties"*, in **Polypropylene Handbook,** Ed., E. P. Moore, Jr., Hanser Publishers, Munich, 1996, p. 237.

17 K. Marcus, *"An Assessment of the Properties of Block Copolymers"*, **Polifin Internal Report,** 1998.

18 A. Eisenberg, "*The Glassy State and the Glass Transition*", in **Physical Properties of Polymers,** Ed., J. E. Mark, 2nd Edition, American Chemical Society, Washington, DC, 1993, p. 61.

19 Y. Feng, X. Jin and J. N. Hay, *"Dynamic Mechanical Behaviour Analysis for Low Ethylene Content Polypropylene Copolymers"*, **J. Appl. Polym. Sci.,** 68, 1998, p. 395.

20 G. M. Kim, G. H. Michler, M. Gahleitner and J. Fiebig, *"Relationship between Morphology and Micromechanical Toughening Mechanisms in Modified Polypropylene"*, **J. Appl. Polym. Sci.,** 60, 1996, p. 1391.

21 *"Untitled"*, **Metallocenes '95 Conference,** 1995, p. 521.

22 K. Marcus, *"Copolymer Project Part 1: A Statistical Study on the Correlation Between Mechanical and Molecular Parameters: BNP Copolymers"*, **Polifin Internal Report,** 1997.

23 J. W. Nicholson, **The Chemistry of Polymers,** The Royal Society of Chemistry Paperbacks, Cambridge, 1994, p. 90.

24 K. Marcus, C. Steinhobel, M. Domingo, N. Marshall, *"The Physical, Mechanical and Rheological Properties of Polypropylene: The*

Influence of Molecular Weight Averages and Molecular Weight Distribution", in **International GPC Symposium '96,** 1996, p. 3.

25 R. F. Becker, L. P. J. Burton and S. E. Amos, "*Additives*", in **Polypropylene Handbook,** Ed., E. P. Moore, Jr., Hanser Publishers, Munich, 1996, p. 177.

26 E. Seiler, *"Recent Developments with Polypropylene by Polymerization in the Gas Phase",* **BASF Internal Report,** 1991.

27 H. Sano, T. Usami and H. Nakagawa, *"Lamellae Morphologies of Melt Crystallised Polyethylene, Isotactic Polypropylene and Ethylene-Propylene Copolymers by the RuO_4 Staining Technique",* **Polymer,** 27, 986, p. 1497.

28 A. Reimschuessel and V. Kramer, *"Techniques of Optical and Electron Microscopy Applied to the Characterisation of Polymers",* **SPE. ANTEC,** 1988, p. 1199.

29 K. Marcus, *"Transmission and Scanning Electron Microscopy to Elucidate the Structure-Property Relationships in Poly-(Propylene-Ethylene) Copolymers",* **Polifin Internal Report,** 1997.

30 A. K. Khandpur, C. W. Macosko and F. S. Bates, *"Transmission Electron Microscopy of Saturated Hydrocarbon Block Copolymers",* **Journal of Polymer Science: Part B: Polymer Physics,** 33, 1995, p. 247.

31 D. C. Bassett, **Principles of Polymer Morphology,** Cambridge University Press, Cambridge, 1981, p. 101.

32 R. A. Phillips and M. D. Wolkowicz, "*Structure and Morphology*", in **Polypropylene Handbook,** Ed., E. P. Moore, Jr., Hanser Publishers, Munich, 1996, p. 113.

33 L. Mandelkern, "*The Crystalline State*", in **Physical Properties of Polymers,** 2nd Edition, American Chemical Society, Washington, DC, 1993, p. 145.

34 E. P. Moore, Jr., *"Introduction"*, in **Polypropylene Handbook,** Ed., E. P. Moore, Jr., Hanser Publishers, Munich, 1996, p. 3.

35 M. Reading, "*Thermomechanical Analysis and Dynamic Mechanical Analysis*", in **Thermal Analysis - Techniques and Applications,** Ed.

E. L. Charsley and S. B. Warrington, Royal Society of Chemistry, year, p.108.

36 H. Cai, K. Luo, D. Ma, J. Wang and H. Tan, *"Structure and Properties of Impact Copolymer Polypropylene. I. Chain Structure"*, **J. Appl. Polym. Sci.**, 71, 1999, p. 93.

37 *"Polifin Polypropylene: The BASF Gas-Phase Process"*, **Polifin Brochure**.

38 R. Greco, E. Martuscelli, G. Ragosta and Y. Jinghua, *"Polyolefin Blends: Morphology, Thermal Behaviour and Mechanical Properties of PP-EPR Alloys Crystallised at Low Undercoolings"*, **J. Mater. Sci.**, 23, 1988, p. 4307.

39 J. N. Hay, J. I. Langford and J. R. Lloyd, *"Variation in Unit Cell Parameters of Aromatic Polymers with Crystallisation Temperature"*, **Polymer**, 30, 1989, p. 489.

40 ASTM Standard D 790M – 92, *"Standard Test Methods for Flexural Properties of Unreinforced and Reinforced Plastics and Electrical Insulating Materials [Metric]"*, **Annual Book of ASTM Standards**, 08.01, 1993.

41 ASTM Standard D 638M – 91a, *"Standard Test Method for Tensile Properties of Plastics [Metric]"*, **Annual Book of ASTM Standards**, 08.01, 1993.

42 F. Ramsteiner, G. Kanig, W. Heckmann and W. Gruber, *"Improved Low Temperature Impact Strength of Polypropylene by Modification with Ethylene"*, **Polymer**, 24, 1983, p. 365.

43 V. Flaris and Z. H. Starchurski, *"The Mechanical Behaviour of Blends of Polyethylene, Polypropylene and an Ethylene-Propylene Block Copolymer at –20 °C"*, **J. Appl. Polym. Sci.**, 45, 1992, p. 1789.

44 H. Cai, X. Luo, X. Chen, D. Ma, J. Wang and H. Tan, *"Structure and Properties of Impact Copolymer Polypropylene. II. Phase Structure and Crystalline Morphology"*, **J. Appl. Polym. Sci.**, 71, 1999, p. 103.

45 J. Karger-Kocsis, J. Varga and G. W. Ehrenstein, *"Comparison of the Fracture and Failure Behaviour of Injection-Moulded α and β*

Polypropylene in High Speed Three-Point Bending Tests", **J. Appl. Polym. Sci.**, 64, 1996, p. 2057.

46 J. Karger-Kocsis, *'Dynamic Mechanical Properties and Morphology of Polypropylene Block Copolymers and Propylene/Elastomer Blends"*, **Polym. Eng. Sci.**, 27 (4), 1987, p. 254.

47 D. J. Lohse, *"The Melt Compatibility of Blends of Polypropylene and Ethylene-Propylene Copolymers"*, **Polym. Eng. Sci.**, 26(21), 1986, p. 1500.

48 M. Yamaguchi, K-H. Nitta, H. Miyata and T. Masuda, *"Rheological Properties for Binary Blends of i-PP and Ethylene-1-Hexene Copolymer"*, **J. Appl. Polym. Sci.**, 63, 1997, p. 467.

49 D. Chundury, A. Scheibelhoffer and V. Bauer, *"Methods to Characterise i-PP/HDPE Blends and PP Copolymers"*, **SPE. ANTEC**, 1988, p. 1243.

50 F. M. Mirabella, Jnr., *"Phase Separation and Kinetics of Phase Coarsening in Impact Polypropylene Copolymers"*, **J. Polym. Sci., Part B: Polymer Physics**, 32, 1994, p. 1205.

51 L. D'Orazio, C. Mancarella, E. Martuscelli, G. Cecchin and R. Correiri, *"Isotactic Polypropylene/Ethylene Co-Propylene Blends: Effects of the Copolymer Microstructure and Content on Rheology, Morphology and Properties of Injection Moulded Samples"*, **Polymer**, 40, 1999, p. 2745.

52 W. F. Msuya and C. Y. Yue, *"The Correlation Between Lamellae Thickness and the Degree of Crystallinity in Semi-Crystalline polymers"*, **J. Mater. Sci. Lett.**, 8 (11), 1989, p. 1266.

53 S. C. Tjong, J. C. Shen and R. K. Y. Li, *"Mechanical Behaviour of Injection Moulded β-Crystalline phase Polypropylene"*, **Polym. Eng. Sci.**, 36 (1), 1996, p. 100.

54 K. D. Rümpler, J. F. R. Jaggard and R. A. Werner, **Kunstoffe**, 78, 1988, p. 602.

55 V. Lorenzo, J. M. Perena and J. G. Fatou, *"Vickers Micro-hardness Related to Mechanical Properties of Polypropylene"*, **J. Mater. Sci. Lett.**, 8, 1989, p. 1455.

56 P. L. Fernando and J. G. Williams, *"The Toughness of Copolymers of Polypropylene"*, **Polym. Eng. Sci.**, 21(15), 1981, p. 1003.

57 H-T. Chiu and W-M Chiu, *"Influence of Mechanical Properties in Carbon Black (CB) Filled Isotactic polypropylene (i-PP) and Propylene-Ethylene Block copolymer"*, **J. Appl. Polym. Sci.**, 61, 1996, p. 607.

58 M. Gahletner, J. Wlfschwenger, C. Bachner, K. Bernreitner and W. Neiβl, *"Crystallinity and Mechanical Properties of PP-Homopolymers as Influenced by Molecular Structure and Nucleation"*, **J. Appl. Polym. Sci.**, 61, 1996, p. 649.

APPENDIX A

PLANT SPECIFICATIONS FOR SOME OF THE GRADES

This section contains the production specifications of some of the copolymer grades investigated.

Grade 2340 PC
MFI: Range 13 – 18, Target 15
% C_2: Range 5 – 8, Target 6.5
Izod notched impact strength @ 23 °C: Greater than 5, Target 7 kJ/m^2
Modulus: Greater than 1100, Target 1400 MPa

Grade 2448 TC
MFI: Range 40 – 55, Target 45
% C_2: Range 8 – 11, Target 9.5
Izod notched impact strength @ 23 °C: Greater than 5, Target 7 kJ/m^2
Modulus: Greater than 1000, Target 1200 MPa

Grade 2540 H
MFI: Range 1.5 – 2.5, Target 1.8
% C_2: Range 9 – 13, Target 11
Izod notched impact strength @ 23 °C: Greater than 35, Target 40 kJ/m^2
Modulus: Greater than 1000, Target 1100 MPa

Grade 2648 PC
MFI: Range 13 – 18, Target 15
% C_2: Range 10.5 – 13.5, Target 12
Izod notched impact strength @ 23 °C: Greater than 10, Target 12 kJ/m^2
Modulus: Greater than 900, Target 1000 MPa

APPENDIX B

XRD SCANS FOR THE VARIOUS COPOLYMER GRADES.

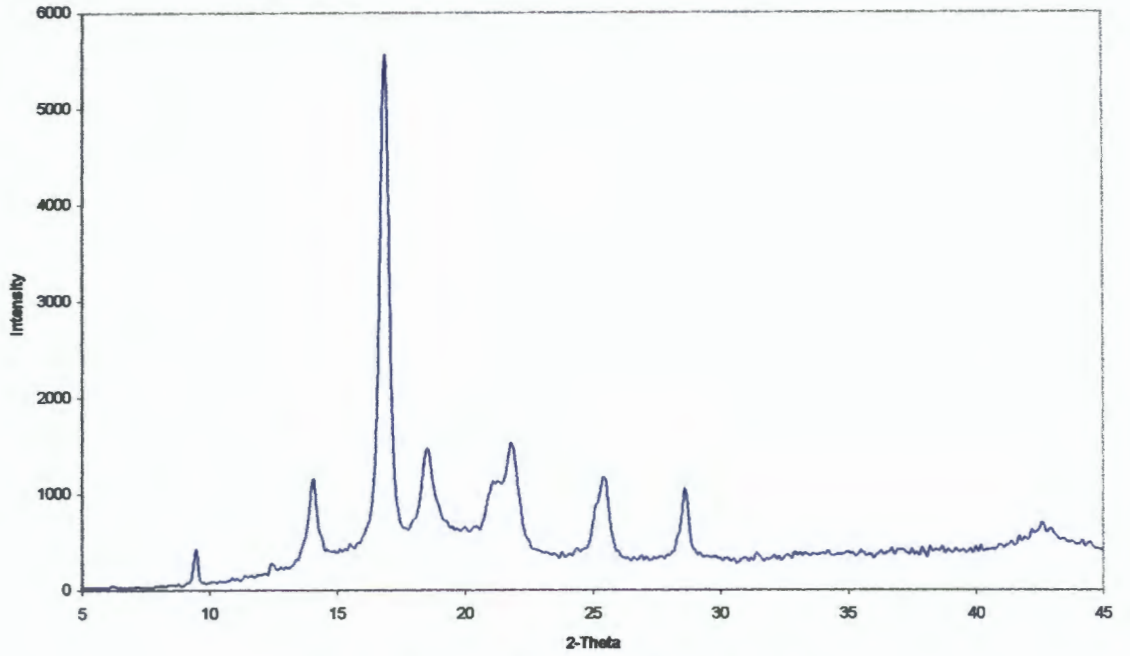

Figure B.1: Grade 2340 PC-1843

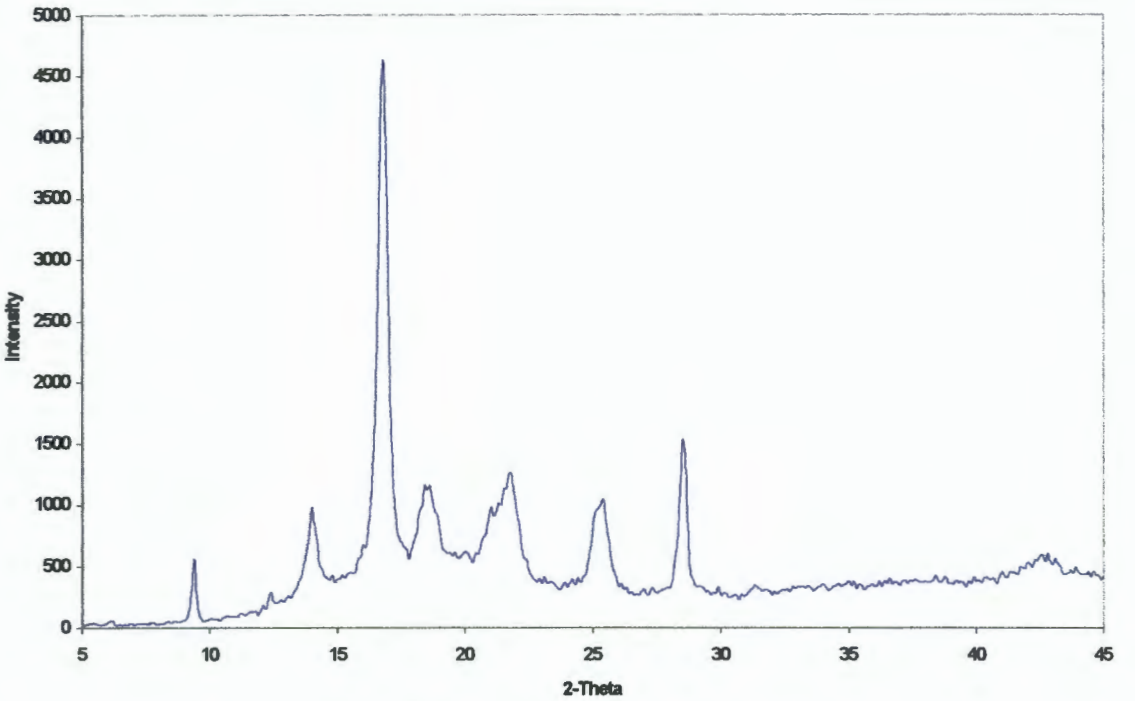

Figure B.2: Grade 2340 PC-3420

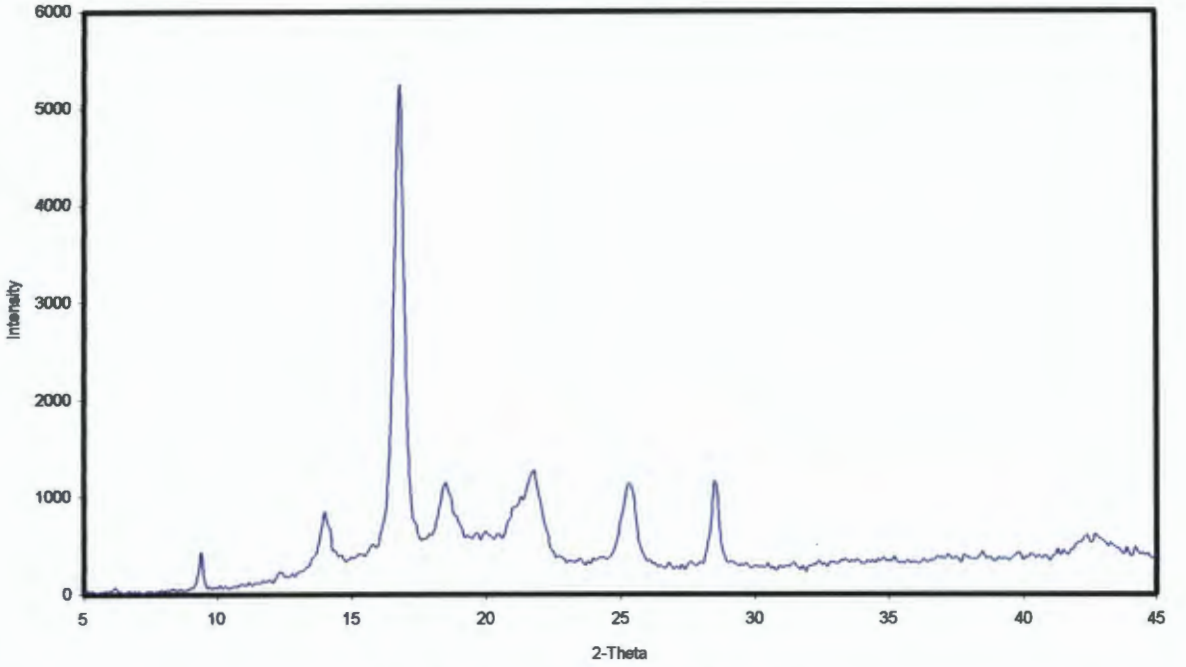

Figure B.3: Grade 2340 PC-3431

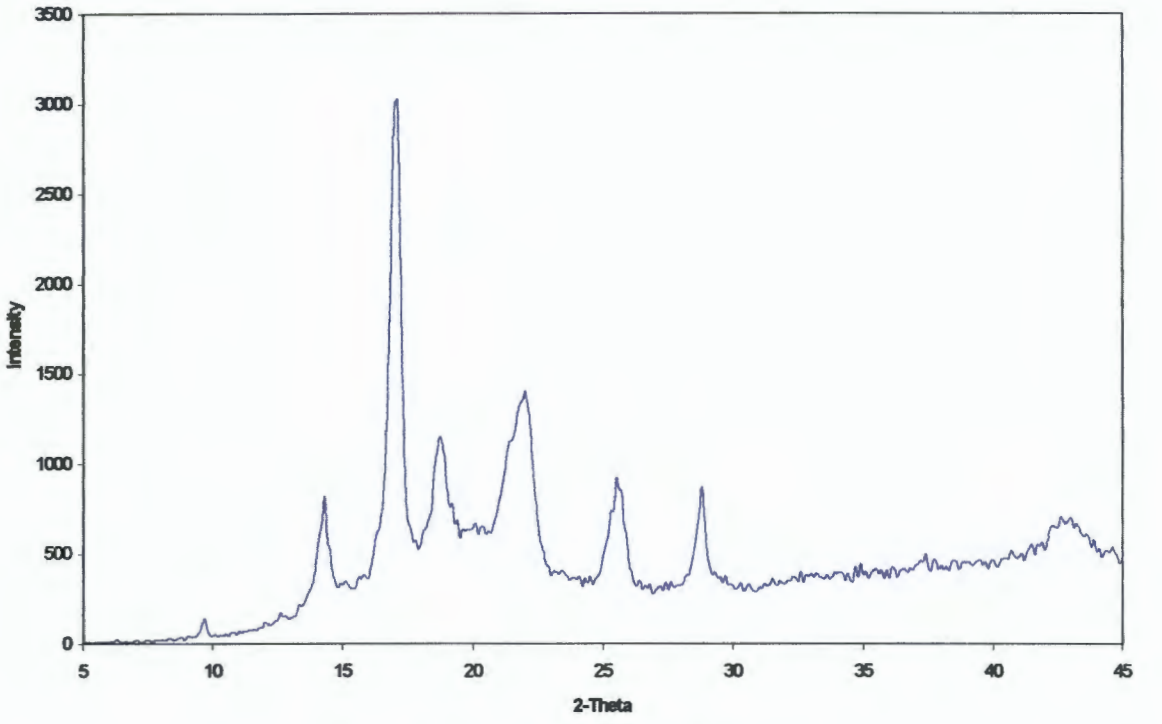

Figure B.4: Grade 2349 MC-2722

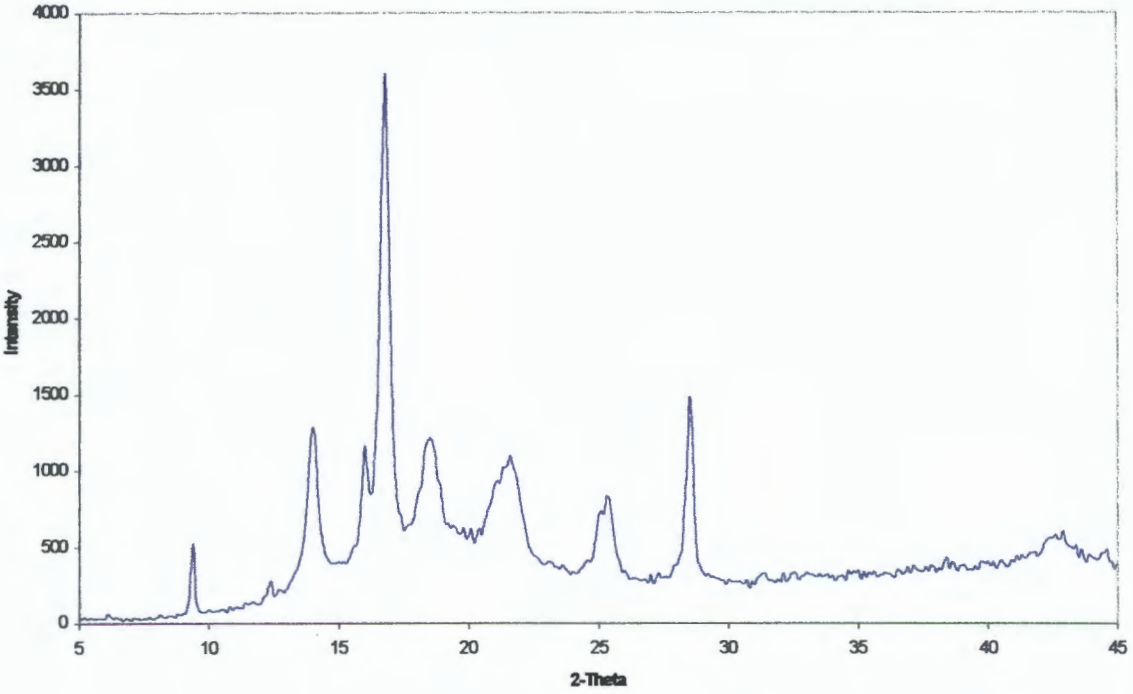

Figure B.5: Grade 2349 MC-3364

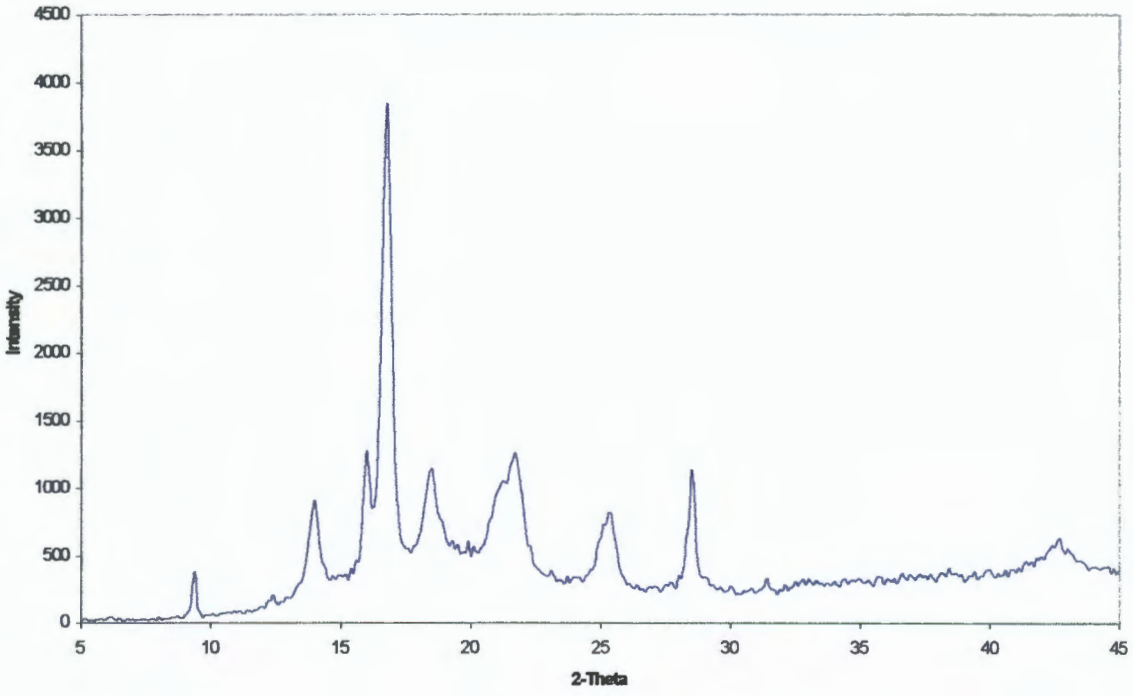

Figure B.6: Grade 2349 MC-3369

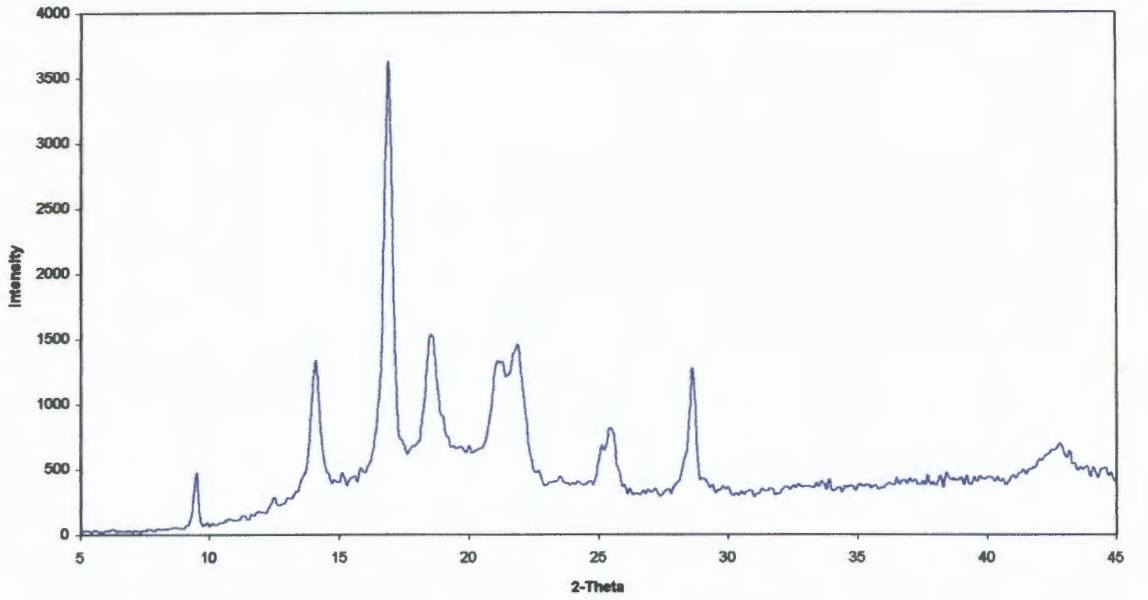

Figure B.7: Grade 2448 TC-2008

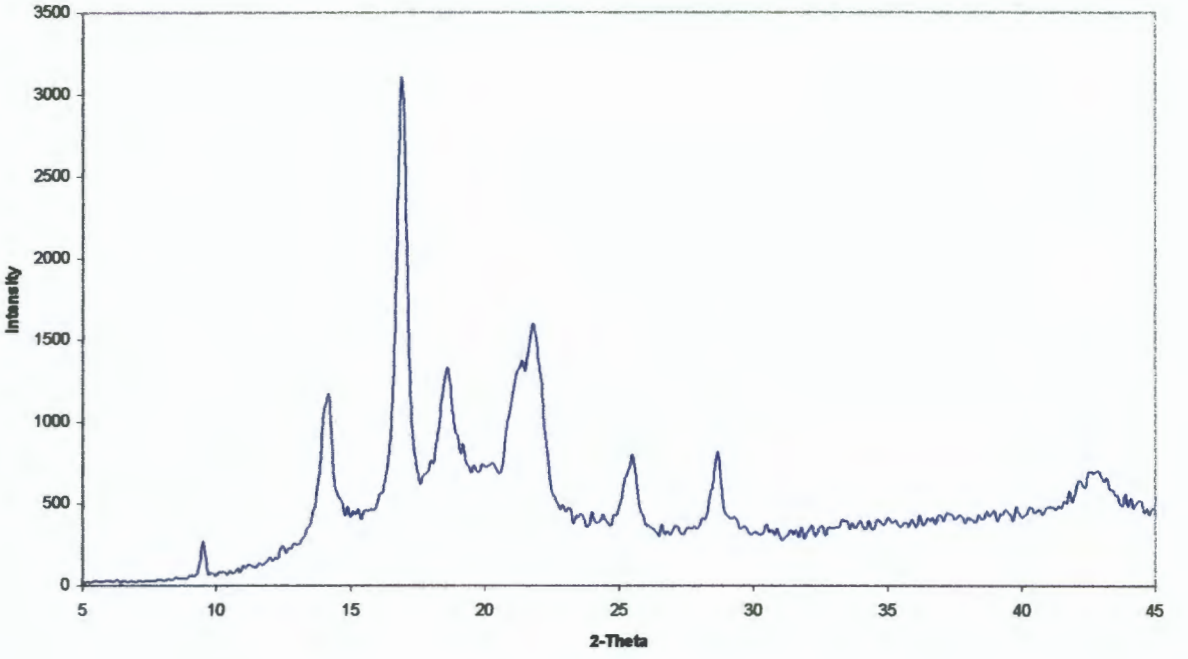

Figure B.8: Grade 2448 TC-2715

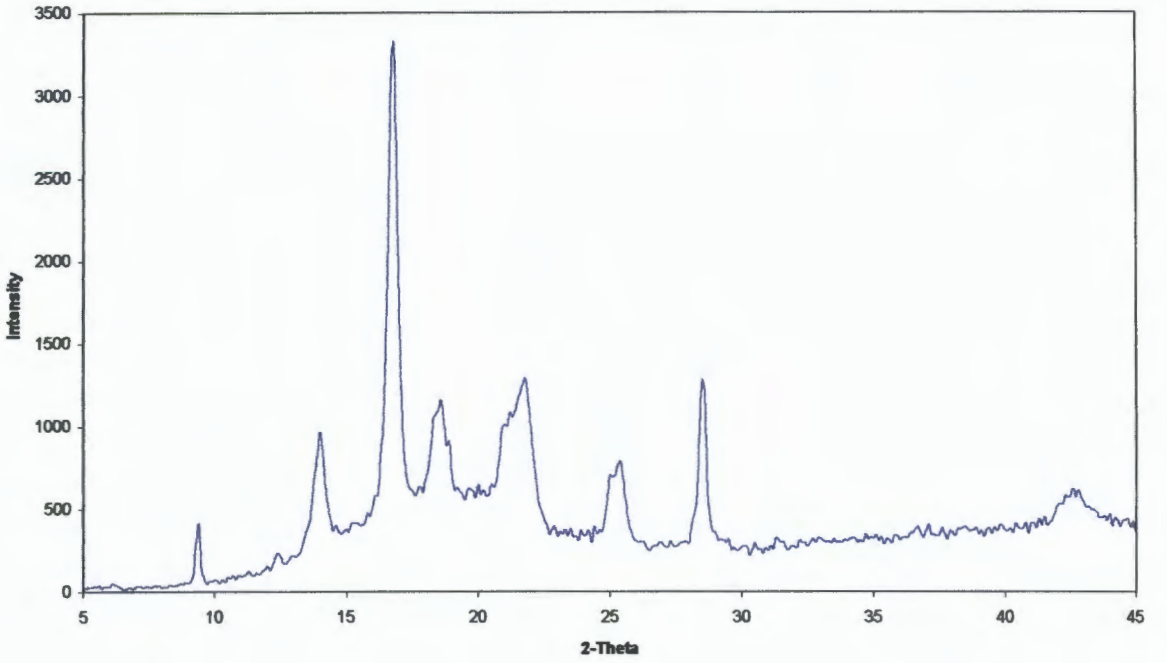

Figure B.9: Grade 2448 TC-3407

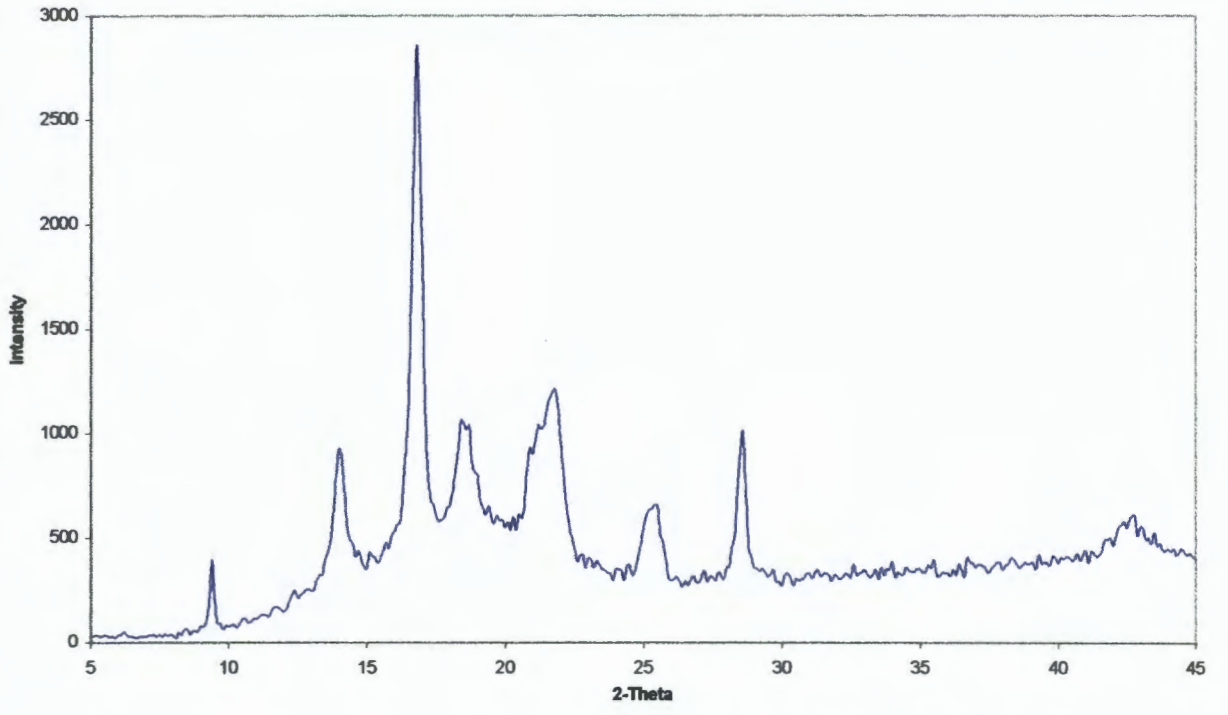

Figure B.10: Grade 2448 TC-3413

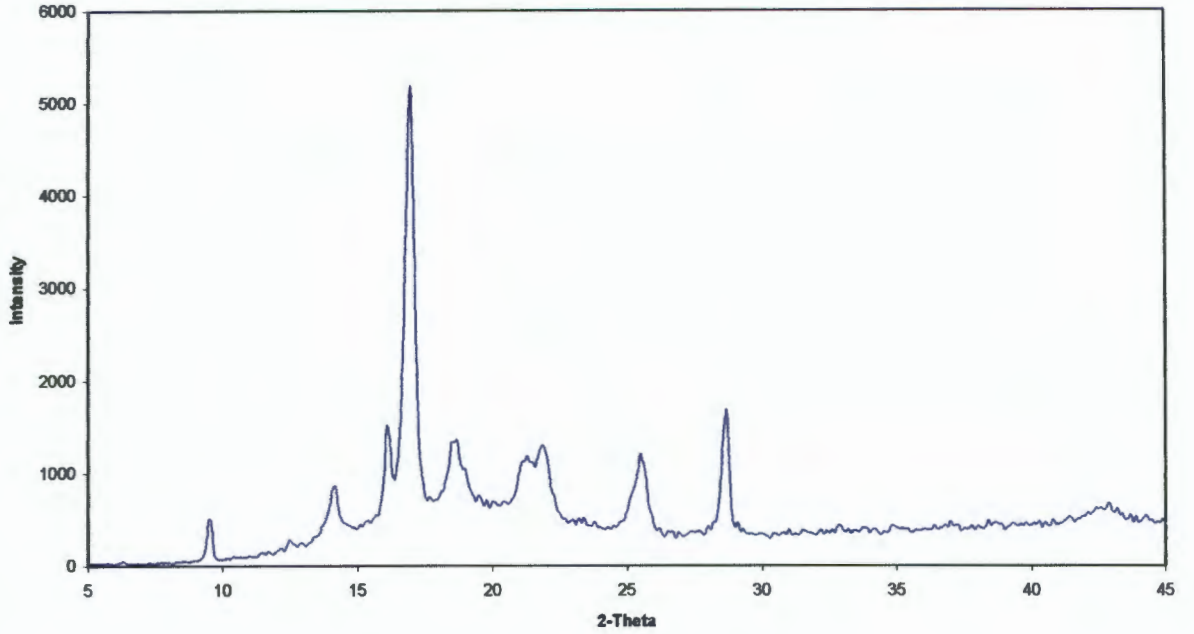

Figure B.11: Grade 2540 H-2177

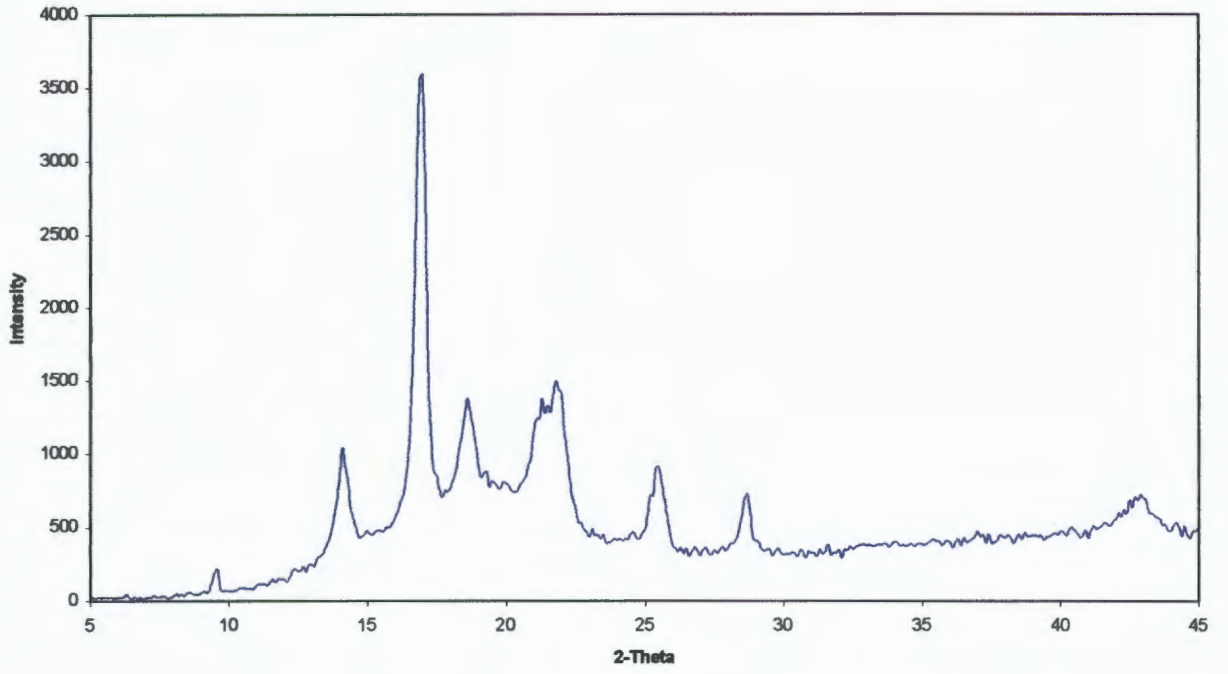

Figure B.12: Grade 2600 PC-390174

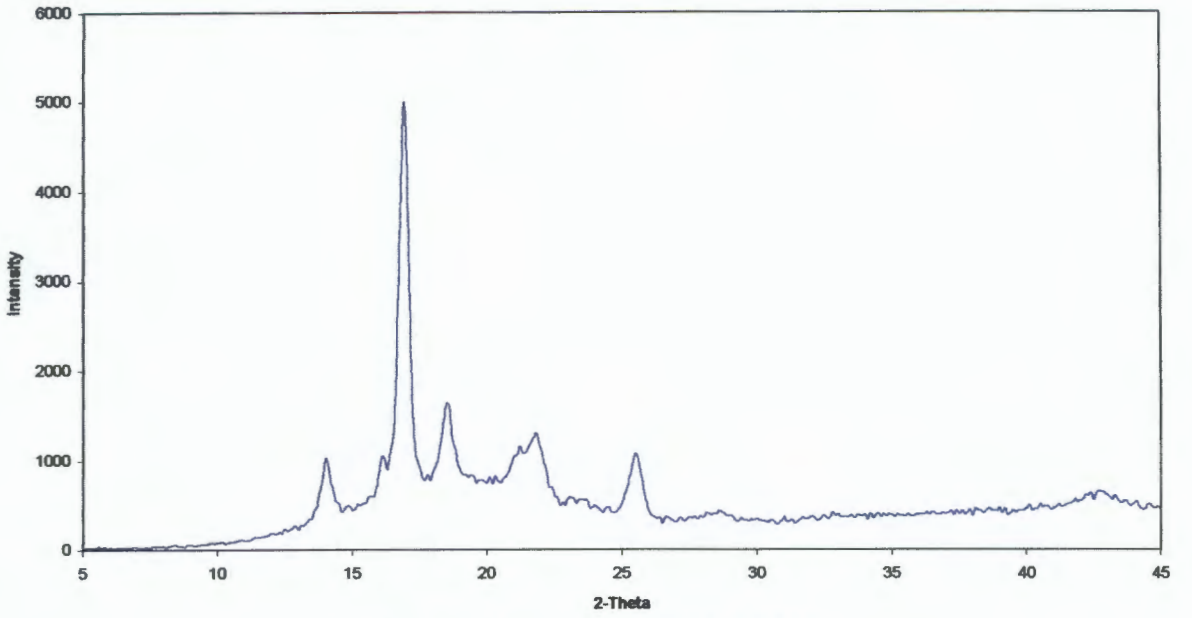

Figure B.13: Grade 2602 E-2699

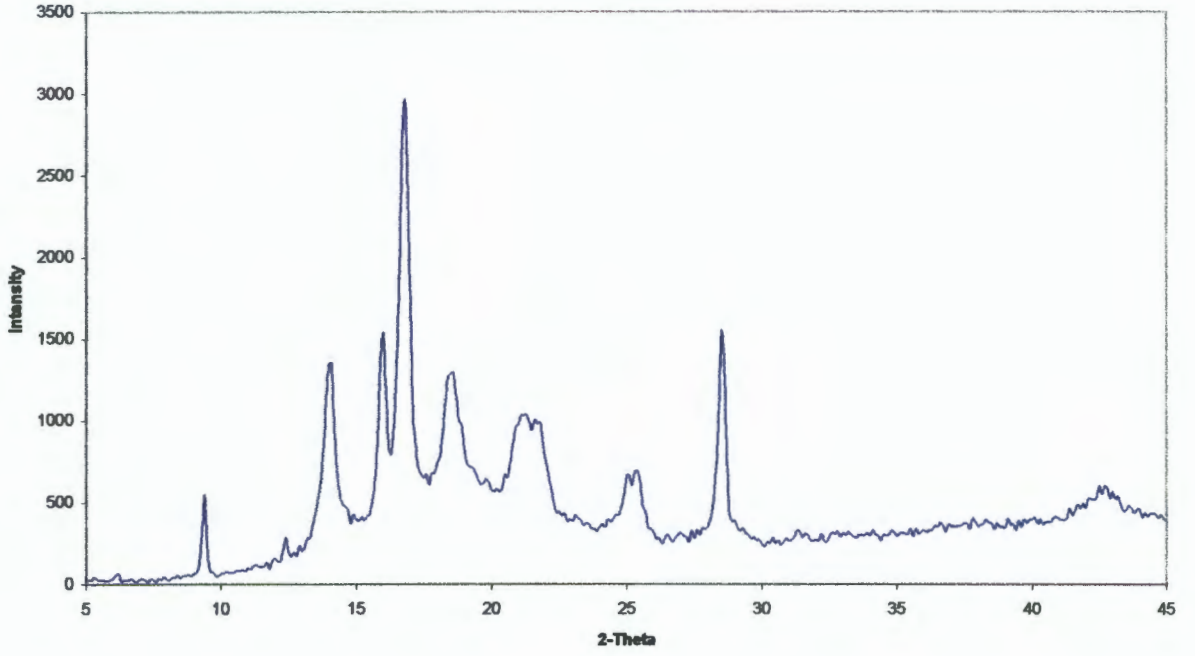

Figure B.14: Grade 2602 E-3399

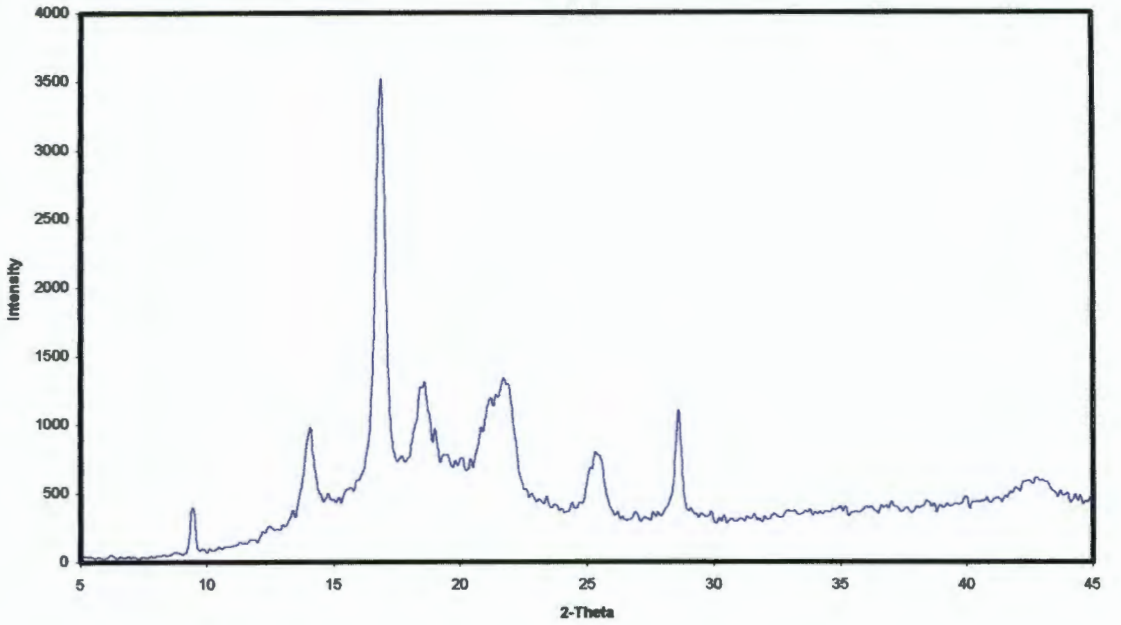

Figure B.15: Grade 2648 PC-1872

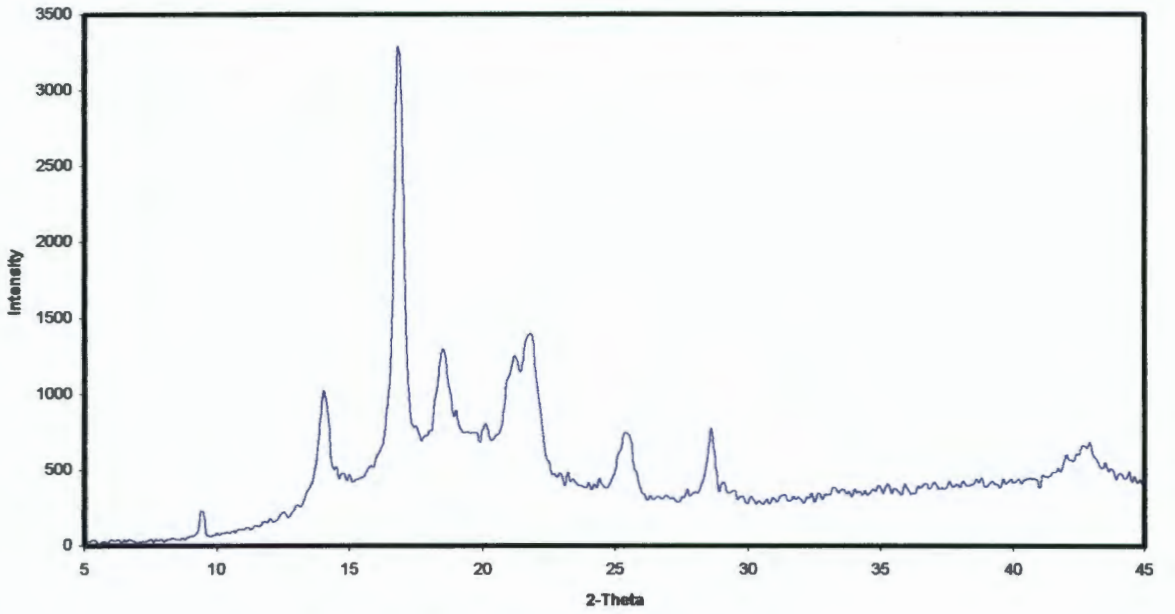

Figure B.16: Grade 2648 PC-2351

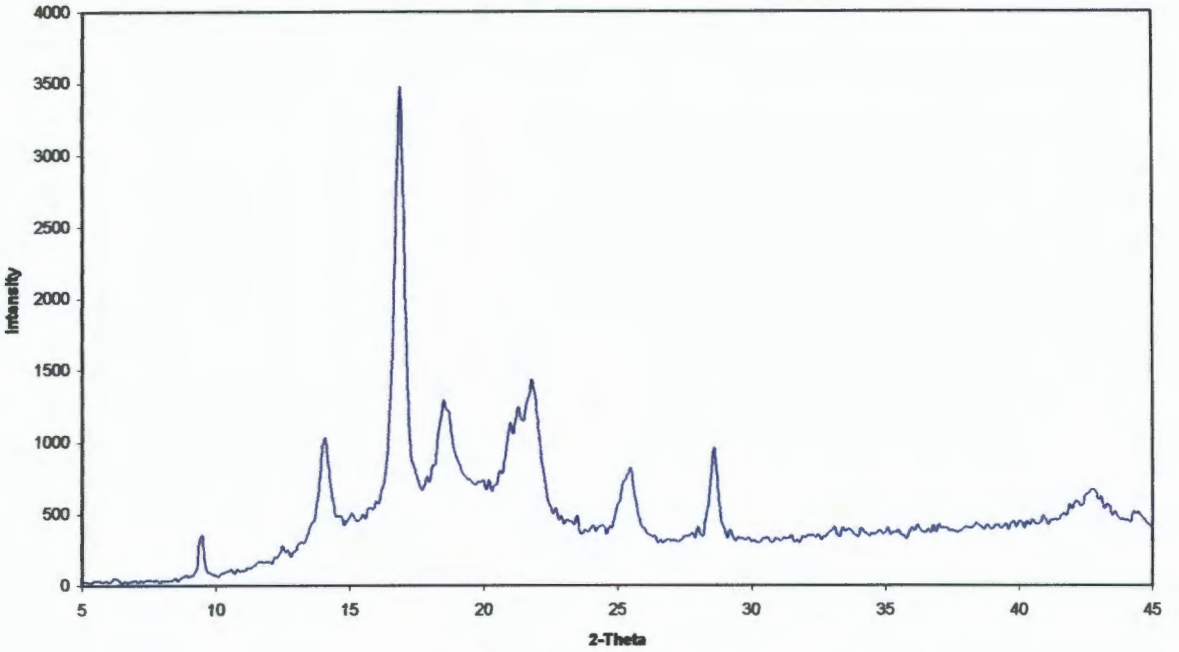

Figure B.17: Grade 2648 PC-2351

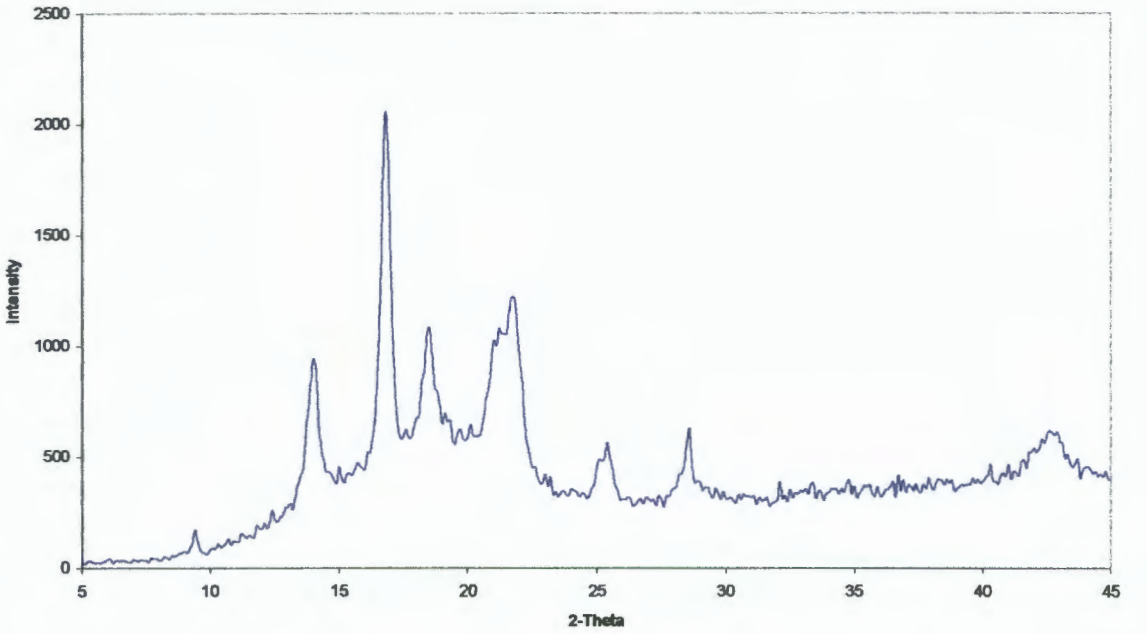

Figure B.18: Grade 2648 PC-2656

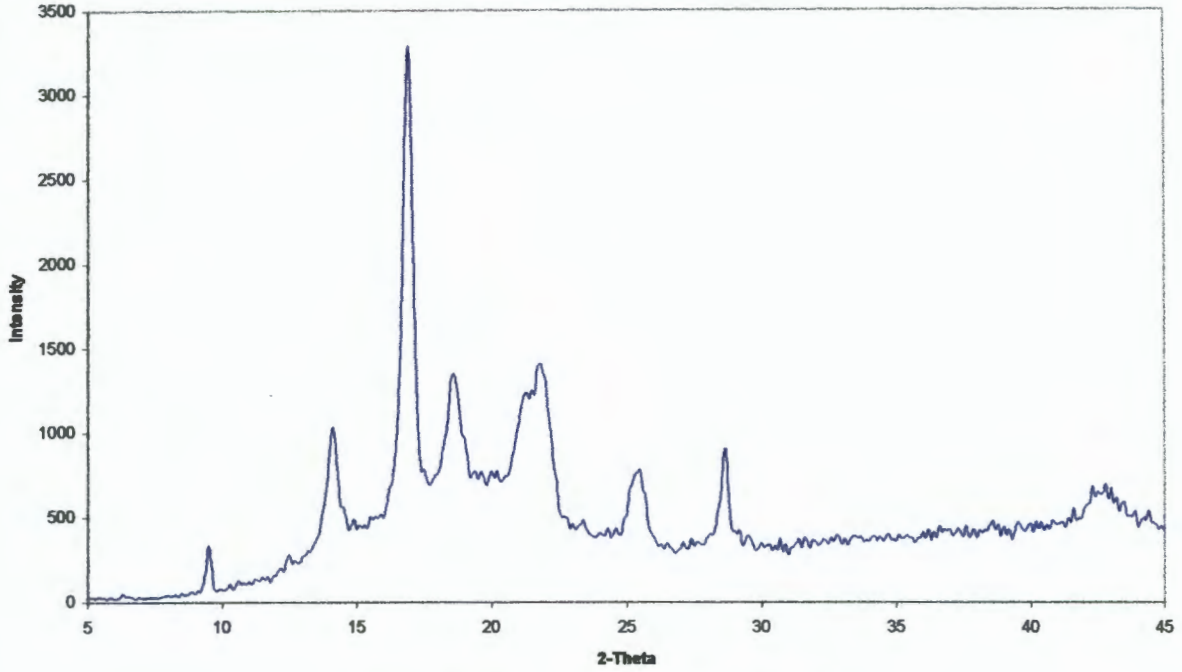

Figure B.19: Grade 2648 PC-2798

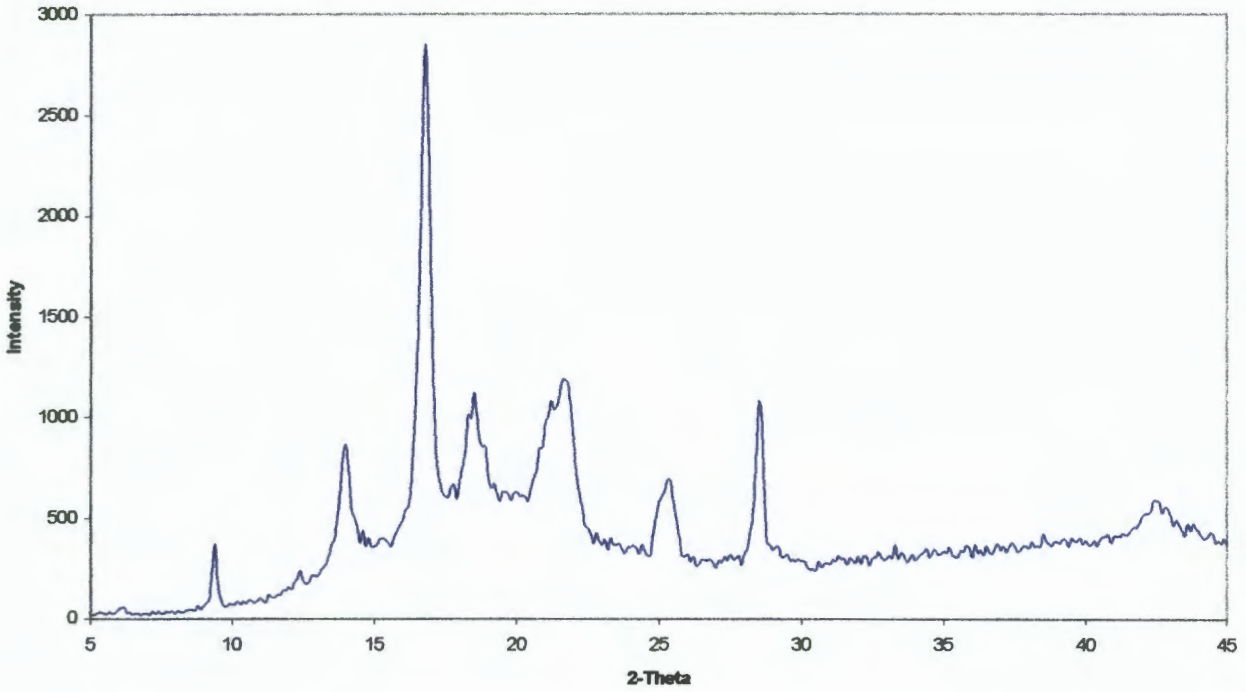

Figure B.20: Grade 2648 PC-3401

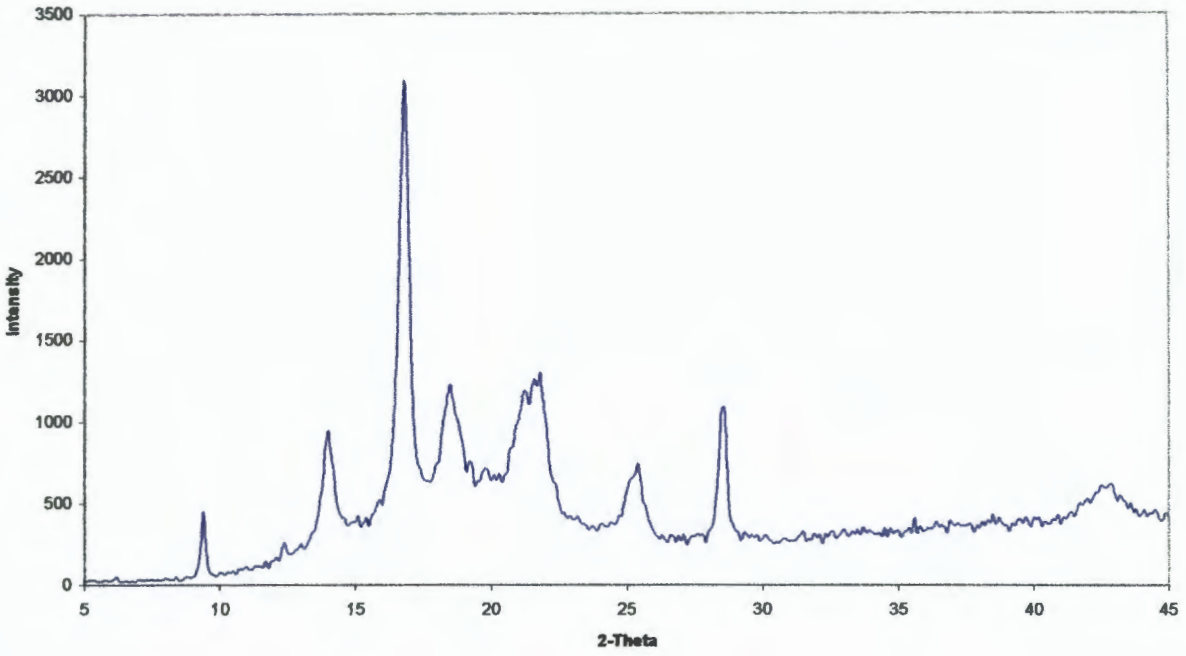

Figure B.21: Grade 2648 PC-3403

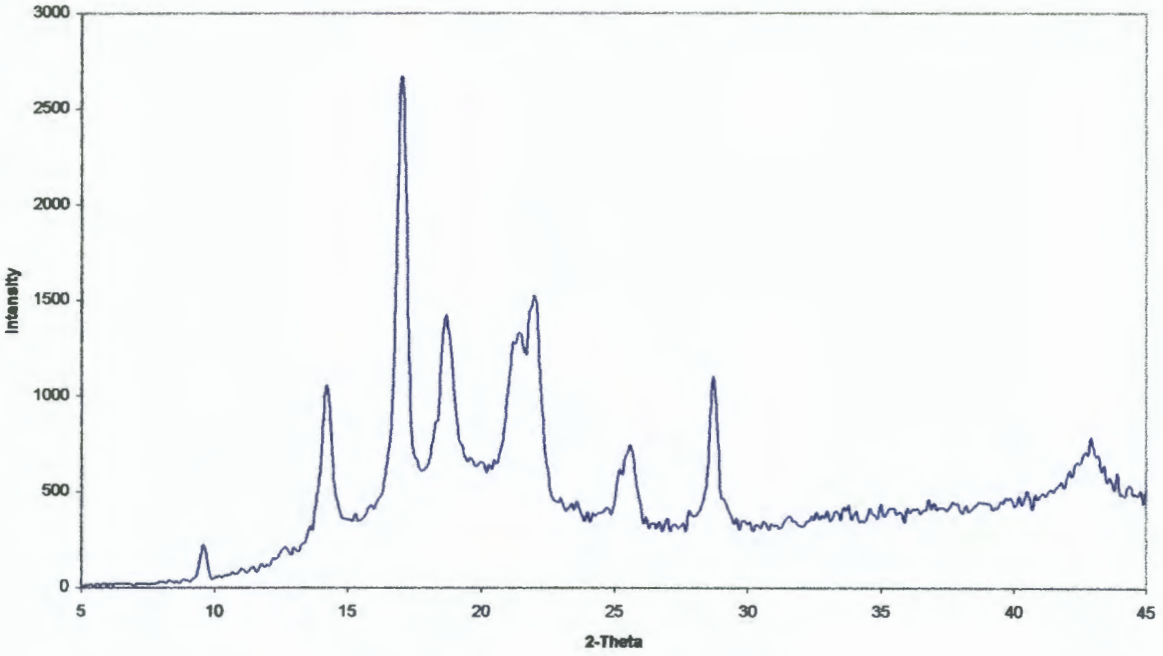

Figure B.22: Grade 2648 RC-1726

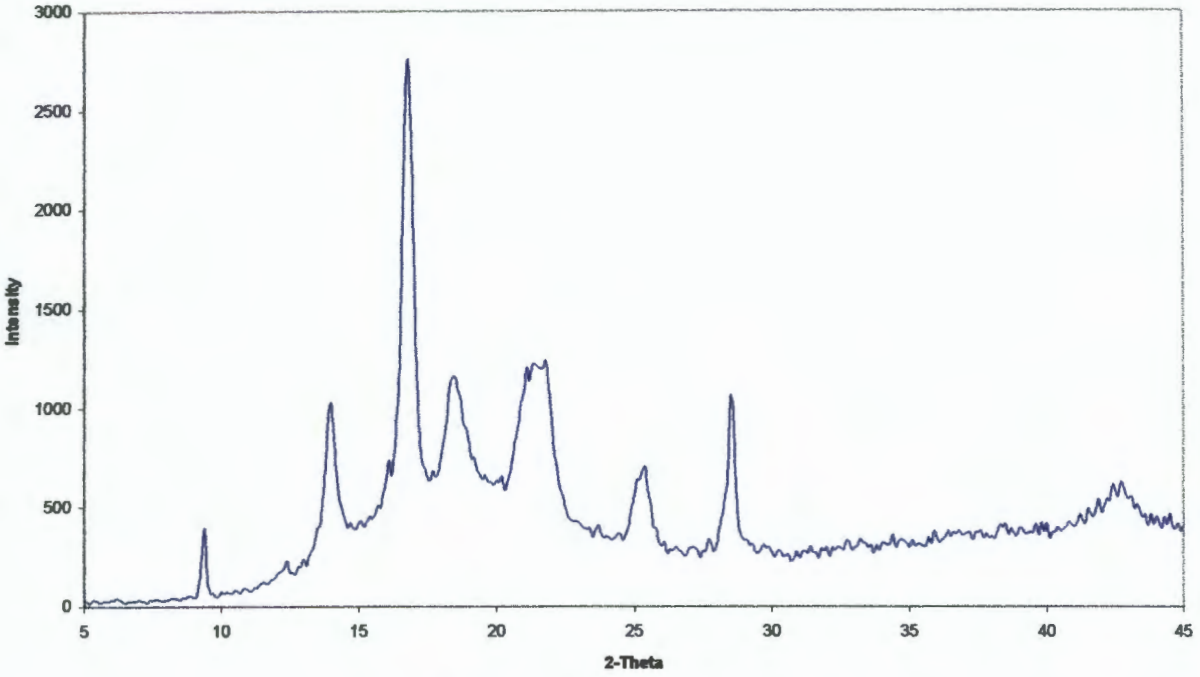

Figure B.23: Grade 2648 RC-3388

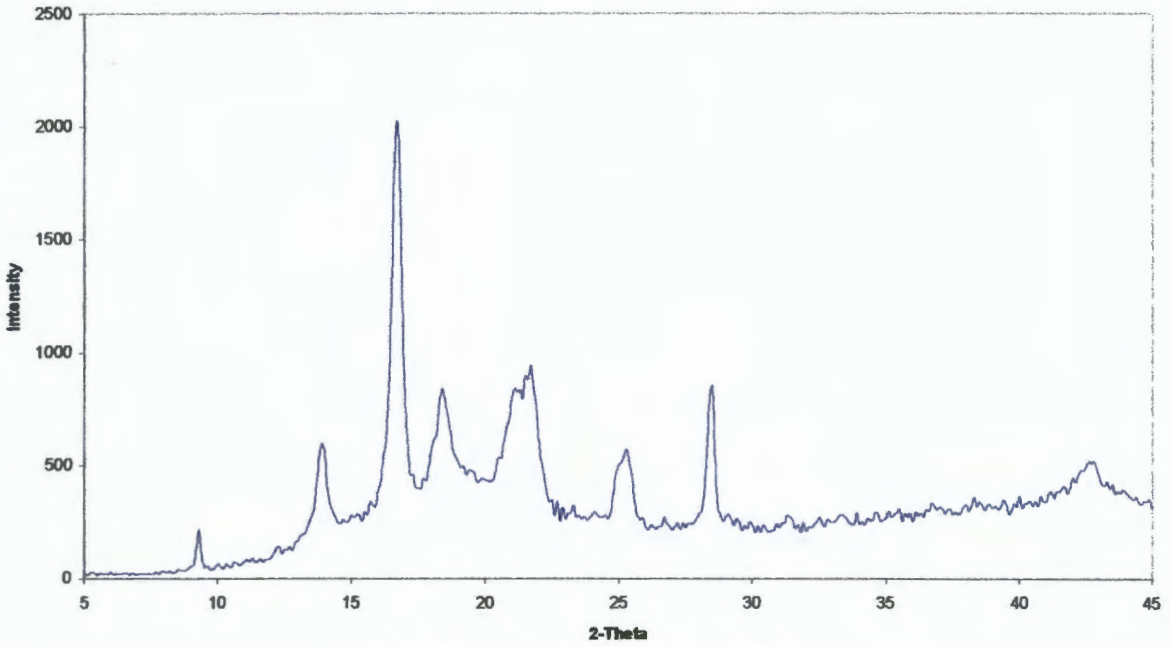

Figure B.24: Grade 2648 RC-3405

n

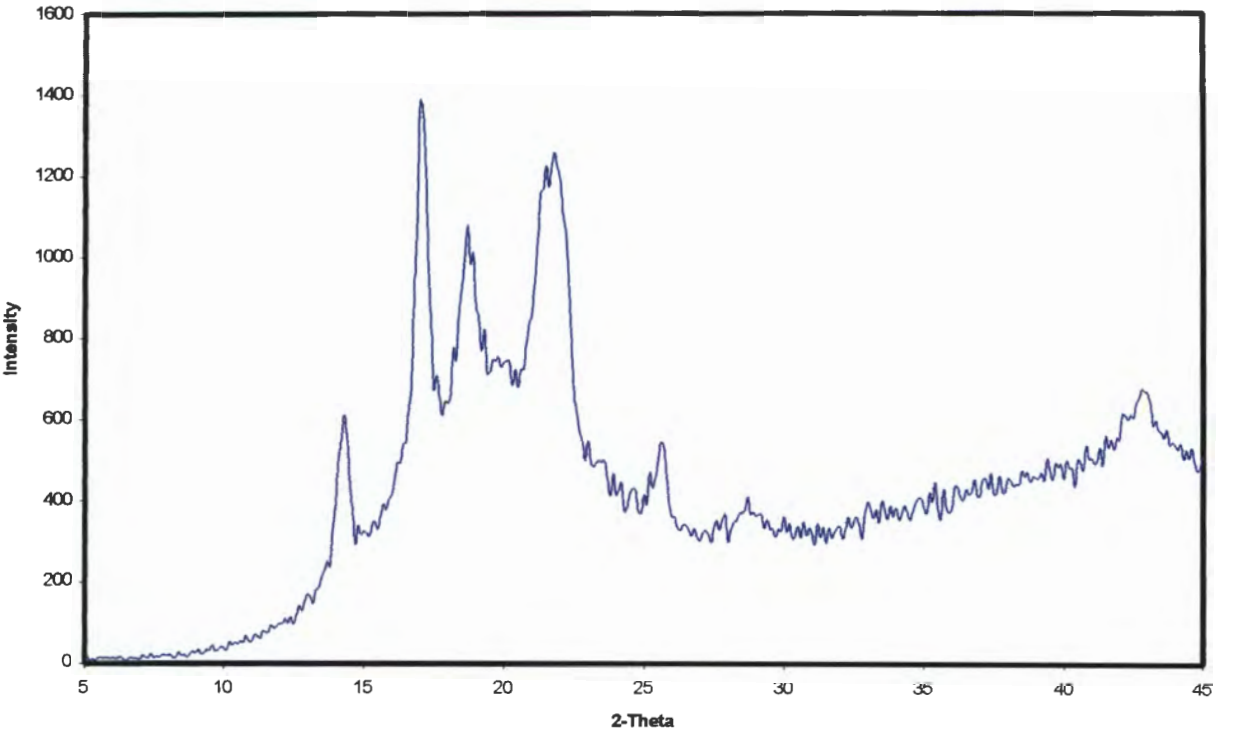

Figure B.25: Grade 2900 H-0708

APPENDIX C

RAW DATA OBTAINED FROM THE CHARACTERISATION OF THE COPOLYMERS.

This section contains the raw data of the results obtained from the characterisation of the copolymer material as a function of ethylene content and melt flow index.

Grade Code	*Ethylene Content (%)*	*MFI (g/10min)*	*Average Impact Strength (kJ/m^2)*
2340 PC-1843	7.1	14	8.7
2340 PC-3420	6.7	16	7.4
2340 PC-3431	4.7	17	8.3
2349 MC-2722	7.6	8	8.1
2349 MC-3364	9.2	8	12.3
2349 MC-3369	6.4	9	7.5
2448 TC-2008	10.2	44.4	9.3
2448 TC-2715	10.0	43	5.2
2448 TC-3407	8.7	48	4.8
2448 TC-3413	9.2	49	5.3
2540 H-2177	11.8	1.7	56.2
2600 PC-390174	11.8	17.2	12.9
2602 E-2699	13.3	0.9	64.7
2602 E-3399	12.1	0.8	43.9
2648 PC-1872	13.1	15	41.3
2648 PC-2337	12	14	42.2
2648 PC-2351	10.9	14	18
2648 PC-2656	11.4	15	9.7
2648 PC-2798	11.5	17	11.4
2648 PC-3401	11.2	17	9.7
2648 PC-3403	12.4	17	15.3
2648 RC-1726	11.4	25	30.3
2648 RC-3388	11.7	20	9.1
2648 RC-3405	11. 8	23	7.6
2900 H-0708	22.4	1.8	54.2

Table C.1: Average batch results for the determination of the impact properties

Grade Code	*Ethylene Content (%)*	*MFI (g/10min)*	*Average Flexural Modulus (MPa)*
2340 PC-1843	7.1	14	1605
2340 PC-3420	6.7	16	1088
2340 PC-3431	4.7	17	1286
2349 MC-2722	7.6	8	1187
2349 MC-3364	9.2	8	986
2349 MC-3369	6.4	9	1237
2448 TC-2008	10.2	44.4	1280
2448 TC-2715	10.0	43	1097
2448 TC-3407	8.7	48	1013
2448 TC-3413	9.2	49	942
2540 H-2177	11.8	1.7	1267
2600 PC-390174	11.8	17.2	908
2602 E-2699	13.3	0.9	685
2602 E-3399	12.1	0.8	897
2648 PC-1872	13.1	15	708
2648 PC-2337	12	14	686
2648 PC-2351	10.9	14	768
2648 PC-2656	11.4	15	867
2648 PC-2798	11.5	17	886
2648 PC-3401	11.2	17	856
2648 PC-3403	12.4	17	904
2648 RC-1726	11.4	25	1197
2648 RC-3388	11.7	20	851
2648 RC-3405	11. 8	23	903
2900 H-0708	22.4	1.8	553

Table C.2: Average batch results for the determination of the flexure properties.

Grade Code	(%) C_2	MFI (g/10min)	Tensile Modulus (MPa)	Tensile Strength (MPa)	(%) Elong.
2340 PC-1843	7.1	14	570	27.7	87
2340 PC-3420	6.7	16	468	27.3	183
2340 PC-3431	4.7	17	505	29.1	131
2349 MC-2722	7.6	8	577	29.6	139
2349 MC-3364	9.2	8	427	23.7	604
2349 MC-3369	6.4	9	476	27.8	114
2448 TC-2008	10.2	44.4	462	23.0	72
2448 TC-2715	10.0	43	479	23.7	65
2448 TC-3407	8.7	48	436	22.3	52
2448 TC-3413	9.2	49	440	23.7	47
2540 H-2177	11.8	1.7	436	24.0	256
2600 PC-390174	11.8	17.2	504	22.1	323
2602 E-2699	13.3	0.9	383	21.1	519
2602 E-3399	12.1	0.8	404	20.8	340
2648 PC-1872	13.1	15	393	20.0	490
2648 PC-2337	12	14	363	20.6	524
2648 PC-2351	10.9	14	380	21.2	603
2648 PC-2656	11.4	15	457	22.8	546
2648 PC-2798	11.5	17	391	22.9	497
2648 PC-3401	11.2	17	407	20.3	407
2648 PC-3403	12.4	17	405	19.6	188
2648 RC-1726	11.4	25	357	21.1	147
2648 RC-3388	11.74	20	397	19.6	94
2648 RC-3405	11.8	23	419	20.9	76
2900 H-0708	22.4	1.8	358	17.3	685

Table C.3: Average batch results for the determination of the tensile properties.

Grade Code	Ethylene Content (%)	MFI (g/10min)	Hardness (HV-25gf)	Degree of Crystallinity (%)
2340 PC-1843	7.1	14	7.9	34.8
2340 PC-3420	6.7	16	6.68	29.2
2340 PC-3431	4.7	17	7.64	30.9
2349 MC-2722	7.6	8	7.94	33.3
2349 MC-3364	9.2	8	5.48	27.2
2349 MC-3369	6.4	9	5.36	32.5
2448 TC-2008	10.2	44.4	5.98	32.2
2448 TC-2715	10.0	43	6.9	32.8
2448 TC-3407	8.7	48	7.34	30.6
2448 TC-3413	9.2	49	5.8	23.5
2540 H-2177	11.8	1.7	4.97	27.4
2600 PC-390174	11.8	17.2	5.2	28.6
2602 E-2699	13.3	0.9	3.06	24.1
2602 E-3399	12.1	0.8	4.56	24.8
2648 PC-1872	13.1	15	5.06	28.8
2648 PC-2337	12	14	4.88	27.9
2648 PC-2351	10.9	14	4.82	27.7
2648 PC-2656	11.4	15	5.54	29.9
2648 PC-2798	11.5	17	4.84	29.3
2648 PC-3401	11.2	17	4.1	27.4
2648 PC-3403	12.4	17	4.66	31.5
2648 RC-1726	11.4	25	5.03	30.2
2648 RC-3388	11.7	20	3.9	24.8
2648 RC-3405	11.8	23	4.82	32.9
2900 H-0708	22.4	1.8	2.36	20.3

Table C.4: Average batch results for hardness and crystallinity determination.

Grade Code	(%) C_2	MFI (g/10min)	Cross Sectional Diameter (μm)	Inter-Particle Spacing (μm)	Spacing to Diameter Ratio
2340 PC-1843	7.1	14	0.84	5.98	7.12
2340 PC-3420	6.7	16	0.78	4.4	5.64
2340 PC-3431	4.7	17	1.31	11	8.4
2349 MC-2722	7.6	8	3.35	12.43	3.71
2349 MC-3364	9.2	8	0.76	4.8	6.32
2349 MC-3369	6.4	9	1.31	9.94	7.59
2448 TC-2008	10.2	44.4	1.02	8.99	8.81
2448 TC-2715	10.0	43	1.47	14.44	9.82
2448 TC-3407	8.7	48	0.57	5.6	9.82
2448 TC-3413	9.2	49	0.86	6.2	7.21
2540 H-2177	11.8	1.7	0.84	5.28	6.29
2600 PC-390174	11.8	17.2	1.7	9.65	5.68
2602 E-2699	13.3	0.9	1.16	4.96	4.28
2602 E-3399	12.1	0.8	0.76	4.4	5.79
2648 PC-1872	13.1	15	1.32	6.93	5.25
2648 PC-2337	12	14	1.3	7.18	5.52
2648 PC-2351	10.9	14	1.57	9.17	5.84
2648 PC-2656	11.4	15	1.29	6.08	4.71
2648 PC-2798	11.5	17	1.52	6.36	4.18
2648 PC-3401	11.2	17	0.83	5.4	6.51
2648 PC-3403	12.4	17	0.74	4.4	5.95
2648 RC-1726	11.4	25	0.84	8.31	9.89
2648 RC-3388	11.7	20	0.88	3.96	4.5
2648 RC-3405	11.8	23	0.68	4.2	6.18
2900 H-0708	22.4	1.8	1.36	6.05	4.45

Table C.5: Average batch results for the microscopy measurements

Grade Code	Ethylene Content (%)	MFI (g/10min)	Average Enthalpy of Fusion (J/g)	Average Melting Temperature (°C)
2340 PC-1843	7.1	14	72.76	166.25
2340 PC-3420	6.7	16	61.08	166.65
2340 PC-3431	4.7	17	64.66	166.28
2349 MC-2722	7.6	8	69.57	168.66
2349 MC-3364	9.2	8	56.84	166.29
2349 MC-3369	6.4	9	68.02	164.54
2448 TC-2008	10.2	44.4	67.37	165.58
2448 TC-2715	10.0	43	68.44	165.81
2448 TC-3407	8.7	48	63.86	164.90
2448 TC-3413	9.2	49	49.1	164.13
2540 H-2177	11.8	1.7	57.30	166.38
2600 PC-390174	11.8	17.2	59.77	165.77
2602 E-2699	13.3	0.9	50.36	164.90
2602 E-3399	12.1	0.8	51.80	166.00
2648 PC-1872	13.1	15	60.26	166.30
2648 PC-2337	12	14	58.33	165.15
2648 PC-2351	10.9	14	57.93	164.73
2648 PC-2656	11.4	15	62.48	165.40
2648 PC-2798	11.5	17	61.16	166.18
2648 PC-3401	11.2	17	57.26	164.54
2648 PC-3403	12.4	17	65.90	164.09
2648 RC-1726	11.4	25	63.01	165.59
2648 RC-3388	11.7	20	51.80	161.73
2648 RC-3405	11.8	23	68.75	165.02
2900 H-0708	22.4	1.8	42.40	165.83

Table C.6: DSC data for the determination of the % Xc and T*m*.

APPENDIX D

RELATION BETWEEN THE DEGREE OF CRYSTALLINITY AND OTHER MECHANICAL PROPERTIES

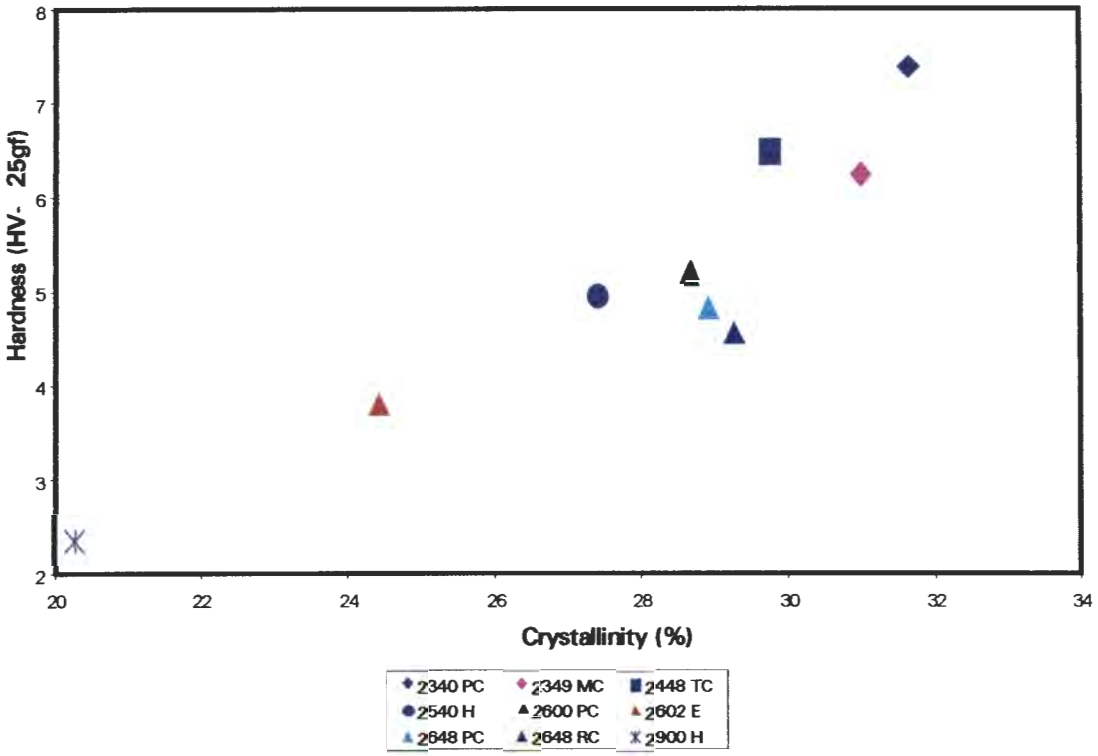

Figure D.1: A plot of the correlation between hardness and the degree of crystallinity.

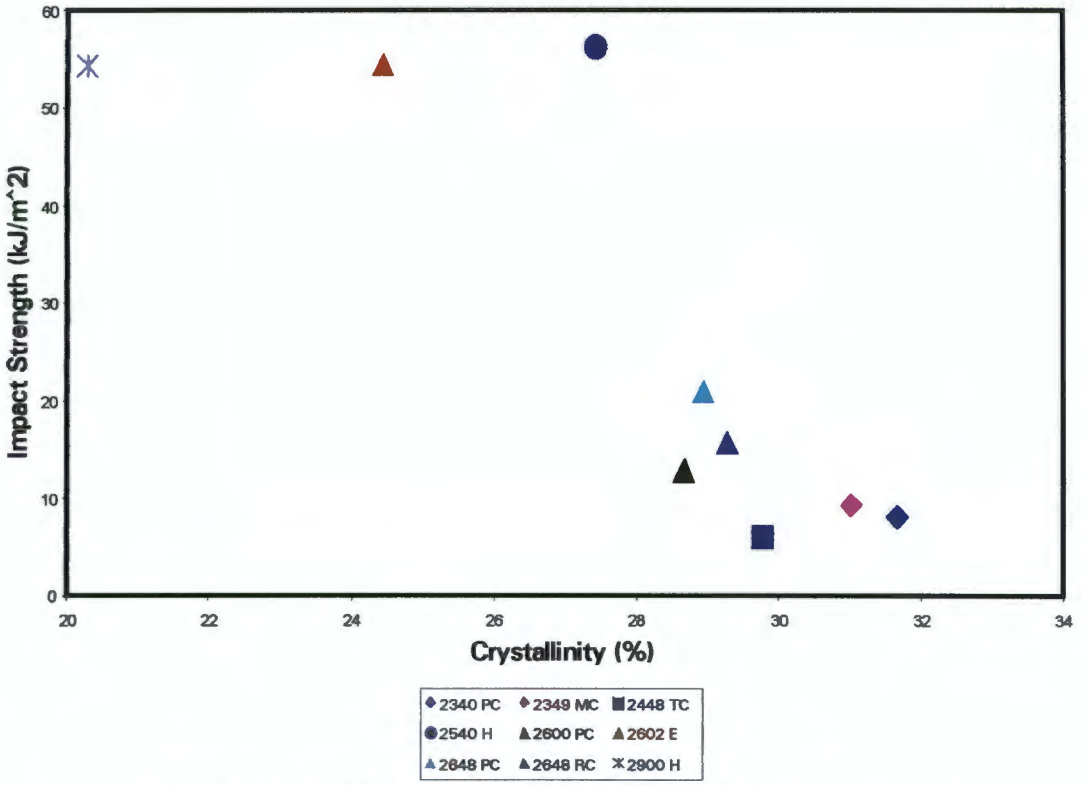

Figure D.2: Effect of the degree of crystallinity on impact strength.

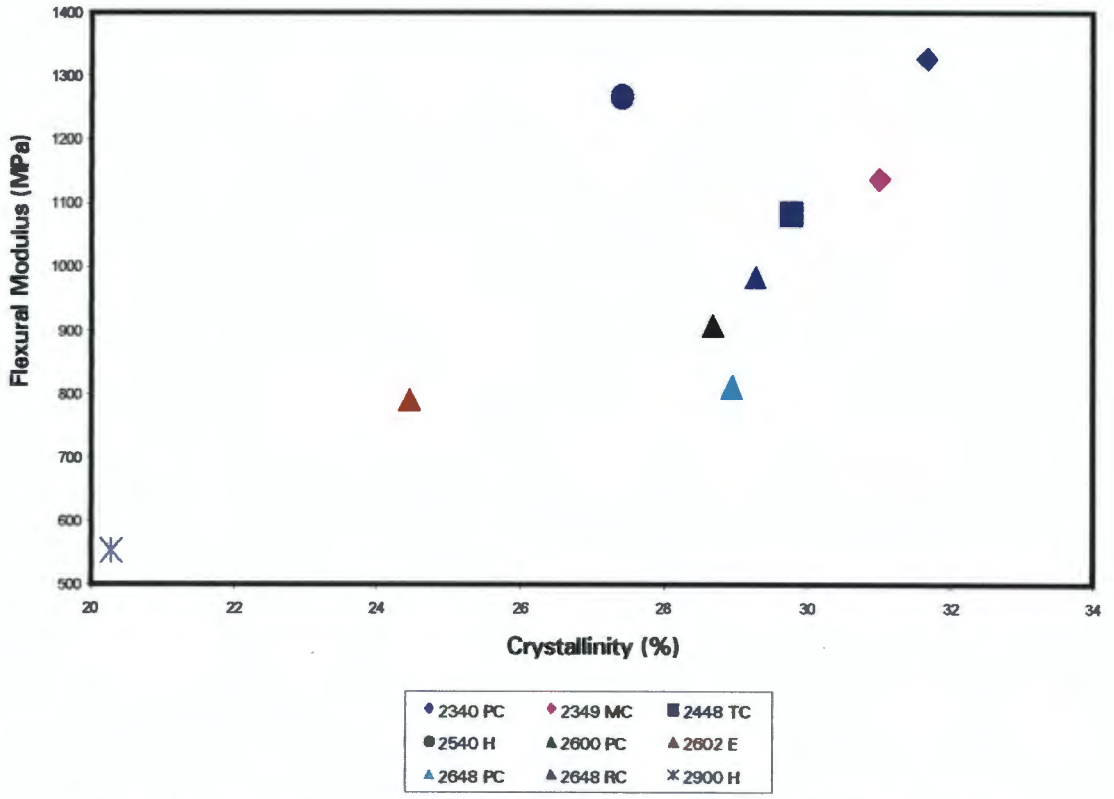

Figure D.3: Effect of the degree of crystallinity on the flexural modulus.

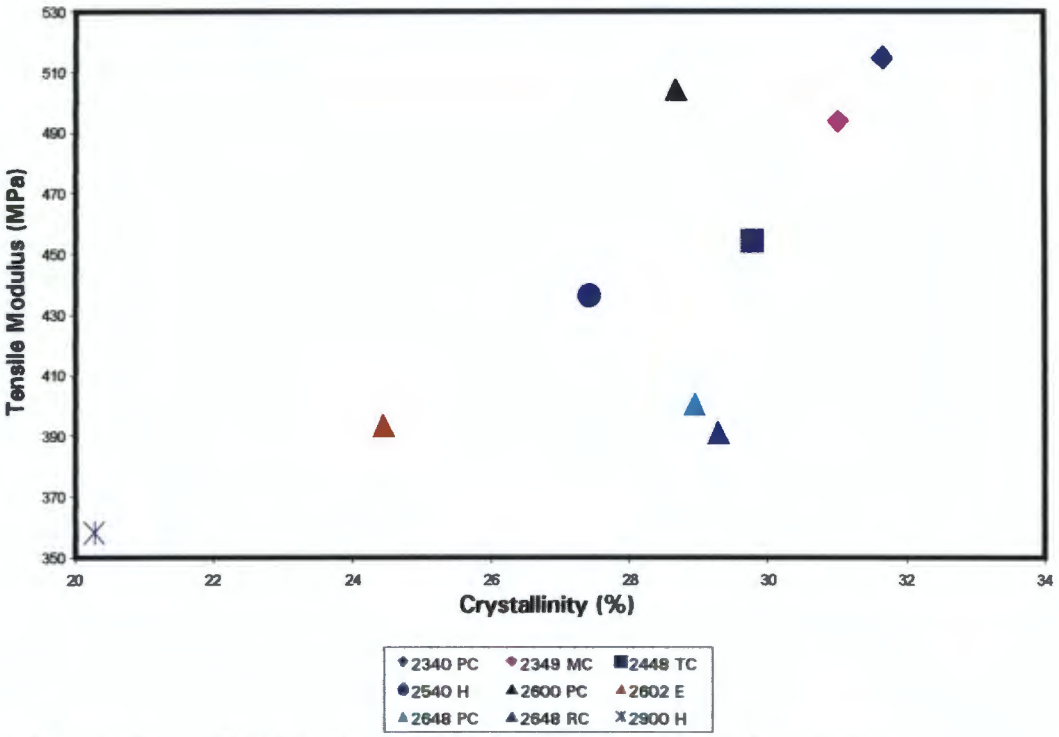

Figure D.4: Effect of the degree of crystallinity on tensile modulus.

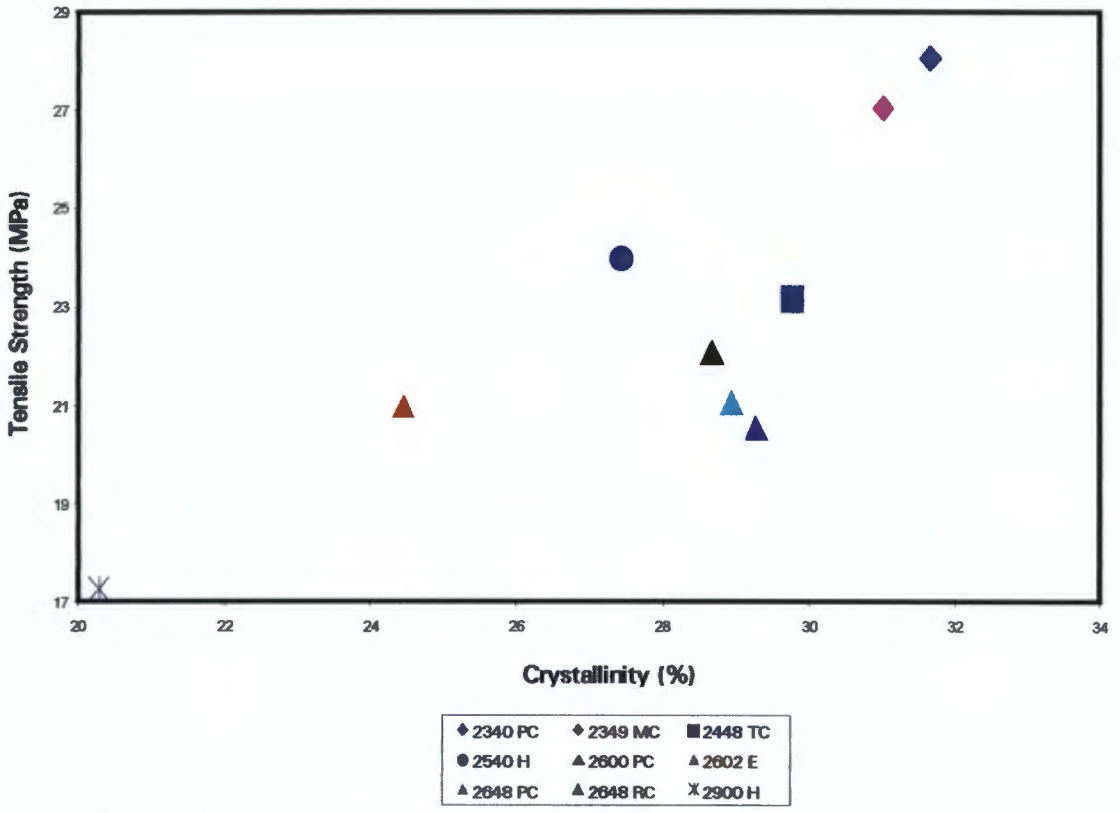

Figure D.5: Effect of the degree of crystallinity on tensile strength.

USE OF ELECTRON MICROSCOPY TO INVESTIGATE THE STRUCTURE OF POLY- (PROPYLENE-ETHYLENE) IMPACT COPOLYMERS

S. Mange, K. Marcus, M. A. Jaffer* and B. Sole**
Department of Materials Engineering, University of Cape Town
*Electron Microscope Unit, University of Cape Town
**Polifin Technical Division, Secunda

Polypropylene has a very good stiffness to cost ratio but suffers from poor toughness at low temperatures. Poly-(propylene-ethylene) impact copolymers were developed to overcome this problem (1). These copolymers can be regarded as a composite consisting of two phases and as such their properties depend on the microstructure of the individual phases. The balance between stiffness and toughness is achieved by controlling the size and the dispersion of the rubber phase within the glassy polypropylene matrix.

The structure of a copolymer with an ethylene content of 13 % was investigated using a Cambridge S200 SEM operating at 15 kV. Notched impact test specimens were immersed in liquid nitrogen and fractured with a plastic hammer to expose the rubber particles. The fracture surfaces were collected and then etched in *n*-heptane at 70 °C for 30 minutes (2). The fracture surfaces were then cleaned in methanol in an ultrasonic bath, fixed on aluminium stubs with a conductive carbide cement and sputter coated with Au/Pd for 10 minutes at 2 kV and 16 mA, to render them electrically conducting.

The quantification of the rubber particle size and distribution was done from SEM photos such as those shown in Fig. 1. The particle size measurement was done using the Joyce Loebl Image Analysis Package. The particle distribution measurement was made by measuring the centre to centre distances of the particles with a ruler. Distribution curves can then be plotted to show the effect that particle size and spatial distribution has on the mechanical properties of the copolymer.

TEM was used to study the microstructure of the rubber phase. A polymer block was machined to fit in an aluminium hollow pin and the combination was then submerged in concentrated chlorosulphonic acid for 4 hours at room temperature. The block was washed in distilled water and then submerged in 0.1 % solution of RuO_4 for 2 hours at room temperature. This solution was buffered at a pH of 7.2 with sodium dimethylarsonate in order to maximise diffusion of the stain through the block. The block was washed again and then sectioned at room temperature or at – 120 °C before viewing in a JEOL JEM-200CX TEM operating at 200 kV.

The rubber particles were found mostly as agglomerates as shown in Fig. 2, although some single particles occurred. This micrograph shows a rubber particle composed of amorphous regions (dark) and crystalline regions (light). Some authors contend that the optimum particle size for a good stiffness to toughness ratio is around 0.4 μm (3).

SEM in conjunction with TEM gives us a good understanding of the copolymer microstructure. The SEM micrographs show the spatial and the size distribution of the rubber particles as seen from the holes left behind through etching. The microstructure of the rubber particles and the matrix is obtained from TEM. The thickness of the interface between the matrix and the particle can also be determined. From such a structural analysis it is possible to understand the differences in mechanical properties between different batches of the same grade. It is also possible to determine the processing conditions that will give copolymers with optimum mechanical properties.

References

1. Lieberman, R. & Barbe, P.C. (1998) In: Encycl. Polym. Sci. Eng., 2nd Ed., 13, 464.
2. Feng, Y., Jin, X. & Hay, J.N. (1998) J. Appl. Polym. Sci., 68, 395.
3. Dwyer, S.M., Boutri, O.M. & Shu, C. (1996) In: E.P. Moore Jr., ed. Polypropylene Handbook, 211.

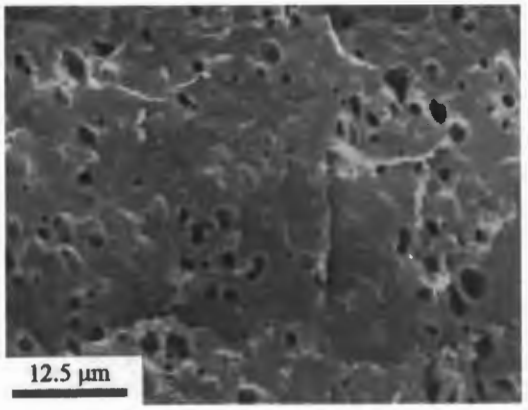

Fig. 1: SEM micrograph showing rubber particle size and spatial distribution

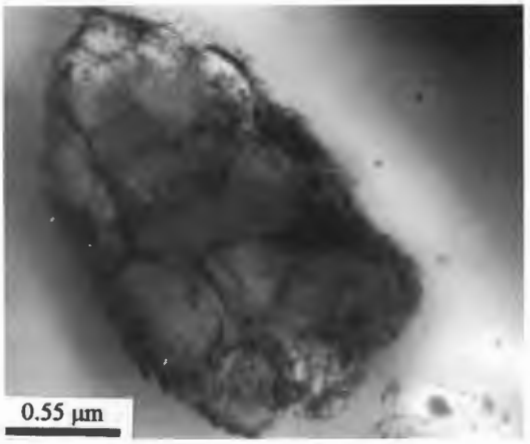

Fig. 2: TEM micrograph showing the microstructure of a rubber particle.